Pipavav Port Project
Volume II of Master's Thesis

Detailed Design, using Mathematical Models: PORTRAY, HISWA and SHIPMA

W.J. de Graaff

March 1994

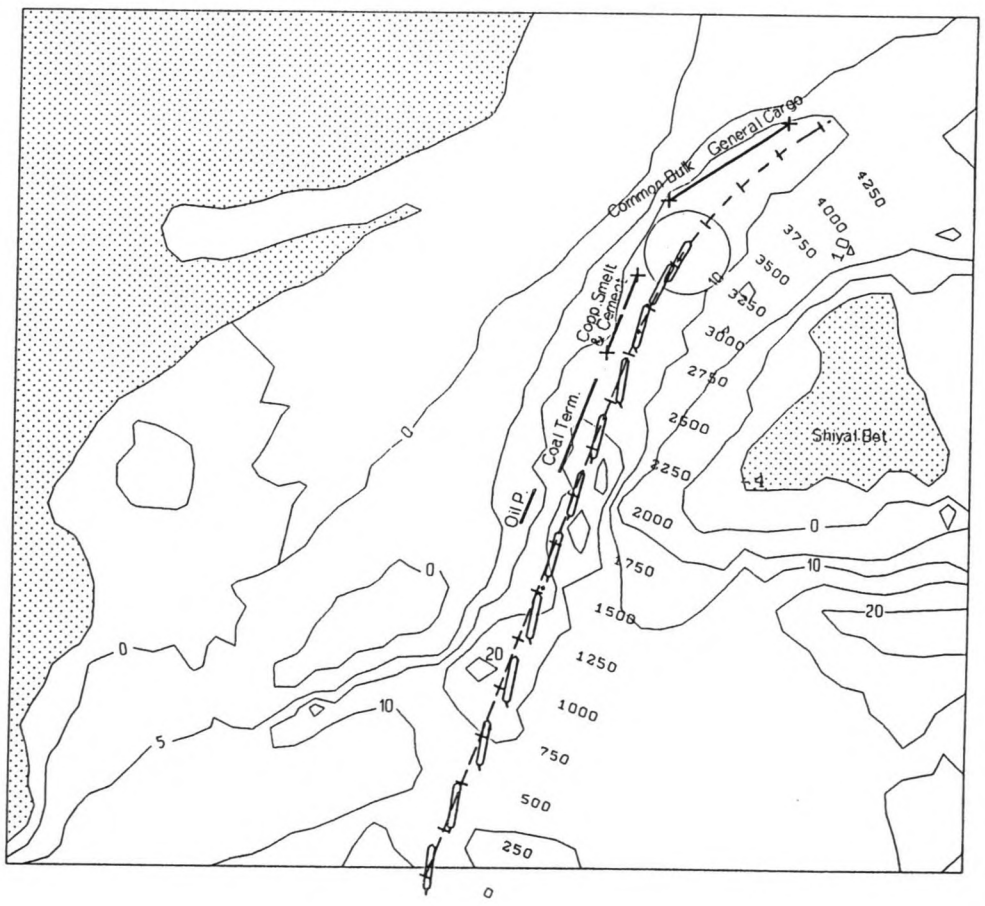

TU Delft
Delft University of Technology

Faculty of Civil Engineering
Hydraulic and Geotechnical Engineering Division
Hydraulic Engineering Group

Pipavav Port Project

Volume II of Master's Thesis

Detailed design, using mathematical models: PORTRAY, HISWA and SHIPMA

W.J. de Graaff

Professor:	Prof.ir. H. Velsink
Daily tutor TU Delft:	Ir. R. Groenveld
Tutor for HISWA TU Delft:	Ir. N. Booij
Tutor DHV Amersfoort:	Ir. M. Schreuder

TU Delft
DHV Environment and Infrastructure

March 1994

Preface

This report is the second volume of Master's thesis. The first volume, which is entitled 'Basic dimensions of the port facilities, based on the traffic forecast' was presented in May 1993. It describes the preliminary design of the projected port of Pipavav, based on a traffic forecast composed by engineers of DHV Environment and Infrastructure.

This second volume describes a more detailed design, resulting from additional studies that were recommended in the first volume. These studies were:

* a wave study on the translation of the deep water wave climate to the near shore wave climate,
* a study on the translation of the near shore wave climate to the port wave climate and
* a nautical study to get a better insight on the possibilities and restrictions of the vessels and infrastructure under several environmental conditions.

The first two studies are performed using two mathematical wave models named PORTRAY and HISWA. The last study is performed using the mathematical model SHIPMA.

This report concludes my Master of Science study at the faculty of Civil Engineering of the Delft University of Technology. I would not have made it without the help of lot of people, of whom I want to mention a few here.

First of all I would like to thank my professor, Professor Velsink, my daily tutor Ir. R. Groenveld, my tutor at DHV, Ir. M. Schreuder and my tutor at hydraulics Ir. N. Booij, for giving me the opportunity to graduate in the field of ports and waterways, an interesting part of Civil Engineering.

Second I would like to thank my parents and family for their moral and financial support without which it would have been impossible to start and finish this study.

Finally I want to thank all my friends for their time and support they have invested in this last stage of my career, especially Mr. Eric Warnaars and Mr. Vincent de Jong, for their constructive thinking and for their patience in correcting my english.

W.J. de Graaff,
Delft, May 9, 1994

Table of contents

Summary

The bay of Pipavav, India has been investigated for a feasible development of a new regional deep water port. This master's study contributes to the DHV Environment and Infrastructure feasibility study for a preliminary masterplan study based on a tentative traffic and shipping forecast.

In Volume I of this study a preliminary design of the port was made. This design comprised of the dimensions of the terminals, the storage requirements, the cargo handling equipment and the navigation channel, turning and berthing basins. Also a general layout of the port's land and water areas as well as a phased development of the port are described.

In Volume II a more detailed design was made, specifically of the hydraulic aspects of the port. A wave climate study and a nautical study were undertaken to get an estimate of the port and terminal downtime, the accessibility of the port and to evaluate the preliminary design.

The wave climate study was done using the mathematical models PORTRAY and HISWA. PORTRAY is a ray model, specifically written to predict wave activity inside harbours, but it could not be used for the bathymetric complex tidal basin of Pipavav, so HISWA was used alternatively.
HISWA is a mathematical model that uses wave propagation over a grid rather than along rays and on a slowly sloping foreshore seabed. It performed well and was used to describe the exceeding of certain wave height/period combinations at specific locations inside and outside the port. This portrayed a strong wave attenuation starting at circa 80% near the oil products terminal, near the entrance of the port, to circa 8% near the multi-purpose terminal, at the rear of the port. The waves are refracted such that they are incident between 3° and 18° with the moored vessels. Terminal downtime due to waves varied from 20 days at the oil products terminal to 0 days at the multi-purpose terminal.

In the final part of this study a nautical study was performed using the mathematical simulation model SHIPMA. With this model the entrance manoeuvre of a 60,000 DWT bulk carrier was simulated under various environmental conditions. The manoeuvre was investigated with regular and extreme wind, waves and currents conditions. Currents proved to be the dominating factor. The study showed that, due to a good alignment of waves and currents with the navigation channel and the terminals, vessels can enter the port with tugboat assistance under all ebb conditions and with flood up to a flow velocity of 1.4 m/s. This resulted in a channel downtime of 22 hours spread out over one year.

The results of both studies were combined with the results of a site investigation. With these results the terminal and the port downtime were estimated. It was concluded that the tidal basin is well protected for wave penetration and the port can be sailed well, due to a good current alignment. It is suggested that the oil product terminal is relocated or better protected and a that the crude oil jetty is reorientated to get a better compromise between current a wave alignment for this terminal.

1 Introduction

1.1 General

As was established in Volume I there is a need for a new deep water port with good cargo handling facilities and accessibility. The main issue now is whether the selected site -near Pipavav- can meet these requirements.

To determine this, a feasibility study was started comprising a phased masterplan up to the year 2010. In this masterplan the preliminary dimensions were determined of quays, storage requirements, cargo handling facilities, the harbour layout and the layout of the channel and basins. The basis for this preliminary design was a traffic forecast for both the commodity types and the ship sizes, up to the year 2010, drawn up by port officials and engineers from DHV. Using empirical rules and preliminary assumptions a general layout was determined that is extensively described in Volume I of this report, entitled 'Basic design of the port facilities, based on the traffic forecast'. The assumptions that were made and the design rules that were used are listed below.

a) PIANC-ICORELS design rules concerning gross underkeel clearance in exposed waterways.
b) Wave climate study for the translation of the deep water wave climate to a near shore wave climate with the use of the program COWAVE, made by DHV and
c) a study of the wave climate inside the harbour using a graphical diffraction method described in the Shore Protection Manual [21], also made by DHV.
d) Queuing theory for the calculation of the number of berths using $M/E_2/n$ and $E_2/E_2/n$ distributions as well as estimated average waiting costs and average construction costs.
e) Multi-criteria analysis for the determination of the best cargo handling configurations at the different terminals.
f) Several design rules concerning the required berth length and the dimensions of the channel, turning basin and the berthing basin, as described the UNCTAD manual and several other text books.

The following will discuss, how this preliminary design can be refined by establishing a more concrete basis for the assumptions made, by conducting additional studies.

a) The gross underkeel clearance depends upon many factors. In Volume I the empirical rules as formulated by the PIANC-ICORELS commissions, 15% of the draught in exposed channels, were used to get a first estimate of the required channel depth. These rules were based on Euro-Maaschannel conditions for ships of 200,000 DWT and over. Since the average ship size calling at Pipavav will be significantly less, with a much larger wave response, this was slightly increased to 20% of the draught. To get a better estimate of the required depth more data is needed on the expected wave height, period and direction, a better insight in the ship's wave

response as well as an estimate on the expected chance of a ship touching the bottom. This could be achieved by making a hydraulic model of the area, studying the ship's wave response in a wave response model, and making a thorough cost benefit study on accepted risk of a ship touching bottom or running aground. Also a sedimentation study which would provide insight in the sedimentation/erosion rate in the bay of Pipavav would give a more accurate estimate of the required depth of the channel and basins.

b) The deep water wave data obtained from the KNMI was adapted in such a way that it could be described as a number of specific wave height/wave period combinations for both sea and swell waves. The translation of this deep water wave climate into a near shore wave climate was done with the program COWAVE. This is an energy based shoaling/refraction program, assuming straight parallel depth contours. This is a schematization which introduces a degree of uncertainty in the near shore wave climate which can not be neglected. A more realistic hydraulic model would greatly reduce this uncertainty.

c) The translation of the near shore wave climate to the port wave climate was done using diffraction diagrams described in the Shore Protection Manual [21]. The assumption made here was that the foreshore rock on either side of the entrance to the West Channel would act as breakwater tips. This assumption is questionable since these 'tips' barely dry at the lowest tide (CD +0.0m) and their diffractive capacity would therefore be overestimated. No additional refraction/shoaling calculations were performed on the waves resulting from the diffraction. The port wave climate thus obtained is a rough (pessimistic) approach which gives an indication of the situation in front of the berths, however, any calculations based upon these results would certainly have to be reviewed critically. Application of a more complete and realistic hydraulic model would significantly increase the validity of any conclusions drawn from this port climate.

d) For the determination of the required number of berths the queuing theory was used, in combination with estimated costs of ship waiting time and for the construction of additional berths. For a better assessment of the costs of ship waiting time data should be available on the kind of ships (age, type, etc), the value of the cargo (e.g. computers or fertilizer), as well as a more accurate estimate of the time in port. Better insight in the costs of berth construction could be achieved by making a comprehensive cost estimate of the construction of an additional berth. The optimum number of berths could be obtained by building a traffic infrastructural simulation model of the port with (random) ship generators and service points in which all kinds of priority rules and e.g. breakdown of port facilities could be simulated. This would also require a good estimate of the port downtime which can be estimated, based on a wave frequency distribution (height and

period), which follows from a hydraulic model study.

e) The determination of the cargo handling facilities was done in Volume I firstly by making an inventory of commonly used equipment for the various processes which involve the handling of cargo. This list was then judged in a multi-criteria analysis with four weighed criteria to determine the most appropriate configuration per terminal. The number of criteria could be increased and their respective weighing factors should be more thoroughly investigated. Also a sensitivity analysis should be performed to investigate whether a certain configuration is suited for the Pipavav situation. Apart from a multi-criteria analysis several other methods could be used such as a monetary evaluation or building a simulation model of the landside operations.

f) With respect to the remaining general design rules which were used to determine the preliminary dimensions of the berthing basin, turning basin, storage areas, etc.; these rules can be replaced with more advanced design tools through an improved insight in the design parameters in general, which can be realized through the various studies recommended above.

It goes beyond the scope of this paper to carry out all the suggested studies. Therefore this Master's thesis will be limited to carrying out two of the above mentioned studies, leading to a more detailed port design. The objectives for this Master's study are set out in the next paragraph.

1.2 Objectives

The main objective of this Master's study is to investigate the suitability of the tidal basin near Pipavav for the development of the port described in Volume I. This will be achieved by making a hydraulic and a nautical model study. The preliminary design of the port as described in Volume I will serve as a boundary condition for these studies.

The objective of the hydraulic model study is to gain insight in the wave climate inside and outside the port. From this model study conclusions will be drawn about the downtime due to waves at the various terminals. An evaluation of the natural conditions of Pipavav will provide information on downtime due to factors other than waves. The results of this model study will also provide input for the nautical model study.

The objective of the nautical model study is to gain insight in the infrastructure of the preliminary design and the vessel's behaviour under various environmental conditions.

The results of both studies will be used to adapt the port masterplan to the extent necessary by refining the port dimensions used in the preliminary design of Volume I. These port dimensions are discussed in section 1.3.

1.3 Port dimensions

Before the actual set up of this report is discussed a consideration will follow on the port dimensions mentioned in the objective.

Port dimensions can comprise, the dimensions of port structures or the depth and width of channels and basins, but the loading rate of cargo handling equipment can also be considered as a port dimensions.
In general, these dimensions can be thought to be dependent upon variables or so called design parameters. Parameters are either given facts which can not be influenced or data that can be influenced, but is accepted as a boundary condition.

There are different types of parameters. One can discern operational parameters, such as security regulations; cost parameters, such as interest rates; and mechanical parameters, such as maximum production rates. The parameters that are most interesting for this study are the hydraulic and nautical parameters and are presented in table 1.1.

Thus port dimensions are all those unknowns of a port that are needed to make a (preliminary) port design. These dimensions depend on boundary conditions such as tidal variations or a traffic forecast. These data are called design parameters. On the one hand one can discern hydraulic parameters, those that influence the hydraulic models to be used and other hydraulic calculations, such as squat and on the other hand the nautical parameters, influencing the nautical model study and other nautical aspects of the port such as capacity calculations.

Hydraulic parameters	Nautical parameters
- tide	- ship characteristics
- waves	- ship dimensions
- seiches	- traffic intensity
- currents	- information on ship's position and weather conditions
- bathymetry	- aids to navigation (port)
- wind/weather	- navigational aids (ship)
- sediment transport	- tugboat/pilot assistance
- salinity	- accepted risk of touching bottom and running aground
- soil characteristics	

Table 1.1 Hydraulic and nautical parameters.

Some of the above parameters can overlap the two groups and some dimensions can change to parameters once they have been determined. For example, once the harbour and channel layout or the breakwater alignment have been determined, they will serve as boundary condition for the mathematical models and thus change to parameters. This only indicates the iterative character of the design process.

The port dimensions which will be the object of study are listed in table 1.2, together with the design parameters on which they depend. Some of these can be drawn directly from data presented as boundary conditions while others will need to be calculated in order to be useful in the determination of the design variables.

Port dimensions	Depend on
* number of berths	* effective loading capacity (un)mooring hours number of ship calls workable days per year waiting/construction cost ratio
* berth orientation	* bathymetry current patterns wave direction
* berth height	* ship dimensions tidal variation waves
* quay length	* number of berths ship size
* berth location	* bathymetry soil characteristics required dimensions (LxB) phased development
* berth structure	* type of commodities soil conditions wave penetration size and type of ships
* channel width	* ship dimensions waves ship characteristics currents wind traffic intensity info on position & conditions aids to navigation (port) navigational aids (ship) tugboat assistance accepted grounding chance
* channel depth	* ship dimensions waves ship response squat/trim dredging tolerance sedimentation tidal window net keel clearance accepted chance of grounding
* channel location	* bathymetry dredging costs layouts possible (curves)
* turning basin diameter	* ship size tugboat assistance currents
* turning basin depth	* (see channel depth)
* turning basin location	* operational criteria
* berthing basin width	* ship size traffic intensity
* berthing basin depth	* ship size sedimentation vertical ship motions tide dredging tolerance

Table 1.2 The design variables that will be object of study.

As can be seen from the listing above, many variables depend on wave height, period and direction in the harbour, indicating the important character of these variables.

The rest of this chapter describes how this study is set up in order to realize the objective.

1.4 Methodology

First the natural conditions of Pipavav will be described. These are parameters that influence the design variables but will not be object of further study, such as the climatic factors.

One of these natural conditions is the deep water wave climate. This deep water wave climate will be used in the determination of the near shore wave climate and the port wave climate. Several methods are available to perform such a translation. The most simple is a manual calculation that assumes straight parallel depth contours. Another method is to use a mathematical model. Two of these mathematical models will be used and compared in this study. The first one is a ray-tracking model, called PORTRAY that is developed at HR Wallingford Ltd., United Kingdom. The second one is a numerical model, called HISWA and which is developed at the Delft University of Technology. The theory behind both models and the simulation results will be discussed and compared. The results obtained from the near shore wave climate will serve as a boundary condition in the determination of the port wave climate. The goal of the port wave climate is to give the wave height, period and direction at several locations in the harbour and their frequency of occurrence. The results of both models will be validated against the results from a physical model built by CWPRS (India).

The final part of this study will be the nautical investigation of the port design. This will be done with the program SHIPMA. This is a fast time simulation program for ship manoeuvring, developed by Delft Hydraulics and the Maritime Simulation Centre the Netherlands. With this program it will be investigated how ships behave under regular and extreme current, wind and wave conditions.

With these results the hydraulic and nautical design variables, which are influenced by the results of the model studies, can be determined more accurately. The major part of the discussion will be dominated by the problem of accessibility and port downtime. In this discussion the parameters obtained from the evaluation of the natural conditions will also be included. This will result in an overall evaluation of the harbour layout made in Volume I with possible suggestions to improve it.

The reason for using two different models can be explained as follows. The first part of this Master's study was done in traineeship at DHV. There, the hydraulic model study was started with the model PORTRAY which was recently purchased by DHV from HR Wallingford, Ltd. However, the results produced by the model, during constructing and testing, were found to be very unreliable. After extensive evaluation and

discussions with experts at Wallingford, DHV and the DUT it was concluded that this model was not suitable. This was largely due to complex bathymetry of the tidal basin of Pipavav. Consequently it was decided that the determination of the near shore and the port wave climate would be done with the model HISWA. In this way it would still be possible to make a sensible evaluation of the port accessibility and the port downtime.

Both models will be described in this paper with the possibility to compare these models with each other. They will be presented simultaneously rather than in succession, but it should be kept in mind that both the determination of the near shore wave climate and the validation of the port wave model were first completed using PORTRAY.

2 Natural conditions

2.1 General

This section gives a general description of the site. The remainder of this chapter summarizes the data on the tides, currents, bathymetry, suspended load transport, waves and winds at the site of Pipavav Port.

The studies are based on data provided by GPPL, the port authorities, Central Water and Power Research Station (CWPRS), Pune India, Consulting Engineering Services, India (CES), the author of a 1984 masterplan for Pipavav and KNMI, the Dutch Meteorological Institute.
The proposed port facility is situated in a tidal basin near Pipavav Bandar, located on the northwest coast of India in the State of Gujarat. Pipavav Bandar is a minor anchorage port, situated at 20°59' North and 71°34' East on the south coast of the Gujarat peninsula. The site is partly exposed to waves from the Arabian Sea, but protected by several islets from wave action from the east and south (see maps in appendix I).

The coast in this area consists mainly of mud and sand flats, mangrove swamps and salt pans. The strong tidal currents however have made rather deep trenches providing locally natural deep water of up to 15m and more. West of Shiyal Bet the West Channel runs, curving in an easterly direction and then forms the East Channel, which is a lot shallower than the West Channel. Around the three islands, Shiyal Bet, Savai Bet and Chang Island, foreshore rock exists which is exposed at lower tides. North of Shiyal Bet the seabed drops sharply to a depth of about 10 m and then rises slowly to the mainland.

A good general impression of the project area and its surroundings from a nautical point of view may be obtained from the West Coast of India Pilot [30].

2.2 Main meteorological features

Information on the general weather conditions is necessary when extreme conditions such as excessive rainfall or poor-visibility can influence the downtime of port facilities or reduce the accessibility of the port in general. In chapter 3 boundaries are set for such extreme conditions.

A summary of the weather climate at Pipavav is reported in the West Coast of India Pilot [30] and in the CES report [11]. The climatic year is divided into 4 distinct seasons, of which the main characteristics are summarized in table 2.1.

Month	Season	Main Characteristics
Dec. - March	Cool Season	Winds NE, dry
April - May	Hot Season	Winds are light and variable, but tropical storms or cyclones may occur
June - Sept.	SW Monsoon	Winds are between SW and W over sea, but mainly W to NW along the coast, rainy
Oct. - Nov.	Interim Period	Light winds with land and sea breezes with occasional tropical storms

Table 2.1 Seasons

On much of the coast of Pakistan and the west coast of India most rainfall occurs during the SW monsoon. The marked seasonal range of rainfall can be drawn from the monthly totals in the climatic tables for the stations Surat and Veraval as presented in the West Coast of India Pilot. These tables also include data on visibility, air temperatures, wind speeds and directions and other relative data. Translated to Pipavav this means:

- The temperature varies from 4°C in January to 42°C in May.
- The relative humidity is high in the monsoon months, reaching up to about 90% in August; low values of about 45% occur in January.
- The annual rainfall in the area is approximately 500 mm, 40% of which occurs in the month of July. June and August account for about another 40% and the remaining 20% is evenly spread over the winter months.
- Visibility is generally good at Pipavav. Mist sometimes develops just before sunrise after a calm and cloudless night. Visibility in the monsoon normally deteriorates during rain showers and squalls. The West Coast of India Pilot gives a frequency of poor visibility (less than 5 miles) of 2% in January and 35% in July.
- The mean sea surface temperature varies from 24°C to 25°C in January to some 28°C in May.

2.3 Wind

Information on wind speeds, direction and duration is important for several design variables. Extreme wind speeds can cause terminals to shut down and in general it influences the required additional width of the access channel to compensate for the drift angle.

Direct wind recordings or observations are not available in the Pipavav area. Wind speed and directional rose diagrams as derived from observations from ships are presented in the CES report [11] and reproduced in table 2.2. A graph showing the frequency of exceeding for the wind speed, summarized for all seasons, is presented in figure 2.1.

Wind speed (Bft)	Frequency in hours per period											
	Dec - March			April - May			June - Sept			Oct - Nov		
	NNW	N	NNE	W	WNW	NNW	SSW	WSW	W	NNW	N	NNE
1	49	49	49	32	29	49	9	15	0	58	81	41
2	148	131	122	148	122	131	20	67	107	197	148	197
3	197	244	197	241	203	261	67	261	189	227	180	261
4	180	238	26	113	203	212	67	343	351	81	148	99
5	32	32	23	0	17	17	29	293	180	0	41	32
6	17	17	9	17			15	113	49	17		15
7							17	32	32			
8								9	3			
Other direct/calm			1141			558			646			545

Table 2.2 Wind climate 1961-1966.[1]

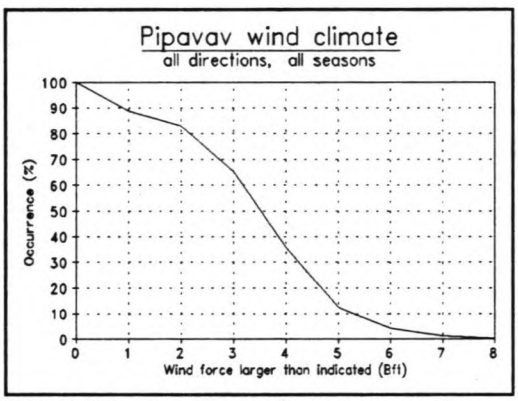

Figure 2.1 Exceeding wind speeds.

According to the India Pilot [30], tropical storms (wind force 8-9) and cyclones (wind force 12) may occur during the hot season, from late May to the first half of June, and during the interim period, from late October through the first three weeks of November. The average frequency of severe tropical storms or cyclones in the adjacent Arabian Sea is about one per year. In the CES report [11] it is estimated that the probability of a cyclone depression passing through the Gulf of Khambat is once in six years and that, during the worst storms, the wind speeds may reach 120 km/h.

2.4 Tide

The tide is of great importance in the design of a harbour. It has an influence on all hydraulic variables to a certain extent and is therefore one of the more important parameters. This section describes the tides, the occurrence of tidal ranges and their relation with the water levels. Tidal data is available from various sources [3], [4], [5], [26] and [30]. The tidal levels are summarized in table 2.3.

Source	MHHW	MLHW	MSL	MHLW	MLLW
[3],[5]	**3.00**	**2.30**	**1.76**	**1.10**	**0.60**
[4]	3.19	2.37	1.76	1.16	0.50

Table 2.3 Tidal levels for Pipavav.

[1] Based on ship observations in the region 17°-21° North and 69° East to coastline, see figure 2.10. Storm hours can be divided over several days.

All tides are composed of both semi-diurnal and diurnal components, the latter introducing an inequality in successive heights of high or low waters and in the times. When this diurnal inequality reaches a certain limit it becomes more informative to list the average heights of the higher and lower high and low waters, rather than the average spring and neap values. This is obviously the case in the region of Pipavav. There seems to be a small difference in the levels between the various sources. Since [3] and [5] are the most recent these values will be adopted as *the* tidal levels for Pipavav.

From the table can be read that the mean higher tidal range (spring) is 2.40 m while the mean lower range (neap) is 1.20 m.

CWPRS report 'Tidal Observations' [26] summarizes water level measurements taken at the new port site of Pipavav Port, between 3-2-1988 and 8-4-1988. This data has been used to further analyze the tidal data in the area. The high and low water levels are studied to determine the frequency of occurrence of a certain tidal range. The cumulative density functions of the observed tidal ranges for flood and ebb in the measuring period are shown in figure 2.2 through 2.5.

Distinction has been made between the flood range and the ebb range. The flood range is the range from low water to consecutive high water. The ebb range is the range from high water to consecutive low water. This is specifically done to analyze the relation between the tidal ranges and the current velocities, because the same tidal range with flood and ebb can result in different tidal velocities, due to the difference in duration between flood and ebb. As a result of the limited measuring period, this resulted in a slight difference between the 50% probability of the flood and ebb ranges.

The mean tidal range is approximately 1.85 m during flood and 1.95 m during ebb. For about 10%-15% of the tides, the flood and ebb ranges exceed the 3.0 m. The mean higher range of 2.40 m is exceeded for about 20%-25% of the tides.

Now it is known how often a certain tidal range occurs. The occurrence of these tidal ranges can now serve as a basis to find the occurrence of all related parameters such as high and low water levels and the tidal currents. The same data as before [26] has been used to construct a scatter diagram to link the tidal ranges to high and low water levels (figure 2.6 and 2.7). With the mean higher range of 2.40m the high water level ranges from 2.35m to 3.55m. With mean lower range of 1.20m the low water level ranges from 1.00m to 1.60m.

The highest astronomical tide (HAT) can be found using the tables in the Admiralty Tide Tables [3] and amounts to CD +3.72m for Pipavav. In data used for the analysis of the tides, water levels below Chart Datum were found. The basis for Chart Datum is therefore not known. It could either be defined as the lowest astronomical tide (LAT) or established from historic water level data. It is assumed here, that LAT equals CD.

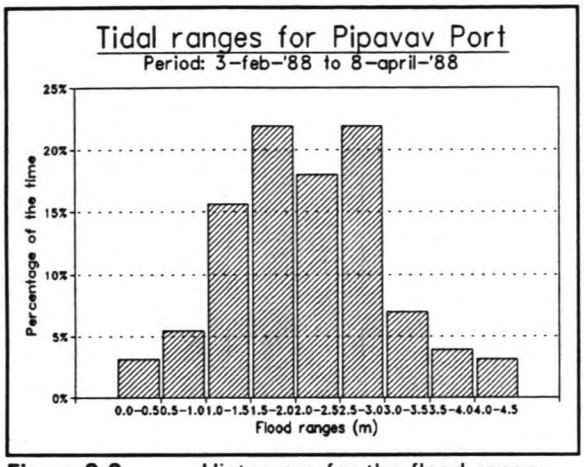

Figure 2.2 Histogram for the flood range.

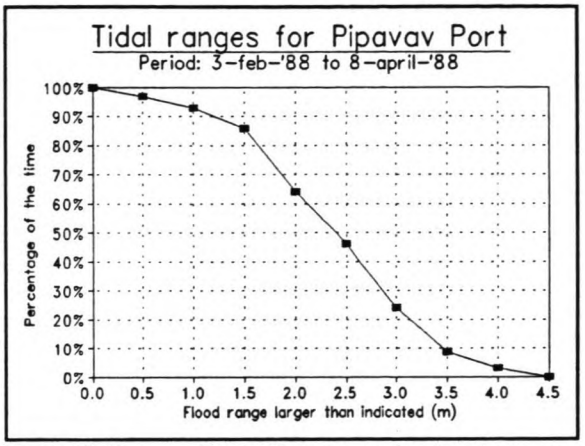

Figure 2.3 Exceeding curve for flood range.

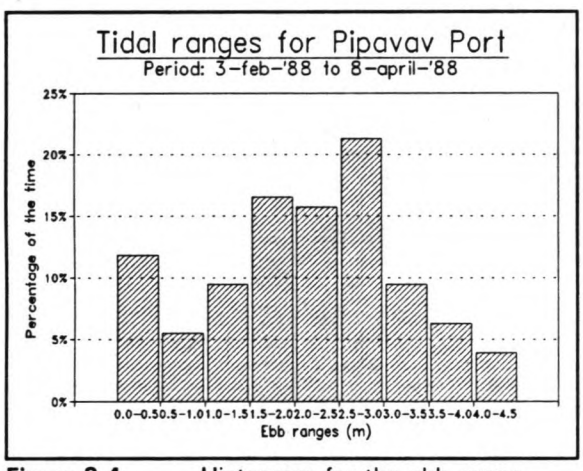

Figure 2.4 Histogram for the ebb range.

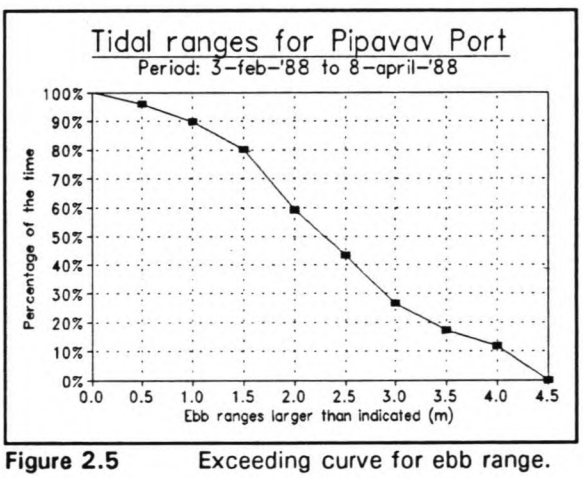

Figure 2.5 Exceeding curve for ebb range.

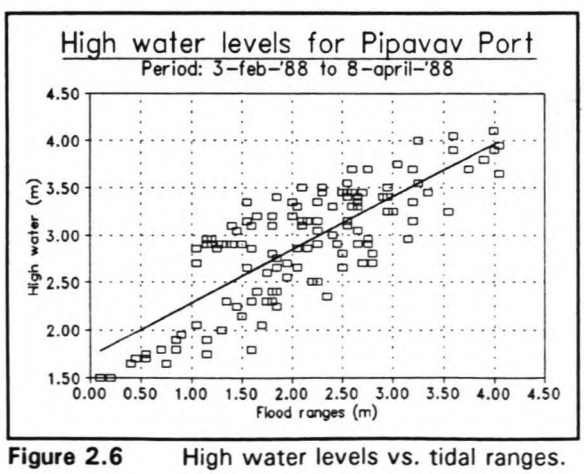

Figure 2.6 High water levels vs. tidal ranges.

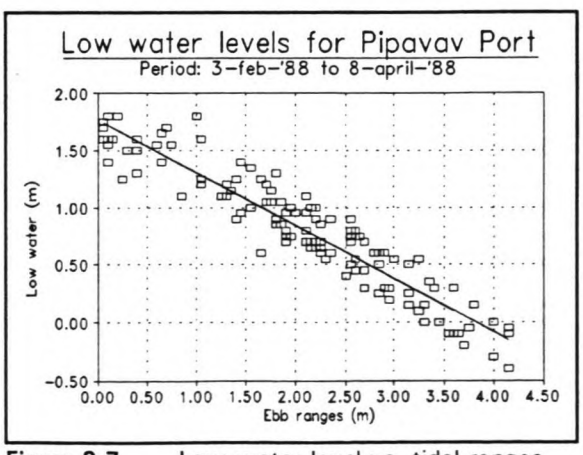

Figure 2.7 Low water level vs. tidal ranges.

2.5 Currents

Currents influence the drift angle of ships entering or leaving the port and they influence the orientation of the berths as the berths should generally be aligned to the currents to avoid nuisant current patterns around moored ships. Information is therefore needed on current velocities, directions and frequency of occurrence.

Data on currents is available from various sources. The tidal data has been used to determine the frequency of occurrence of certain tidal ranges. These tidal ranges have been linked to the current velocities.

This section describes the relation between the tidal ranges and the currents. The flood and ebb currents are described resulting in a table with frequencies of exceeding for different locations near the proposed facilities.

CWPRS report [8] lists current velocities measured at four locations. These locations are:

- L-1 in Motapat Creek near Pipavav Bandar,
- L-2 at the entrance of Motapat Creek,
- L-3 in front of the reclamation and
- L-4 in the navigation channel west of Shiyal Bet.

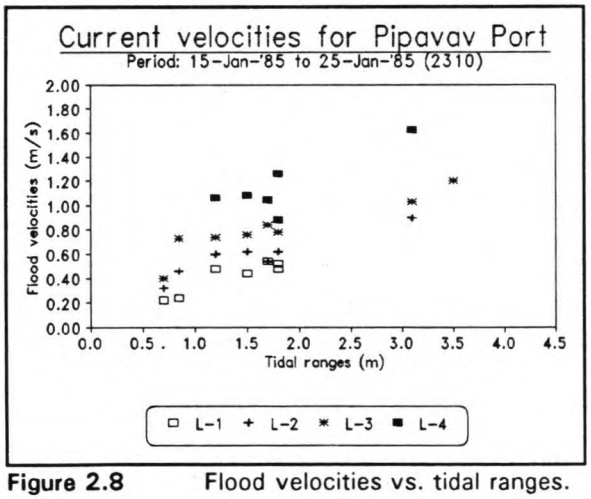

Figure 2.8 Flood velocities vs. tidal ranges.

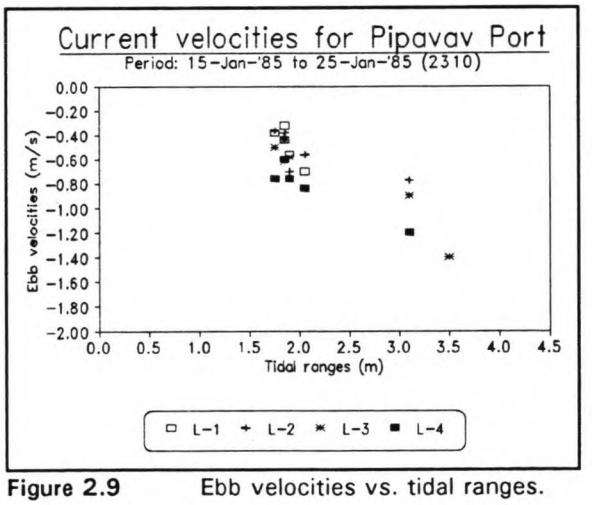

Figure 2.9 Ebb velocities vs. tidal ranges.

These locations are indicated on the map in appendix I.
Similar as with the water elevations, a diagram has been constructed which shows the flood and ebb velocities against the tidal ranges. Different diagrams are made for locations 1 and 2 and locations 3 and 4. The data on locations 2, 3 and 4 is supplemented with the information presented in [4], [9], [13] and [30].
The constructed diagrams are reproduced in figures 2.8 and 2.9. These show a correlation between the velocities and their tidal ranges. Table 2.4 summarizes the results from these figures, giving information on current velocities and their occurrence.

A description on the direction of the tidal currents can be found in the West Coast of India Pilot. It states that the tidal currents, running along the shore of Gujarat, branches near Pipavav. The inner branch runs through the West and the East Channel. Since the navigation channel is projected in the deeper parts of the West Channel, the currents follow the general alignment of the channel. The terminals are projected parallel to the channel axis.

In several studies, performed by CWPRS, the alignment of the so-called steamer berth has been investigated [9], [14] and [23]. This has caused several realignments resulting in the present orientation of the reclaimed area. As was mentioned, in Volume I, the reclamation has already been constructed and will be incorporated into the new multi-purpose terminal.

Tidal range with percentage of exceeding.		Current velocity in front of the reclamation. Location L-3 (m/s)		Current velocity in the access channel. Location L-4 (m/s)	
		Flood	Ebb	Flood	Ebb
80%	1.05 m	0.67	-0.22	0.92	-0.40
50%	1.85 m	0.82	-0.53	1.14	-0.72
20%	2.75 m	1.00	-0.91	1.35	-1.00
1%	4.05 m	1.28	-1.48	1.69	-1.47

Table 2.4 Relation between the current velocities and the tidal ranges.

2.6 Deep water wave climate

Direct observations or recordings of the normal wave climate at Pipavav are not available. Information on the wave climate outside and inside the port will therefore have to be obtained otherwise. The deep water wave climate will be the basis of calculations for the near shore wave and the port wave climate. Both calculations will provide essential information for virtually all design variables which makes the deep water wave climate extremely important.
For the study with PORTRAY use is made of an adapted version of the deep water wave climate (as presented in the DHV feasibility report), based on a separation of the whole climate in sea and swell waves, which is also described in this section.

Wave data was obtained from the KNMI (Royal Dutch Meteorological Institute). It contains 5813 observations of wave height, wave direction and wave period in a 30-years period (1961-1990) from the area 17.0°-20.9° North and 69.0°-71.9° East (see figure 2.10).

It can be questioned whether all these observations were really 'deep water waves' as ships usually sail close to the coast. It can also be disputed whether the percentage of 'storm waves' is accurate since ships tend to avoid rough weather, especially with modern forecasting. Since answering these questions is almost impossible and it is assumed that

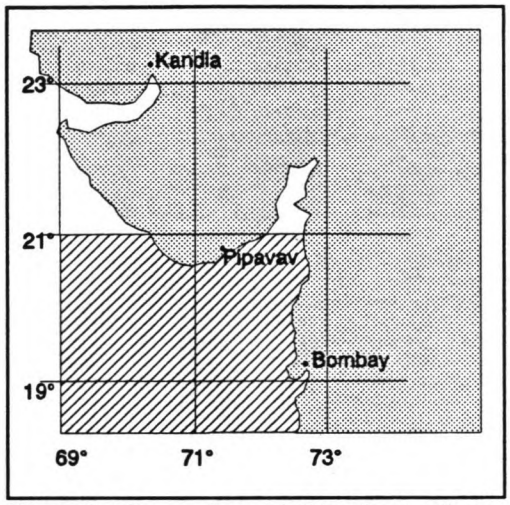

Figure 2.10 Area of ship observations.

any deviation would be minor (this only concerns the longer and higher waves, with a low frequency of occurrence). These observations are therefore adopted as a good representation of the genuine deep water wave climate. The wave heights in the tables are based on visual observations. This 'visual' wave height (H_v) is normally close to the significant wave height (H_s). It is assumed that the visual wave height equals the significant wave height.

The observations as presented in the KNMI data, are divided over the seasons as follows:

Cool season (December-March)	:	2318 (39.9%)
Hot season (April-May)	:	1146 (19.7%)
SW monsoon (June-September)	:	1681 (28.9%)
Interim period (October-November)	:	668 (11.5%)

The observed wave data is classified in 12 wave directional sectors (30° intervals), 22 wave height classes from 0-10m (0.5m intervals), and 6 wave period classes. A wave direction of, for instance, 90° actually means that waves are approaching from a 75°-105° sector. A wave height of 3.5m actually means 3.25m-3.75m.

Looking at the map of Pipavav (appendix I), it can be seen that the port facilities can be affected by waves coming from easterly and southerly directions. The island group and the coast west of Pipavav shield the facilities from other incident angles. Waves travelling through the East Channel will come from a 60°-120° bearing. Waves travelling through the West Channel can affect the port facilities coming from a 90°-240° bearing. In table 2.5 the frequencies of occurrence for the different directions and seasons are summarized. Figures 2.11 and 2.12 show the number of days per year that a certain wave height or wave period is exceeded.

Seasons	Wave direction							Total 60°-240°	Other direct. /calm
	60°	90°	120°	150°	180°	210°	240°		
Dec-March	6.08	1.68	0.47	0.39	0.35	0.39	0.43	9.79	90.21
April-May	0.17	0.52	0.44	0.35	1.05	3.40	11.87	17.80	82.20
June-Sept	0.17	0.42	0.18	0.48	0.95	11.90	45.87	59.96	40.04
Oct-Nov	7.19	1.95	0.75	1.05	2.10	2.69	3.14	18.86	81.14

Table 2.5 Frequencies of wave occurrence per direction and season.

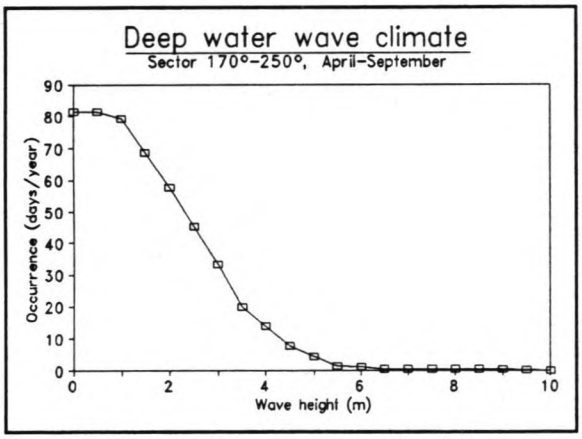

Figure 2.11 Exceeding curve for H_s.

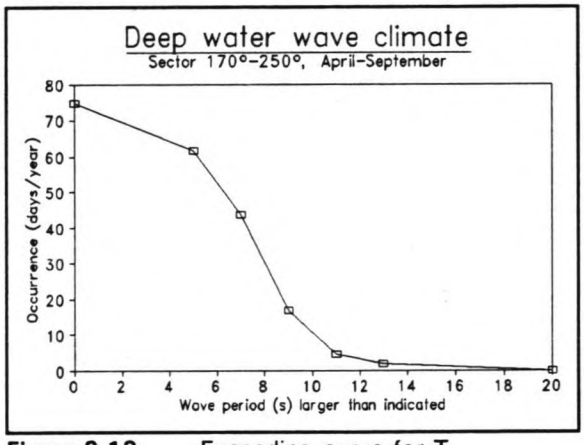

Figure 2.12 Exceeding curve for T.

The site is only exposed to waves from the East, that originate in the Gulf of Khambat. These waves will be locally wind generated waves and it is not very likely that these waves will significantly affect the site. The origin of the (larger) waves (i.e. deep sea) lies southwest of Pipavav.

As highlighted in the table above, it can be concluded that the most interesting seasons concerning the wave climate for Pipavav Port are the Hot season (April-May) and the SW monsoon (June-September). During these seasons, wave directions are more frequent in the range of 180°-240°. The predominant wave direction is 210°-240°, occurring in 57.8% of the time during the SW monsoon. A summary of the wave climate for these directions in these seasons is presented in table 2.6. The wave direction 180° is also included in this table because waves coming from this direction can run straight into the West Channel and could prove to be a very significant direction.

Wave height (m)	Frequency in days per year							
	180°		210°		240°		Total	
	Occur	Exceed	Occur	Exceed	Occur	Exceed	Occur	Exceed
1.0	0.41	1.73	2.76	16.07	7.39	61.42	10.56	79.22
2.0	0.16	0.86	2.12	10.27	10.14	46.53	12.42	57.65
3.0	0.09	0.45	2.30	6.06	11.03	26.96	13.42	33.47
4.0	0.09	0.18	1.38	2.71	4.75	10.96	6.22	13.85
> 4.0	0.09	0.18	1.33	2.30	6.21	14.66	7.63	17.14

Table 2.6 Deep water wave climate summarized for April-September.

The deep water wave climate that was used by CWPRS in 1974 to investigate the suitability of the tidal basin of Pipavav for the location of a new deep water port was based on ship's observations plying in the same region (as the ones obtained from the KNMI) but for a shorter period namely from 1961 until 1966.

In the 1961-1966 wave climate the wave heights of 2m and 3m were exceeded for 37 and 13 days per year respectively. One can see that this was an underestimate and it implies that Pipavav Port could be subject to a larger wave attack than originally assumed.

2.6.1 Adaptation of the deep water wave climate for PORTRAY

For the feasibility study done by DHV the deep water wave climate, as presented in the previous section, was separated into two period classes to reduce the total number of direction-height-period combinations. This calculation method is not used for the determination of the port wave climate, but it is described for completeness sake's.
The 6 different wave period classes were reduced to 2 classes, one class for 'sea conditions' and one for 'swell conditions'[1]. For 'sea conditions', there is a close relation between wave height and period, depending on wind speed and duration in the local wind field. When unlimited fetch and unlimited duration is presumed a specific period can be found for each specific wave height. This relation can be read from the 'graphs for the determination of the significant wave height H and the wave period T in sea state from the wind speed U and the duration t or the fetch F' that can be found in various text books like the Shore Protection Manual [21]. This relation does not exist for 'swell conditions' as waves under this heading have travelled away from the local wind field or still remain after the wind has dropped. The total climate is now divided in a 'sea' part and a 'swell' part where sea applies to a certain part around this 'unlimited fetch-duration period' and the remaining area is covered by swell. A more

[1] This doesn't mean that sea and swell waves can not coincide.

detailed description of this separation method can be found in appendix II.
For this translation of the climate only the directions 210° and 240° were considered as these deemed to be the only significant directions in view of their high frequency of occurrence, see also table 2.5. The new representation of the deep water wave climates for the hot season and the SW monsoon are listed in appendix III. The frequency of occurrence of a certain wave class during one of the seasons is expressed in number of days per year.

2.7 Soil conditions

Data on the soil conditions provide essential information for several design variables. Knowledge about the type of soil in the areas to be dredged, for instance, largely influences the type of dredging equipment to be used and implicitly the costs involved with the dredging operation. It also exerts influence, in case of soft soil, on the location of the nautical depth, which can reduce maintenance dredging quantities. In this study the soil characteristics will only be used to determine wether a pile foundation is the only possible foundation type and hence, what the character of the berths will be; open pile structure or a closed, vertically faced wall.

In March 1985 and again in June 1991 soil investigations were carried out in the area of the ongoing works, i.e. the quay and reclamation area, which is also the location for the future multi-purpose berth. On both occasions several bore samples were taken and tested in a laboratory.

From the samples taken in June 1991, located in the area of the projected block wall, a longitudinal soil profile can be derived which is presented in appendix IV.

The soil stratification can be described as follows:
- The top layer consists of soft mud.
- Between CD -12m and CD -16m the soil mainly consists of firm to very firm clay (CH and CL).
- Below the upper layer (highly weathered) rock exists, with SPT-values of $N \geq 100$.

Hardly any information is available on soils in the areas to be dredged and in the location of the proposed dedicated berths. From bore samples made in 1985 it appears that in front of the reclaimed area weathered to hard rock exists below CD -20m and above this layer firm clay and dense sand up to about CD -10m. Additional soil investigations will have to be done in the next phase of engineering to obtain more information in areas to be developed, not covered by the present samples.

2.8 Bathymetry

To make a good layout of the port, i.e. the location of the berths, the channel and the turning basin, it is essential to have a good insight on the local bathymetry. In this way it is possible to search for a balance between reclamation and dredging quantities, the distance from the site to the shore and natural alignment to bottom contours. This section describes the local bathymetry using several maps and cross sections at various locations in the basin.

Several depth soundings were supplied by the port authorities. These charts were all issued before the completion of the reclamation and restricted to a rather small area in front of the proposed facilities. Other, more complete, bathymetric data is available from admiralty charts 2034 'Pipavav Anchorage' (1:25,000) [4] and 1474 'India West Coast, Savai to Veraval' (1:300,000) [5] which are dated in 1968 and 1991 respectively.

The foreshore slope at deep water is rather regular. The 20m contour lies at a distance of some 40 km from the shore. The contour pattern near shore is very irregular with local scour holes of CD -27m and flat shoals of only 0.30m below chart datum. A lot of foreshore rock and submerged reefs can be found at either side of the entrances of the East and West Channel of which some dry at the lower tides.

On the map in appendix I lines indicate where cross sections of the basin are drawn. These 15 cross sections are reproduced in appendix V. Cross sections 7 and 8 are drawn again, but now from a hydrographic survey made at the new site in April 1985, 4 months before completion of the reclamation. A comparison between the two different surveys shows that no significant changes have occurred in the intermediate 17 years.

According to [11], the present bathymetry seems to be stable, which is supported by the comparison of sections 7 and 8. However, relatively small scale interventions could change the local flow pattern, which in its turn could trigger large scale morphological changes in the area. To understand the possible consequences better, a study should be carried out on the overall hydro-morphology of the basin as well as local effects of quay construction.

In section 8 a sketch shows how the reclamation and quay wall construction diminish the wet cross sectional area. The reduction at CD +0.00m and CD +3.00m amounts to 25% end 12% respectively. This explains why current measurements in 1988 resulted in 10%-20% higher values in front of the reclamation. The construction of more port facilities will have a similar effect in other cross sections.

2.9 Other natural conditions

Other natural conditions that can influence the design variables are:
- suspended load transport
- salinity
- seiches

Suspended load transport
CWPRS report 2310 [8] gives tables of the water sample measurements undertaken at locations L-1, 2, 3 and 4. These water samples give information on the suspended sediment in this area. The measuring period was 10 days, during the NE-monsoon period and the measurements were restricted to daylight only. Also seabed samples were taken to determine the nature and the size distribution of the material in this area. The D_{50} of the samples taken at L-1, 2, 3 and 4 were 0.006mm, 0.0064mm, 0.25mm and 6.75mm respectively. This can be classified as medium silt to medium gravel [6]. No measurements were done on sediment transport along the bottom.

The data now available, is not sufficient to make any reliable calculations of the sedimentation of the proposed dredging areas. Additional measurements of suspended sediment and sediment transport along the bottom as well as recent and full scale hydrographic surveying and measuring over a longer period, especially during the SW-monsoon, are necessary. Moreover it is beyond the scope of this paper to make a detailed sedimentation study. However, based on experience of DHV specialists in similar situations, a rough estimate of sedimentation of about 20% to 30% of the capital dredged volume after one year is thought to be realistic.

Salinity

A change in the salinity of the water can lead to additional sinking in of ships when sailing into less salty waters within the harbour boundaries. This additional sinking in should be accounted for in the determination of the depth of the channel and basins.

The tidal basin of Pipavav is openly connected on two sides with the Arabian Sea. Thanks to the tidal currents running through the port area, and the absence of a fresh water inflow a change in salinity does not have to be accounted for. Additional sinking in due to salinity changes will therefore not occur.

Seiches

Due to the open character of the tidal basin of Pipavav no enclosed water masses exist. Also the port design has a very open character. The coast at the edges of the basin consists of flat sloping mud beaches and mangrove. This means that circumstances needed for resonance of very long waves, with all its disastrous effects, are not present. The effect of seiches on the port facilities will therefore not have to be incorporated into the port design.

3 Operational limits

The operational limits are those circumstances where port operations are impeded, due to environmental conditions. The port operations which may be affected are:

- boarding of pilot (10 km off the coast)
- waiting in the anchorage area
- tying up of tugboats (2 km outside the port)
- sailing in the navigation channel
- berthing manoeuvre
- moored condition
- loading or discharging process
- leaving the berth and port

Environmental conditions that can hamper or prevent port operations are:

- waves
- currents
- wind
- water level
- mist, rain, temperature, etc.

Each of the port operations is bounded by its own limiting conditions, which can vary depending on the type of vessel, mooring arrangements, berth structure and orientation, soil type, meteorological conditions and many more. An attempt is made to formulate the limiting conditions for each stage related to its relevant ship size, mooring arrangement or whatever other factor influences these conditions. These conditions are drawn up after consulting various textbooks on port design, of summary of which is presented in appendix VI. However, no author has yet been able to formulate *the* acceptable wave height/wave period combination nor any other concrete operation limit. The reason for this is that there are too many different parameters which influence these conditions and that there are various different norms in the ports throughout the world. In this paper an attempt is made to give indicative values for 'average' circumstances in the Pipavav case. Average in this case means that, for instance, no distinction is made between stiff fender systems or soft fender systems, because this would introduce too many variables.

3.1 Definition of limiting criteria

In this section the limiting conditions for each port operation will be described.

Boarding of the pilot

When a pilot is requested by an approaching vessel, the ship will be some distance offshore. The exact distance varies for ports and situations throughout the world. A maximum distance of 10km offshore is assumed for the Pipavav situation.
The pilot can board the vessel either by sea or by air.
When the pilot boards a vessel by sea, the most important factors

governing this operation are the visually observed wave height and the wind speed. PIANC bulletin no. 32 [12] claims that it becomes extremely difficult for pilots to board the vessel when this observed wave height exceeds 3m and when the wind speed exceeds 20 m/s.
When the pilot arrives by helicopter there will be some minimum atmospheric conditions that control this operation. Each port has its own rules. To give an example, that can serve as an indication of the Pipavav situation; the rules that apply for Rotterdam, for helicopters that are equipped to fly on their instruments, are:

* minimum ceiling 45.7m
* minimum horizontal visibility 800m
* maximum wind speed 28 m/s.

Boarding of pilots by air is not relevant in the case of Pipavav, but is added for the sake of completeness.

Waiting in the anchorage area

It is hard to comment on the limiting factors for the anchorage area. Generally it can be assumed that these conditions are the least conclusive in the whole chain of entering, manoeuvring and mooring, since ships have to be able to remain in the anchorage area to 'ride out' a storm.

Tying up of tugboats

The tying up of tugboats will start at some distance outside the port to ensure enough stopping distance, in case the tying up fails. It will last approximately 15-20 minutes. The actual distance from the berth is determined by many factors, such as weather conditions, ship length, whether the ship has bow propellers, etc. In general, a distance of 2km should suffice, so depending on the location of the berths the tying up should start further offshore.

This operation is limited by the shorter waves (4s-7s) with a wave height of approximately 1.5m. It is the shorter waves that disturb the auxiliary craft, due to their limited length. According to Thoresen [17] a wind speed of 12-15 m/s or a significant wave height of 1.0m - 1.3m must be taken as guideline limits for safe operation of modern mooring boats or launches.

Sailing in the navigation channel

Manoeuvring in the navigation channel is governed by limiting conditions for the vessel itself and for the tugboats and other auxiliary craft towing the vessel to the berth.

A vessel sailing in the channel is subject to six modes of freedom; three translatory and three rotary (see figure 3.1). In each of these modes of freedom the vessel has its own natural period of oscillation. Resonance will occur when the apparent period of the joint excitation force of waves, wind and current is close to one of these natural periods of oscillation of the sailing vessel. Of the six modes of motion, roll, pitch and heave are the most important. Of these, the latter two are rather

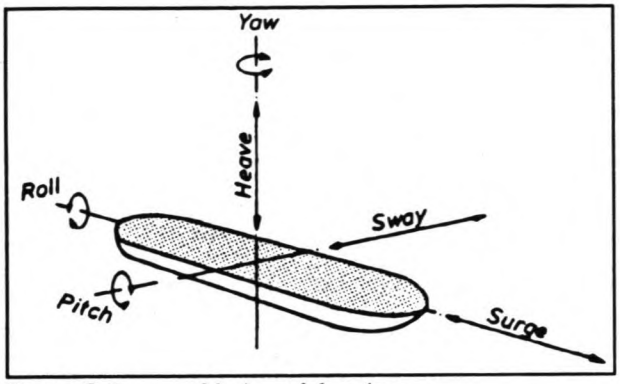

Figure 3.1 Modes of freedom.

damped motions, meaning that resonance is less likely to occur. Roll is a motion which a quite resonance sensitive. According to [18] the natural roll period of merchant type ships in deep water is usually between 10s and 17s. The natural periods of pitch and heave would be in the same range, however, since these are damped motions due to a decreased water depth, the danger of resonance is less. These modes of motions therefore have less consequence, where roll can cause significant decrease in rudder efficiency.

Whether some (range of) wave height/wave period combination will significantly disturb the sailing in the channel, or even prevent this, is very hard to determine. This depends on many factors such as the wave period, the wave height, the wave direction, the natural period of oscillation of the vessel, the sailing speed of the vessel, the depth of the channel, the acceptable risk of a vessel touching the bottom, the material of the sea bottom and even the value of the ship and its cargo. It is therefore quite difficult to give limiting wave height/wave period combinations for sailing in the channel. However, the data available from this literature review, *can* assist in the determination of the required channel depth for the design vessel.

Other factors that affect a safe manoeuvre through the channel are cross winds, cross currents, insufficient water depth and reduced visibility.
Depending on the loading condition of the vessel (e.g. a fully loaded tanker or a tanker in ballast) a cross wind of 15-20 m/s can become decisive, according to [12].

Cross currents force the vessel to navigate with a drift angle. Working Group IV of ICORELS, PIANC poses that for safe navigation, the drift angle tangent should be less than 0.25.

Reduced visibility due to fog and heavy rain may also hamper the ship's approach of the harbour or it's departure. The effect can be reduced by aids to navigation and navigational aids, such as ship and port radar, electronic positioning systems, high intensity lights and good communication. According to [12] the limits may vary between 200m and 500m, dependent on ship size, available navigation aids, the communication system, the traffic intensity and local conditions.
Reference [17] reports that fog in Norway is defined as a weather condition in which the visibility is less than 1000m. In general, visibility between 500m to 1000m can be acceptable for the manoeuvring and berthing process inside a harbour. As a general rule, most oil and gas terminals will close for arrival and berthing or deberthing and departure of tankers if the visibility is between 1000m and 2000m.

Berthing manoeuvre

Environmental conditions affecting the berthing manoeuvre have a double effect. They influence both the vessel and the auxiliary craft. Therefore a sufficient number of tugboats will have to be provided to ensure the maximum allowable berthing speed permitted by the fender system, in use. In [18] it is mentioned that berthing with wind speeds higher than 12.5 to 15 m/s is considered to be unsafe and therefore not allowed. Reference [17] specifies this, by giving a wind speed of 10 m/s, as berthing limit for ships with lateral wind area of more than approximately 5000 m^2 and a wind speed of 15 m/s with a wind area of less than 3000 m^2.

Generally it can be said that when safe manoeuvre through the channel cannot be guaranteed the berthing manoeuvre will also be cancelled.

Moored condition

A moored vessel exposed to waves, wind and current can start to ride on the waves. When the period of the waves comes close to the ships own natural oscillation frequency, the ship can be subject to uncontrollable movements, caused by resonance phenomena. These movements can, to a certain extent, be influenced by adjusting for instance the fender and mooring system or the berth orientation. Excessive vessel movement, influences cargo handling rates which means a loss in efficiency or even total disruption of the cargo transfer process. In severe cases, it may cause the rupture of mooring lines resulting in major damage to ships and port structures.

The most interesting modes of movement for a moored ship are roll, yaw, surge and sway. Although the ship is no longer a free floating vessel the natural periods of oscillation are still different for the various modes of movement; only they are now largely influenced by the fenders and mooring system, which forms, together with the ship, a multiple mass-spring system. The roll motion is the one least affected by the moorings, in other words close to that of a free floating vessel. Contrary to the roll motion, the surge and sway motions are largely governed by the elastic properties of fenders and mooring lines. Stiff moorings give short natural periods of oscillation, whilst soft moorings lead to long periods. Extreme values for third generation container or ro-ro vessels would probably be, say, 15s to 20s for hard fenders and all steel mooring lines, and 120s to 150s for Yokohama type fenders and all nylon or polypropylene mooring lines.
The yaw motion is appreciably affected by both the properties of the mooring system and the hydrodynamic characteristics of the ships. T_n will normally be in between that of the roll motion and that of the surge/sway motion.

Several authors give acceptable limiting motions for different types of moored ships, while others give acceptable wave heights at various types of berths. The fact is that the wave heights in themselves are not the limiting factor for safe mooring and safe operation, but the actual ship

motions. The expected wave heights at the berths can be calculated relatively easily through various mathematical models, but the relation between a certain wave, wind and current attack on a ship and its actual response is hard to establish. Only carefully reproduced scale models can give information about this relation. But specific information about the used fender and mooring system and the response characteristics of the expected ships at all berths has to be available. A composition of the limiting values for cargo handling operations, used by various authors[1], is presented in table 3.1. In this table it is assumed that the ships are moored with an average mooring and fendering system and that the limiting ship motions or wave heights will be exceeded before the maximum acceptable mooring line force of fender force is exceeded.

Terminal	Limiting ship motions (m or °)						Acc.
	surge	sway	heave	yaw°	pitch°	roll°	H_s
Common bulk (exp)	± 1.0	± 1.0	± 0.3	± 1.0	± 1.0	± 3.0	1.0
Common bulk (imp)	± 0.5	± 0.5	± 0.3	± 1.0	± 1.0	± 1.0	1.0
General Cargo	± 0.5	± 0.3	± 0.3	± 0.3	± 0.5	± 1.0	1.0
GenCarg/Cont/Ro-ro	± 0.5	± 0.3	± 0.3	± 0.3	± 0.5	± 1.0	0.8
Cement (exp)	± 1.0	± 1.0	± 0.5	± 1.0	± 1.0	± 3.0	1.0
Copper Smelter (exp)	± 1.5	± 0.5	± 0.5	± 1.0	-	-	1.5
Copper Smelter (imp)	± 1.0	± 0.5	± 0.5	± 1.0	± 1.0	± 1.0	1.0
Coal (imp)	± 1.0	± 0.5	± 0.5	± 1.0	± 1.0	± 1.0	1.0
Oil Products (exp)	± 1.5	± 0.5	± 0.5	± 1.0	-	-	1.5
Crude Oil Jetty (imp)	± 2.0	± 0.5	± 0.5	± 1.0	-	-	1.5
Crude Oil SBM (imp)	± 2.0	± 0.5	± 0.5	± 1.0	-	-	2.5

Table 3.1 Limiting ship motions and acceptable wave heights for cargo handling operations of moored vessels.

If the values for the limiting ship motions given in this table are accepted, there would still be a problem in determining when these limits would be exceeded. To determine these limits, the relation between a wave of a certain height and period and the consequential (moored) vessel motions must be known. Since no general rules are applicable in this situation the wave response characteristics of every expected ship must be known. It can be seen that this would be extremely difficult even if the uncertainties that already exist in the shipping forecast are ignored.

Thus, although the ship's motions are the limiting factor for a moored ship, the acceptable wave heights mentioned in the last column will be used to determine the limiting operational conditions. The last question

---

[1] The titles and the authors of the textbooks used in this literature review are presented in the reference list on page 113. The principle references used are [17], [18], [15], [12] and [16].

that has to be answered is the period-range for which the moored ships in Pipavav are expected to be sensitive. Velsink [18] gives acceptable wave heights in the period-range of 7-12s, above which the loading and unloading operations will have to be stopped. Typical surge and sway oscillations will occur for wave periods of 15-20s up to 120-150s, while roll oscillation will usually occur with wave periods between 10s and 17s. Furthermore Velsink mentions that in case of swell larger than 12 seconds a good orientation of off-shore oil terminals is a necessity.

Per Bruun [16] gives allowable maximum movements for ships with a length of 200m and over, in waves with periods between 60s and 120s.

Thoresen [17] reports that in harbours for fishing boats or small ships, the shorter periodic waves (less than about 6-8 seconds) normally determine the berthing and acceptable movement conditions for the ship. For larger ships, it is the longer periodic waves (above 20 seconds), that can cause serious movements and forces in the mooring systems. For a traditional mooring system, a typical natural period for a large ship would be one minute or more. He gives acceptable wave heights for periods up to 10s, with the note that for larger periods the values have to be reduced.

The definition of clear boundaries for safe mooring conditions, reduced cargo handling rates or evacuation criteria, is very difficult. The vessels that are expected at Pipavav range in size from 10,000 DWT product tankers to 25,000 DWT multi-purpose vessels to 60,000 DWT coal carriers. These types of vessels can be qualified as medium size. In the Pipavav situation it is assumed that the vessels will probably be most perceptive for waves in the range between 8s and 20s. Longer waves can also affect the moored vessels, but the occurrence of these longer waves is very small (see section 2.6) and they will therefore not be included in the downtime calculations.

Loading or discharging process

The type of discharging or loading process is an important determining factor for the allowable wave heights at the berth.

At liquid bulk terminals the loading and discharging is done through flexible devices like loading arms and hoses, which can tolerate rather large ship motions.
The loading of bulk commodities with continuous shiploaders also tolerates rather large ship movements. Surge motions in the order of magnitude of the length of the hold and sway motions in the order of magnitude of the width of the hold are tolerable.
The discharging procedure for bulk carriers can tolerate much less motion than the loading procedure. This is inherent to the process. First, the discharging device has to extend inside the holds and will be in contact with the cargo. And second, near the completion of the process, front-end shovels will be used in the holds to bring the cargo to the discharging device.
The loading and discharge of general cargo require that stevedores work

in the hold close to the hook of a shore crane or of ship's own gear. For discharge, forklifts are commonly used in the holds to bring cargo units to the hook. This obviously limits acceptable ship motions. These motions increasingly reduce cargo handling rates.
Loading and discharging of cellular container ships are extremely sensitive to all types of ship motion because of the small tolerances (a few inches) between horizontal dimensions of containers, which are being lowered or raised and horizontal dimensions of cell guides and cells.
Ro-ro operations are adversely affected both by ship motion and by resulting ramp motion. Only very limited motion may be tolerated.

Cargo transfer is not only hampered by waves, but also by wind and thunderstorms with heavy showers. In reference [17] and [19] it is assumed that equipment such as heavy lifting equipment for cargo and containers, loading towers and loading arms, etc., will not operate in wind speeds
stronger than about 20 m/s.
Because of the danger imposed by thunderstorms for the handling of inflammable cargo, it is recommended that loading and discharging activities be interrupted in that case.
Heavy showers can hamper the loading and discharging of bulk commodities, especially with moisture sensitive goods such as rock phosphate, because of the large open holds of bulk carriers.

Each of the mentioned cargo transfer processes has its own limiting parameters, resulting in different limiting conditions. The type of process was incorporated into the determination of the composition of the values of acceptable wave heights in table 3.1.

Leaving the berth

Under extreme meteorological conditions ships will have to leave the berth to ride out the storm outside the port. This will prevent possible rupture of mooring lines with all the damage that it may cause. It will be clear that when a ship is instructed to leave the berth, sailing conditions should be such that the ship can leave port safely. This implies that there must be an accurate weather forecast, since it is expected that safe mooring and sailing conditions will be exceeded within the next several hours. The more reliable this weather forecasting is, the less unnecessary port closure will be occur. Thoresen [17] states that when wind speeds over 10 Beaufort are expected, oil and gas tankers will normally leave the berth. If they should stay at the berth, 10 Beaufort is the approximate limit. In this case they should be ballasted and moored with emergency mooring.

Leaving the berth under normal conditions is also restricted to certain minimal conditions. When a vessel leaves port it will not have complete rudder control due to its slow starting velocity. Leaving should therefore be prohibited for wind speeds over 8 Beaufort and/or current speeds over 2 knots, unless tugboat assistance is provided and given that the conditions for sailing in the channel are not exceeded.

Other factors

Of course the above mentioned factors are not the only ones that influence the operationality of a port. Other factors such as:

* breakdown of loading or discharging equipment,
* periodical maintenance,
* traffic intensity,
* tugboat non-availability and
* calamities,

can also hamper or even completely prevent port operations.

Whether and how often the cargo transfer process is interrupted due to a breakdown of the cargo handling facilities depends on the number of connected installations (reclaimers, belts, loaders) and their respective operational reliability. The possibility of changing to a different transport line can reduce the non-availability. Manufacturers usually give an operational reliability of approximately 90%. Of course breakdown of equipment can only occur when it is used.

Periodical maintenance will usually be scheduled for the more quiet periods. In case of a high occupancy of the terminals, however, this can still lead to downtime due to maintenance.

The chance that the one-way channel is in use by another vessel or that the tugboats are not available in time, could cause some waiting time for approaching or leaving vessels.

Calamities such as cyclones passing through the area or blockage of the channel by a stranded ship are such rare events, that downtime due to calamities should only be incorporated in a peak downtime calculation and not an average, such as this one.

3.2 Limited port operations

This section describes what the specific conditions are for the Pipavav situation whereby the aforementioned port operations are limited. This is discussed by summarizing the effects per environmental condition.

3.2.1 Waves

In this section values are given for the limiting wave heights with their period(-range) that will be used in the HISWA models for the near shore and port wave climate and the SHIPMA model. Table 3.2 lists the wave height and the period range for which cargo handling operations will have to be ceased. It should be noted that the values presented in this table are high end values, so that with a more thorough investigation these limits could probably be relaxed.

Location	Limitation for	H_s (m)	T (s)
10km offshore	pilots	3.0	4-7
2km outside port	tugboats	1.5	4-7
Port basin	launches and mooring boats	1.3	4-7
Fixed oil jetty	100,000 DWT tankers	1.5	>12
SBM	100,000 DWT tankers	2.5	>12
Oil products	25,000 DWT prod.tankers	1.5	8-20
Coal terminal	60,000 DWT coal carriers	1.0	8-20
Copper Smelter Export	10,000 DWT prod.tankers	1.3	8-20
Copper Smelter Import	25,000 DWT coal carriers	1.0	8-20
Cement terminal	20,000 DWT coal carriers	1.0	8-20
Common bulk Export	30,000 DWT coal carriers	1.0	8-20
Common bulk Import	40,000 DWT coal carriers	1.0	8-20
Gen. Cargo/Cont./Ro-ro	25,000 DWT multi-purpose	0.8	8-20

Table 3.2 Operational limits with respect to waves.

3.2.2 Currents

When port operations are limited by currents is hardly described in the studied literature. The only criteria mentioned are, that the maximum drift angle tangent of a sailing ship should not exceed 0.25 and that vessels should not be allowed to leave the berth without the assistance of tugboats, with current velocities over 2 knots, and then only when the current is directed head on.

What the drift angle of the vessels is, depends on several factors, such as the type of ship (e.g. equipped with bow propellers), the sailing speed and whether or not it is assisted by tugboats. To get an indication; a vessel sailing with an actual speed of 4 knots needs a cross component of the current of ¼*4= 1 knot, to exceed the maximum drift angle tangent. Knowing that the angle of the currents and the channel axis will generally not exceed 20°, it is very unlikely that the maximum drift angle can be exceeded as a result of currents alone. In combination with a cross wind, however, it is possible. This is of course dependent on the vessel size, i.e. the lateral windage area. Investigation of the drift angle of the design ship (60,000 DWT bulk carrier) under regular and extreme conditions will be done with the nautical simulation model SHIPMA (see chapter 7).

With regard to the other criterium, it can be said that leaving the berth under these conditions is not allowed except when tugboat assistance is provided.

With respect to maximum allowable current speeds, it is assumed that

when these are exceeded the berthing or deberthing will be postponed until more favourable conditions ensue, since the currents are induced by the tide. However, this situation will rarely occur and therefore will not significantly influence the accessibility of the port.

When ships enter port during flood they will first be turned and then berthed. With ebb the procedure is reversed. This is done to always have the current head on when berthing. Ships will on the other hand never leave the port during ebb. It is not possible to keep the vessel under control with currents stern on, because it would have to give reverse power which destabilizes the ship such that not even tugboats can control it.

3.2.3 Winds

Maximum wind speeds for port operations are described more extensively and listed below:

-	boarding of pilots by air	28 m/s
-	boarding of pilots by sea	20 m/s
-	cargo handling with loading arms and towers	20 m/s
-	leaving the berth without tug assistance	19 m/s
-	sailing in the navigation channel	15-20 m/s
-	berthing for vessel with $A_{lat} < 3000$ m^2	15 m/s
-	tying up of tugboats	12-15 m/s
-	berthing for vessel with $A_{lat} > 5000$ m^2	10 m/s

A laterally projected wind area larger than 5000 m^2 is not expected for the vessels projected to arrive at Pipavav. Assuming that the winds are equally strong over the entire project area and that all vessels are obliged to call for tug assistance, then the tying up of tugboats becomes the most determining factor for sailing ships, and cargo handling berthed ships.

A wind speed of 15 m/s, or Beaufort 7, is only exceeded for about 1% of the time (see section 2.3). This means that impediment of port operations will almost never occur. In combination with currents and waves some port operations might however be affected. This will be investigated with the nautical simulation model SHIPMA (see chapter 7).

3.2.4 Water level

If unrestricted port access were provided for all vessels expected at Pipavav the channel would have to dredged to a depth of CD - draught of the design vessel - the gross underkeel clearance. On the other hand, port access for the largest vessels could be restricted, through the use of a tidal window, to a limited period of the tidal cycle. An economical optimization study of dredging costs and the costs of waiting time would determine the optimal channel depth. In Volume I it is assumed that a tidal window of 4 hours should be enough in the Pipavav situation. What the channel depth at this water level should be will be determined in chapter 8.

3.2.5 Other meteorological conditions

Port entrance and other port operations are impeded when the visibility is bad or in case of heavy showers or thunder storms. The minimum visibility for large oil tankers is 1000m-2000m, for pilot boarding this is 800m and for the other vessels and tugboats and other auxiliary craft this is 500m.

In section 2.2 is stated that the visibility is generally good at Pipavav. Mist sometimes develops just before sunrise after a calm and cloudless night. The West Coast of India Pilot gives a frequency of poor visibility, defined as less than 5 miles, of 2% in January and 35% in July.

It can be concluded that a visibility of less than 2000m will almost never occur, and that when it does, it will hardly affect the overall downtime of the port. Impediment due to heavy showers or thunder storms will neither influence the overall downtime.

3.2.6 Other factors

The remaining factors, that can cause impediment of port operations are breakdown of cargo handling equipment and periodical maintenance.

In the first phase the average occupancy is approximately 25%. This is low enough to schedule maintenance in a way that it would not affect cargo handling operations. Downtime due to breakdown would amount to approximately 9 days per year (see section 8.1).

In the second phase the average occupancy is approximately 40%. This is slightly higher than for the first phase. Now downtime due to maintenance can occur with an estimated 3 days per year. Downtime due to breakdown is estimated to have increased to approximately 14 days per year (see section 8.1).

3.3 Conclusions

It appears that the only circumstances whereby port operations are impeded are waves, a basic terminal shut down for equipment breakdown and periodical maintenance and possibly excessive wind, wave and current conditions for sailing vessels. The latter will be investigated in chapter 7. The calculation of the downtime due to waves will be determined in chapter 6.

When all factors are known, their correlation should first be established before their effects can be added to get an estimate of the total port downtime.

4 Description of mathematical models

4.1 General

As has been established in section 1.3, it is of great importance, because of its interrelated character, to obtain accurate information on the near shore and the port wave climate. Since direct wave recordings inside or near the basin of Pipavav do not exist, this information must be obtained otherwise.
Wave observations made aboard ships, plying in the region south of Pipavav have been obtained from the KNMI. Based on these observations, a deep water wave climate has been derived, which is discussed in section 2.6. This climate serves as a boundary condition for a mathematical model, with which the near shore wave climate can be calculated. This near shore wave climate, in turn, serves as a boundary condition for the calculation of a the port wave climate.

The near shore wave climate can be obtained using several techniques or calculation methods. Each of these methods will have its inherent limitations and advantages. Manual calculations can give a general impression but will always be subject to large simplifications, especially regarding the bottom schematization. On the other hand, the use of graphical and mathematical models will be more laborious. In this study the use of a mathematical model is chosen for the reason mentioned in section 1.1 (unacceptable simplification) and to obtain some skill in using such a model before starting on the, more complex, harbour model.

In general, a mathematical model of harbour wave disturbance can be used where a preliminary assessment of wave conditions is required or where a number of different harbour layouts are to be compared. A mathematical model will give information on wave activity suitable for many engineering purposes quickly and at low cost. The mathematical model approach will work particularly well in cases where the bathymetry and the geometry of the harbour are fairly simple and where the wave processes occurring in the harbour are well understood and represented in the mathematical model. For example, a mathematical model can often be used in feasibility studies or to examine and compare a number of breakwater layouts and their effect on wave disturbance.

For a more complex layout, where there are processes, which are not included in the mathematical model, or where accurate quantitative information on wave disturbance or ship movement is required, then a physical model can be used.
In this study a mathematical model approach will be incorporated. A physical model study could be part of the next phase of engineering.

As it will appear, in the course of this study, the model PORTRAY, in combination with the bathymetric complex port basin of Pipavav, was not suitable to simulate the harbour wave disturbances. That is why the wave study was repeated using the model HISWA. This chapter describes the mathematical background of both models.

The final part of this study will be the nautical investigation of the port. This will be done with the fast time simulation program SHIPMA. The theory behind this program will also be described in this chapter.

4.2 PORTRAY

The model PORTRAY is developed by Hydraulics Research Ltd., Wallingford, United Kingdom to predict storm and swell wave activity inside a harbour or marina. The acronym PORTRAY speaks for it self as it uses a technique in which rays are tracked inshore from the harbour entrance, in the direction of wave travel. For each set of wave conditions at the harbour entrance, the model will provide wave height phase and direction at all points on a specified grid. Hence, wave disturbance at a variety of mooring positions can be calculated for particular incident wave conditions in a single run of the model.

For a description on the mathematical backgrounds of the physical processes that are included in PORTRAY is referred to various textbooks such as the Shore Protection Manual [21]. The technique of ray averaging, a technique, which is used by PORTRAY to calculate the wave disturbance and at the same time smooths the rapid variation of wave height near caustics and ray crossings, a known effect of single ray methods, is described in appendix VII. The next section will roughly describe what the model stands for, how boundary conditions are implemented and what results can be produced with this model. Furthermore, this section will describe what cannot be modelled with PORTRAY and how this may affect the wave climate study.

PORTRAY is based on a ray tracking technique. Wave rays are lines everywhere perpendicular to the wave crests. As waves approach the coast and enter the harbour, height and direction of the waves will change, under the influence of several physical processes.

Among the mechanisms which redistribute energy are refraction and shoaling, due to depth variation, diffraction by breakwaters and partial or complete reflection from harbour boundaries. In addition, it can also model the effects of seabed friction and wave breaking on wave activity inside the harbour. The first four processes are always included in the calculations, the last two only when desired. PORTRAY does not include the effects of waves being generated by wind within the model area.

Wave *refraction* and *shoaling* can be shown to be governed by Snell's law, under the assumption that waves are linear and that a wave in water of local depth, will behave similarly to a wave in water of constant depth. Rays are tracked in the direction of wave propagation and the wave heights are calculated using the principle of conservation of energy between neighbouring rays. This is the principle used in PORTRAY.

The method used to represent wave *diffraction* by breakwaters is based on the Sommerfeld solution for diffraction of waves by a semi-infinite breakwater in water of constant depth. The basic idea is that the initial energy and phases of the rays representing diffraction at the breakwater

tip are determined from the far field solution to the semi-infinite breakwater problem. This leads to three sets of rays being sent out from the breakwater tip to represent diffraction. These are two sets sent out at specified intervals from the line of the shadow boundary ray, one set into the sheltered (lee side) and one into the unsheltered area and a third set of rays radiating out from the breakwater tip.

Reflection is also modelled by PORTRAY. The objects from which rays will be reflected are represented in the model by a series of straight lines, each with a separate reflection coefficient. If a ray strikes the object, i.e. the ray path intersects with one of the lines representing the object, the ray is reflected numerically.

In the model the effects of *seabed friction* may be calculated using either a linear or non-linear formulation, with a maximum wave height reduction due to bottom friction of 50%. Larsen gives a linear differential equation for bottom friction. For non-linear friction the formula due to Bretschneider and Reid is used.

Effects of *wave breaking* are taken into account in the model after the wave height has been altered by refraction, shoaling and friction. A breaking coefficient is supplied by the user.

Effects which are not represented in the model are *wind generated waves within the model area, wave overtopping* and *long period resonance*. It is not believed that these effects will have a significant influence, inside the port, in this particular case. Wind generated waves will generally be of a lower period and height (because of small fetch) and will therefore not affect traffic in and near the harbour nor moored ships at the quay side. Wave overtopping is not relevant, for the first goal is to investigate the harbour without the use of a breakwater. Long period resonance is not likely to occur in the harbour basin, because there are no enclosed water masses; the basin is bordered by flat beaches that will prevent such resonance effects.

4.2.1 Boundary conditions

The wave disturbance model built with PORTRAY is enclosed by several boundaries. One is a representation of the seabed, including the natural coastline, the next is a representation of the harbour boundaries, i.e. the actual structures, such as breakwaters and quay sides, and the third is the 'sea side' boundary from which the wave trains are simulated.

An approximation of the true topography of the study area, is required by PORTRAY. This is achieved by constructing a rectangular mesh over the area of interest and then taking the depth values at each nodal point. The model automatically divides each rectangle in two right angled triangles. The seabed beneath each triangle is assumed to have a constant slope, so the depth at any point within the triangle can be determined by linear interpolation using the depths at the vertices. The accuracy of this representation depends on the grid size and the seabed topography. The lattice of cells obtained in this manner serves as a basis for the ray

tracking subroutines of PORTRAY. As the ray leaves one cell, its position and direction become the entry conditions for its journey across the next.

An approximation to the actual layout of the harbour being studied is required so that the mechanisms of wave reflection and diffraction can be modelled. This is achieved by specifying the boundaries as a series of line segments within the grid squares. Each line segment is assigned a reflection coefficient which corresponds with the properties of the structure it is representing. In addition the connectivity of these lines to each other is also required, together with details of the points where diffraction by a breakwater tip is to be represented. The method of modelling structures allows their position to be specified accurately, avoiding a 'saw tooth' effect that can occur in other models.

Each run of the model is for a single combination of incident wave height, period and direction. Wave conditions at the model boundary may have been predicted using data from measurements, observations or a mathematical refraction model. These wave conditions will usually be specified as a significant wave height (H_s), mean zero crossing period (T_z) and mean direction, parameters representative of a certain sea state. As input to the model the RMS wave height should be specified rather than H_s. In addition, the mean wave direction at the entrance of the sector of interest is specified, together with the peak wave period and a chosen fixed water level.

The initial ray paths are now determined either in accordance with the expected behaviour of waves as they are being diffracted by a breakwater at the harbour entrance (PORTRAY's 'harbour mode'), or being sent out from an incident ray-starting line some distance offshore (PORTRAY's 'coastal mode'). The rays are then tracked forward to the entrance, considering refraction and shoaling and once they are inside the harbour again refraction and shoaling, but also diffraction by subsequent breakwaters or jetties, and reflection from other harbour boundaries are taken into account. If bed friction or wave breaking is likely to be significant their effects can also be included.

4.2.2 Stability conditions

There are some rules and restrictions as to how the boundary conditions and the data must be implemented in the model. Of these the following are discussed: the spectral character of sea states, the grid spacing, the ray density and lateral transfer of wave energy.

In order to fully represent the effects of propagation of a wave spectrum it would be possible to do many runs covering all the important period components and then combining wave heights throughout the model area, using linear superposition, to give 'spectral' wave conditions. This

work[1] has shown that a single run of the model at the peak wave period of the incident wave spectrum will normally give results that are close to those calculated from a combination of runs. This will lead to considerable savings in computer time and effort.

The grid spacing or mesh size is very important. It should be fine enough to represent the topography correctly and on the other hand it is wise to keep preparation time and calculation time within practical limits meaning a courser grid. To get an idea of the required mesh size the PORTRAY manual [25] recommends that it should be such that the depths at two adjacent grid points do not differ by more than 5% or 10%. Smallman [1] states a mesh size of the grid of 2 points per wave length, should be satisfactory. Southgate[2] [24] claims that by using a phase correction method (incorporated in the square averaging technique of PORTRAY), a square size of 2.5 wave lengths should not give an error of more than 4% in the worst case.

The ray density, i.e. the number of rays per square that are sent out from the model boundary, can also be varied. A minimum density would be 1 ray per square, this also means minimum calculation time, and a maximum would be a ray separation of 1m (100 rays per square with a mesh size of 100m). The PORTRAY Manual [25] suggest an optimum of 7 to 10 rays per smallest side of a grid square. Southgate's investigation [24] shows that a ray density of about five rays per square side was shown to give errors generally no worse than 5%.

The assumptions on which PORTRAY is based, Snell's Law and conservation of energy between neighbouring rays, bear a limitation. Diffraction, i.e. a lateral transfer of wave energy, which can be caused by rapid gradient changes in the bed, is not included in the governing assumptions of the model. This can lead to some difficulties in applying the model, particularly in areas where relatively long period waves are incident along the line of a dredged channel.

4.3 HISWA

The model HISWA is developed at the Delft University of Technology for the prediction of stationary, short-crested waves in shallow water with ambient currents. The acronym stands for HIndcast Shallow water WAves.
HISWA is a numerical model to obtain realistic estimates of wave parameters in coastal areas, lakes and estuaries from given stationary wind, bottom and current conditions. The basis of the model is parameterized version of the action balance of the waves.

---

1 The model has been extensively validated against physical models and in most situations, particularly in harbour wave disturbance studies, found to provide accurate results [1].

2 J.V. Smallman and H.N. Southgate are both attached to HR Wallingford and involved with the development of the model PORTRAY

4.3.1 The theory of HISWA

4.3.1.1 Physical background

HISWA is based on the notion of a spectral action balance, which, in the absence of a mean current, reduces to an energy balance. The energy balance approach implies, that for each spectral wave component of the wave field, the rate of energy change is equal to the net effect per unit of time of wind growth, bottom dissipation, etc. In conventional wave models one wave component is followed, across the area of interest, along its wave path (ray). During this journey the effects of wind, bottom, etc, are determined and accumulated until the wave component arrives at the location of interest. In a spectral mode this process could be repeated for all spectral components so that eventually the full two-dimensional spectrum is determined at the location of interest. However, in HISWA the procedure is somewhat different.
The technique which is used in HISWA is similar to the above described discrete spectral technique, but it differs from it in two respects; the wave field is not described with a full discrete two-dimensional spectrum and wave propagation is not along wave paths but across a grid. In HISWA the spectrum is discrete spectral in the directions and parametric in the frequencies. That is to say, in each spectral direction two quantities are propagated: a frequency-integrated energy density and a mean frequency. Both quantities vary across the geographic area. HISWA computes this variation by integrating the local effects of wind, bottom and currents while propagating, with these quantities, at the group velocity of the mean frequency, across a grid in the area of interest. HISWA has as many wave components as it has discrete spectral directions. The computations are carried out for each wave component separately on the basis of two evolution equations. The physical phenomena which are accounted for in these equations are:

- refractive and shoaling
- wind growth
- bottom dissipation
- surf dissipation and
- current dissipation.

These phenomena are addressed below. Diffraction is not taken into account.

Refractive propagation

In HISWA, wave propagation is computed for each of the above described wave components. This propagation is separated in rectilinear propagation and refraction. The first of these two gives propagation in x,y-space based on linear wave theory, including bottom and current induced shoaling. And, because energy does not propagate along a ray but across a grid, refraction is accounted for by shifting energy from one direction to another during propagation.

Wind growth

The wind induced development of the wave energy and the mean wave frequency are considered for each spectral wave direction separately and independently from other spectral directions. The formulations are taken from empirical information in an idealized situation, under the assumption that in that situation the directional energy distribution has a universal shape. Wind growth in HISWA thus includes implicitly all processes of undisturbed wave generation and dissipation. The effect of currents on wind generation is included is included by using the apparent local wind speed and direction (i.e. relative to the mean current) rather than the real wind speed and direction.

Bottom dissipation

In shallow water some wave energy is dissipated in HISWA by bottom friction. This dissipation is determined with a fairly conventional nonlinear bottom friction formulation including the effect of a mean current.

Surf dissipation and added white capping

In extremely shallow water or if a certain wave steepness is exceeded, the waves will break. The bottom induced wave breaking is called surf breaking while the steepness induced breaking is called white-capping. The corresponding energy dissipation is determined in HISWA with a bore model for those values that are higher than a certain threshold value. Only the total rate of energy dissipation is thus determined. The total energy dissipation thus obtained is proportionally distributed over the wave directions. The directional characteristics of the waves in HISWA are therefore not affected by breaking.

Current dissipation (wave blocking)

In a strong adverse current some wave energy is carried away by the current. This is energy which in a fully spectral model is carried by wave components that cannot travel against the current. This energy is removed from the wave field in the HISWA model through high frequency dissipation.

4.3.1.2 The numerical procedure

The evolution equations used in HISWA are partial differential equations of the first order with the two horizontal coordinates (x and y) and the spectral wave direction (θ) as independent variables. The dependent variables are the action density per spectral wave direction $A(x,y,\theta)$ and the mean frequency (action averaged) per spectral wave direction $f_{av}(x,y,\theta)$. The state in a point in the (x,y,θ)-space is determined only by what happens in the upwave direction of this point.

The computational region is a rectangle covered with a rectangular grid. The x-axis is chosen in the down-wave direction (i.e. roughly the mean wave direction); normal to the x-axis is the y-axis. The computation

starts at the up-wave boundary x=0 and proceeds in positive x-direction. After the states in all points on a line in y-direction have been determined, the computation proceeds with the next line in the grid.

For the propagation in x,y-space an explicit scheme is used (leap-frog), in θ-direction a fully implicit scheme is used (backward Euler). This has certain consequences. Since the numerical scheme is explicit in x,y-space, the computation is only stable under the condition that the ratio of the forward step (i.e. the step in x-direction) and the lateral step (step in y-direction) is lower than a certain limit. The stability condition is:

$$\frac{|\Delta_x \cdot c_y|}{|\Delta_y \cdot c_x|} < 1$$

where D_x and D_y are the step sizes in x- and y-direction respectively and c_x and c_y are the energy transport velocities in x- and y-direction respectively (group velocity of the mean frequency in the HISWA computations). In cases without current this is equivalent with:

$$\Delta_x / \Delta_y < \cot(\theta)$$

here θ is the discrete spectral wave propagation direction. A consequence of this is that waves can be computed only in a sector narrower than 180° (i.e. 90° to either side of the positive x-axis). For economic computations a compromise must be made between the maximum value of θ (as large as possible to have a large directional sector to encompass as much as possible of the directional energy distribution) and a large value for D_x (in order to speed up the computation).

4.3.1.3 Limitations of HISWA

The fundamental limitations of HISWA are the consequences of the assumptions and the simplifications in the mathematical model and the method of computation.

It is not possible to draw any conclusions from the computational results regarding the real shape of the frequency spectrum. The most refined comparison of HISWA results with measurements can only be done in terms of the directional energy density and the directional distribution of the mean frequency.

HISWA can only be used for waves with a relative short residence time in the area under consideration, because the basic formulations do not include time variations. Moreover the wind in HISWA is assumed to be uniform over the region.The dimensions of the computational region must therefore be small compared to the length scale of the wind field.

Diffraction is not modelled in HISWA, so HISWA should not be used in areas where wave height variations are large within a horizontal scale of a few wave lengths. Because of this, the wave field generated by HISWA will generally not be accurate immediately behind obstacles.

The forward stepping procedure in the numerical scheme of HISWA allows only waves propagating in forward direction to be computed. This precludes the computation of wave fields at large angles with each other (e.g. swell perpendicular to locally generated wind waves). It also implies that reflecting or back-scattering waves are not accounted for. It is also not possible to model any structures such as breakwaters or quaywalls which can cause diffraction or reflection.
The depth and currents must be given to HISWA before the computations are carried out. So wave set-up cannot be taken into account by HISWA in a dynamic manner.

4.3.2 Boundary conditions

For the input of a HISWA wave model various grids are needed. These grids can be divided into input grids, output grids and a computation grid. All these grids are relative to a problem coordinate system which can be arbitrarily chosen by the user, but does not have to be specified.

One of the input grids is the bottom grid, to represent the sea bottom. The finer the user makes this grid the more realistic the representation will be. A finer grid means, however, that more values have to be read in, which will cost more computation time. The bottom grid should also contain all the land values. Outside this grid HISWA interpolates to get more values if needed.
Another input grid is the one for the currents. This grid should also be fine enough to resolve relevant spatial detail. Outside the current grid HISWA assumes no currents. Wind and sea bottom friction grids only have to be provided if they are variable over space.

The computational grid must be chosen with care. Its x-axis should be more or less in the mean wave direction and the spacing should be such that the numerical stability condition is met. The upwave boundary of this grid should be located in deep water or otherwise the user has to provide the attenuated wave height and direction.

The output grids are provided by the user to get output values in areas of interest. Also output on a line or a curve can be obtained to suit the users wishes. A special kind of output grid is a nested grid which can be used when the user wants to do a detailed run of an area in which more detailed information is available or where more detailed results are required.

At the upwave boundary the incident wave conditions have to be specified. This can be done in three manners.

* As parameters with a significant wave height, the mean wave period and the mean wave direction.
* As varying across the upwave boundary of the computational grid, specified with the same parameters as above.
* As a spectrum, specified with the variance density and the action averaged frequency.

The results of the computation can be stored in a file which can provide the incident wave field for a so called nested grid.

4.4 SHIPMA

SHIPMA is a fast time simulation program, developed by Delft Hydraulics, to simulate the manoeuvring behaviour of ships, taking into account the influences of:

- the ship's manoeuvring characteristics,
- the kind of manoeuvre and desired track,
- rudder and engine actions,
- tug assistance,
- wind, waves and currents,
- shallow water and
- bank suction.

Rudder, engine and tugs are controlled by a combination of:

- a track keeping pilot,
- a tug controller and
- input data as defined by the user.

The autopilot responds to deviations from the desired track and course angle. In the case of curved tracks and changes in the current-pattern, the autopilot will anticipate on these changes, while taking into account a user defined 'anticipation distance'.

SHIPMA computes the track and course angles of the ship, the required actions from the ruder, the engine and the tugs, on time-step basis during the manoeuvre. All factors acting on the ship and the speeds, rotations and accelerations of the ship will be determined as well, and stored in output files. In addition actual water depths, current velocities, wind speeds, wave heights, tug orders, tug forces and so on, are calculated.

SHIPMA is used in port design and inland waterway studies so as to give the designer an insight into the inherent possibilities and restrictions of the vessels in relation to the infrastructure and environmental conditions.

4.4.1 Mathematical description of SHIPMA

The mathematical model of a manoeuvring ship, in the context of SHIPMA, consists of a set of equations that constitute a relationship between the ship's position and velocities on two subsequent instances of time. The momentary rudder angle and propeller rpm play an important role in these equations. This definition implies that the manoeuvring ship, which is an intrinsically dynamic system, is described as a series of system states (e.g. position, heading and velocity) on subsequent instances of time.

The hydrodynamic forces and moments acting on a manoeuvring ship can be expressed in inertia forces (added mass) and lift and drag forces (velocity dependent). The propeller and rudder forces can also be expressed in terms of lift and drag forces.

The equations of motion are of an Abkowitz [10] type.

$$(m-X_{\dot{u}})\dot{u}-m(vr+x_G r^2)=X_{vel.hydr.}+X_{wind}+X_{wave}+X_{suct}$$
$$(m-Y_{\dot{v}})\dot{v}+(mx_G-Y_{\dot{r}})\dot{r}+mur=Y_{vel.hydr.}+Y_{wind}+Y_{wave}+Y_{tug}+Y_{suct}$$
$$(I_{zz}-N_{\dot{r}})\dot{r}+(mx_G-N_{\dot{v}})\dot{v}+mx_G ur=N_{vel.hydr.}+N_{wind}+N_{wave}+N_{tug}+N_{suct}$$

ψ	=	course angle
δ	=	rudder angle
X,Y,N	=	forces and moments on the ship
m	=	mass
$X_{\dot{u}}$	=	$\frac{X\ force}{\dot{u}}$
$\dot{u},\dot{v},\dot{r}$	=	accelerations
u, v, r	=	velocities
x_G	=	centre of gravity
$X_{vel.hydr.}$	=	velocity-dependent part of hydrodynamic force
I_{zz}	=	mass moment of inertia

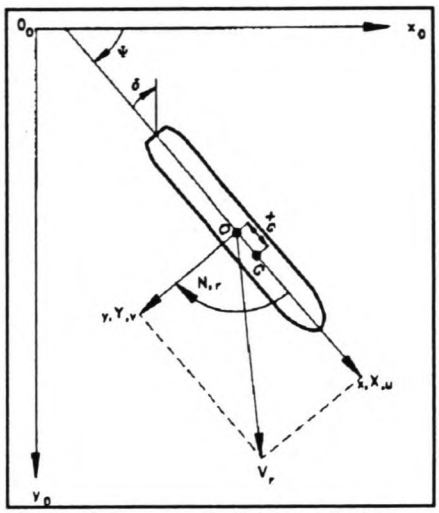

Figure 4.1 Definition of ship-fixed co- ordinate system (x,O,y) and earth fixed system (x_0,O_0,y_0)

The equations are solved numerically on a time-step basis. A predictor-corrector method is applied to compute the new velocities and the new position and course angle.
The left-hand side of the equations of motion of the manoeuvring vessel contain the forces and moments according to Newton's law and the hydrodynamic inertia forces. The right-hand side contains the velocity-dependent hydrodynamic hull forces, propeller and rudder forces and external interaction forces such as wind, waves, tug and bank suction forces.

4.4.2 A birds-eye view of a SHIPMA simulation run

Lots of data must be entered into SHIPMA, before a proper simulation run can be carried out. This information is stored in a set of input files. These input data can be distinguished in three categories:

i. Information about the ship itself, such as:
- ship's dimensions, windage areas, wind angles, wind coefficients,
- ship's hydrodynamic coefficients ('mathematical' ship model),

ii. Information regarding external impacts on a ship affecting the manoeuvre, such as:
- wave field and wave force coefficients,
- bottom schematization,
- wind field,
- current-pattern and water level,
- position of the banks and bank suction coefficients,

iii. General run information and manoeuvring tactics, describing how to perform the desired manoeuvre with regard to a preconceived plan and the environmental demands and restrictions. Preferably this plan should be based upon interviews with local pilots. Items are:
- identifications, desired track and other track data, start values, time-step, stop criterion, kind of manoeuvre and autopilot setting,
- number of tugs, bollard pull forces and tug controller coefficients and
- selection of the required output data.

The mathematical ship model consists of an extensive series of coefficients per loading condition and per h/T (depth/draught ratio). So, for one ship several models can be necessary. These sets of coefficients are determined by both small-scale and full-scale manoeuvring tests. The file, containing these coefficients, holds two sets of coefficients, each for a specified h/T ratio. SHIPMA interpolates the values of coefficients within the h/T interval.

After a successful run a numerical output file is produced and the graphical representations of the results can be made. Thus, it can be investigated if and when maximum rudder and engine power bursts were necessary. Also the tug orders from the tug controller can be looked at to be able to judge the degree of difficultly of the desired track under the given circumstances.

5 Determination of the near shore wave climate

5.1 General

In this chapter the near shore wave climate will be determined. Several techniques may be used in this determination. Three of these will be dealt with below.

First, the near shore wave climate will be assessed using 'manual' calculations. These calculations have been made using a spreadsheet with formulas based on Snell's law, assuming no dissipation and straight parallel depth contours. This method is used to get a first estimate and can also be used as a comparison and validation of the mathematical models.

The second technique used is a mathematical model, named PORTRAY. This model uses a ray tracking technique, combined with a ray averaging technique, to predict wave height, period and direction at designated points on a specified grid. The reason to use a mathematical model was that the manual calculations would introduce to big a degree of uncertainty due to the schematization of straight parallel depth contours.

The third determination will be done using another mathematical model, named HISWA. This is a numerical model which calculates the wave propagation across a grid. This model was used after the validation of the port model results with PORTRAY were found to be too unreliable.
The theory behind the mathematical models is described in chapter 4.

5.2 Manual calculations

The principal physical processes that influence the waves as they travel towards the shore, are refraction and shoaling. Under the assumption of conservation of energy and conservation of wave crests, the ratio of the local wave amplitude and the deep water wave amplitude is described by:

$$\frac{a}{a_o} = \left(\frac{c_{g_o}}{c_g}\right)^{1/2} \left(\frac{\delta b_o}{\delta b}\right)^{1/2} = K_s K_r$$

where K_s and K_r are the shoaling and the refraction factor. While K_s only depends on the wave number (k) and the water depth (h), K_r depends on the bottom topography, the water level, the frequency and the angle of incidence and will have to be determined in every single case.

When we simplify the problem to the two-dimensional situation with straight parallel depth contours the equation can be reduced to:

$$\frac{a}{a_o}=\left(\frac{c_{g_o}}{c_g}\right)^{1/2}\left(\frac{\cos\theta_o}{\cos\theta}\right)^{1/2}=K_s\left(\frac{\cos\theta_o}{\cos\theta}\right)^{1/2}$$

in which θ is the angle of incidence.

Now there exist a simple relation between the deep water wave height and the wave height at any depth offshore. This relation was used in calculations for the near shore wave climate (ignoring wave breaking).
Looking at the offshore depth contours of Pipavav (see figure 5.1) it is possible to schematize the depth contours as parallel lines with a normal at 180° (south), realizing that the deep water condition for the major part of the waves is located at a depth of 50m or less. Calculations of the wave heights at a depth of 10m offshore at a water level of CD +2.00m were performed, using the adapted deep water wave climate as described in section 2.6.1. The results are represented in table 5.1. In this table the wave heights and periods are divided in sea and swell. Calculations of the attenuated wave height and the refracted direction have been made for waves coming from 180°(S), 210°(SSW) and 240°(WSW) bearing. Also the ratio between the deep water wave and the attenuated wave is presented as the product of K_r and K_s. One can see that this scaling factor decreases for longer waves and that it decreases more rapidly for waves with a larger angle of incidence to the normal. It starts to increase, however, for wave periods longer than 9s. This can be explained as follows. Longer waves are refracted stronger than shorter waves, explaining why the scaling factor decreases at first. The simplified equation can be rewritten as:

$$\sin\theta=\sin\theta_o\tanh(kh)=\sin\theta_o\tanh\left(\frac{2\pi h}{L}\right)$$

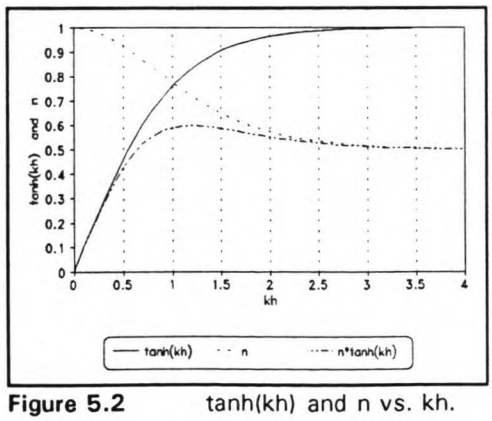

Figure 5.2 tanh(kh) and n vs. kh.

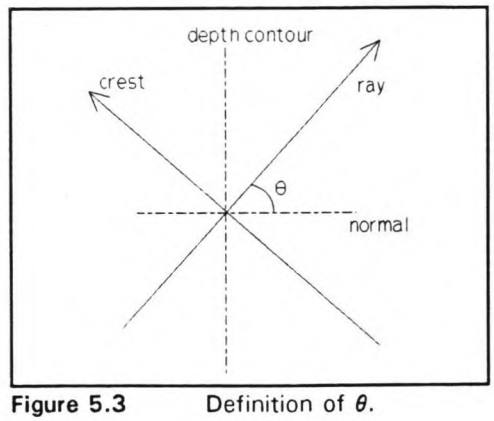

Figure 5.3 Definition of θ.

Using the definitions in the figures above it can be seen that, when the length of the wave increases, the fraction decreases, tanh decreases and sin(θ) decreases. A smaller θ means a larger refraction, which results in a smaller refraction coefficient. K_s depends on the ratio of the group velocities and can be rewritten as:
As can be seen from the figure above the product of n and tanh(kh) increases at first but starts to decrease when the water gets more

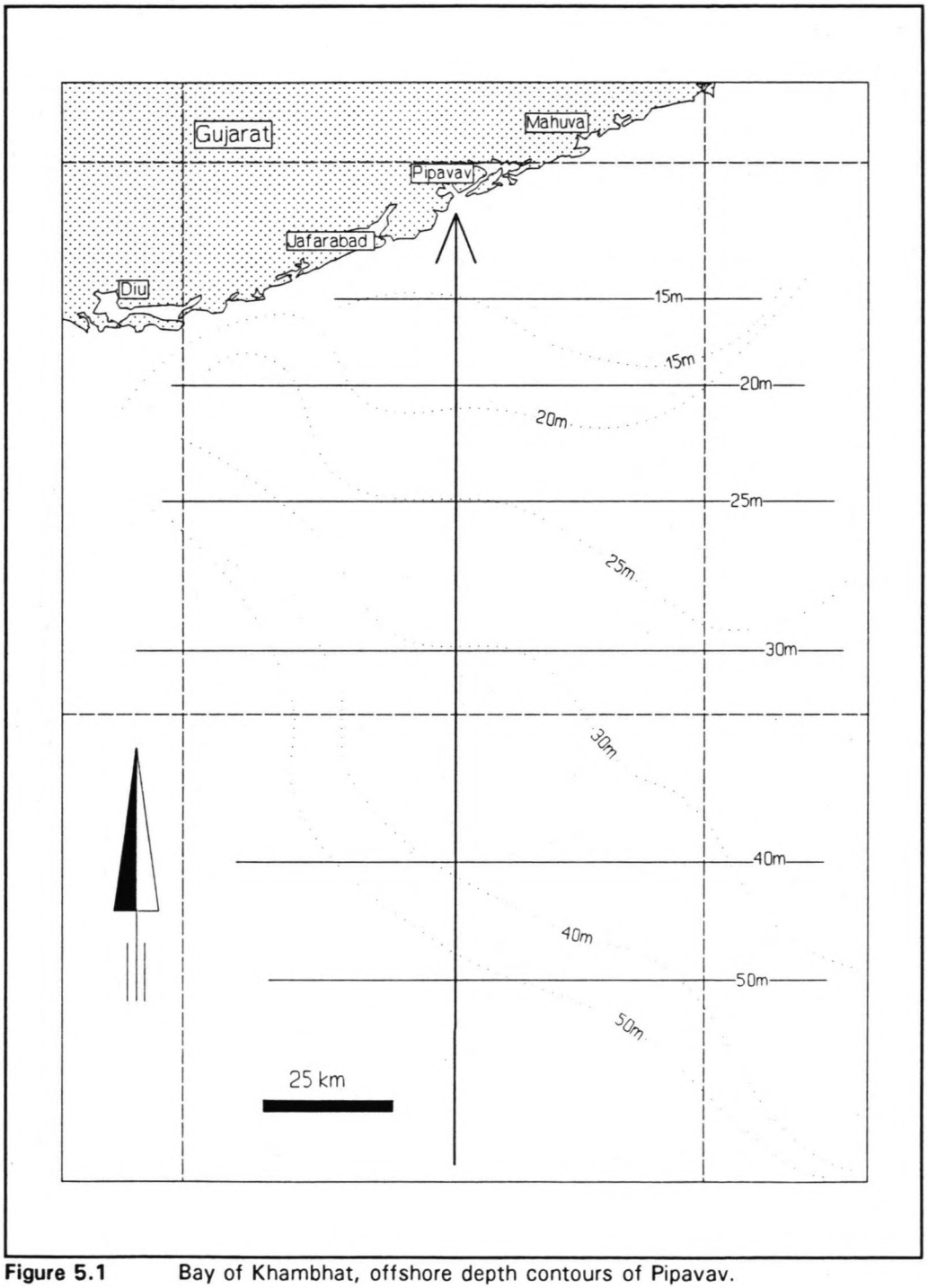

Figure 5.1 Bay of Khambhat, offshore depth contours of Pipavav.

$$K_s = \sqrt{\frac{1}{2n\tanh(kh)}}$$

shallow; at a value of $kh \approx 1.3$, or with a water depth of 12m, for $L \approx 75$m. This means that K_s slowly increases for wave periods larger than 6.5s. This explains the increase of the scaling factor for the higher periods.

Deep water		180°			210°			240°		
Hs	T	H,att	alpha	Kr*Ks	H,att	alpha	Kr*Ks	H,att	alpha	Kr*Ks
Sea for April to September										
0.5	3.0	0.50	180	1.00	0.50	210	1.00	0.50	240	1.00
1.0	4.0	1.00	180	1.00	0.99	210	0.99	0.98	240	0.98
1.5	5.0	1.47	180	0.98	1.42	209	0.95	1.36	237	0.91
2.0	6.0	1.96	180	0.98	1.82	207	0.91	1.65	231	0.82
2.5	6.5	2.46	180	0.98	2.24	206	0.90	1.99	229	0.80
3.0	7.0	2.98	180	0.99	2.67	205	0.89	2.32	226	0.77
3.5	7.5	3.51	180	1.00	3.11	203	0.89	2.66	223	0.76
4.0	8.0	4.06	180	1.02	3.56	202	0.89	3.00	221	0.75
4.5	8.5	4.63	180	1.03	4.03	201	0.89	3.35	219	0.74
5.0	9.0	5.22	180	1.04	4.50	200	0.90	3.71	217	0.74
5.5	9.5	5.83	180	1.06	5.00	199	0.91	4.08	215	0.74
6.0	10.0	6.46	180	1.08	5.50	199	0.92	4.46	214	0.74
6.5	12.0	7.45	180	1.15	6.24	196	0.96	4.95	208	0.76
Swell for April to May										
1.0	7.5	1.00	180	1.00	0.89	203	0.89	0.76	223	0.76
1.5	7.5	1.50	180	1.00	1.33	203	0.89	1.14	223	0.76
2.0	8.5	2.06	180	1.03	1.79	201	0.89	1.49	219	0.74
Swell for June to September										
0.5	8.0	0.51	180	1.02	0.45	202	0.89	0.37	221	0.75
1.0	8.5	1.03	180	1.03	0.89	201	0.89	0.74	219	0.74
1.5	9.0	1.57	180	1.04	1.35	200	0.90	1.11	217	0.74
2.0	9.5	2.12	180	1.06	1.82	199	0.91	1.48	215	0.74
2.5	9.5	2.65	180	1.06	2.27	199	0.91	1.73	215	0.69
3.0	9.5	3.18	180	1.06	2.73	199	0.91	2.22	215	0.74
3.5	10.0	3.77	180	1.08	3.21	199	0.92	2.60	214	0.74
4.0	11.0	4.44	180	1.11	3.75	197	0.94	3.00	211	0.75
4.5	10.5	4.92	180	1.09	4.17	198	0.93	3.36	212	0.75
5.0	12.0	5.73	180	1.15	4.80	196	0.96	3.81	208	0.76

Table 5.1 Calculation of wave heights and directions at CD -10m in front of the port entrance, for deep water waves from 180°, 210° and 240° with the manual method.

5.3 PORTRAY simulations

For reasons explained in section 1.1 a mathematical model was built for the determination of the near shore wave climate. The mathematical model used is the ray tracking model PORTRAY.

For this model, the offshore bottom topography was translated into a grid to represent the sea bottom. As incident wave field the adapted deep water wave climate from section 2.6.1, will be used. As a consequence hereof the bottom grid has to extend sufficiently far offshore to provide deep water conditions for the longest wave. The minimum provided 6water depth, on the grid used in the offshore model, is about 52m. The error made for the longest wave of 225m (12s) is:

$$1-\tanh\left(\frac{4\pi^2 h}{gT^2}\right) = 1-\tanh(1.45) = 1-0.896 = 0.1 \quad (10\%)$$

For a wave of 10s this is already reduced to 3%. Since these waves hardly occur (waves with periods higher than 10s occur only 10 days per year) this error is accepted.

The orientation of the grid was chosen such that both waves from 240° as waves from 150° would not make too large an angle with the x-axis (a requirement for PORTRAY simulations). This resulted in an orientation of the x-axis of 126° bearing. The width of the bottom grid had to be such that waves coming from 150° up to 240° would be able to reach the site. This resulted in a grid with dimensions 150 x 187.5 km^2.

For the mesh size of the bottom grid various suggestions are done (see section 4.2.2). The most realistic (Southgate) [24] suggestion claims that a square size of 2.5 wave lengths should be enough. The reason why these grid requirements are so strict is that the bottom grid is used as computation grid. A finer grid means more accuracy of the results.

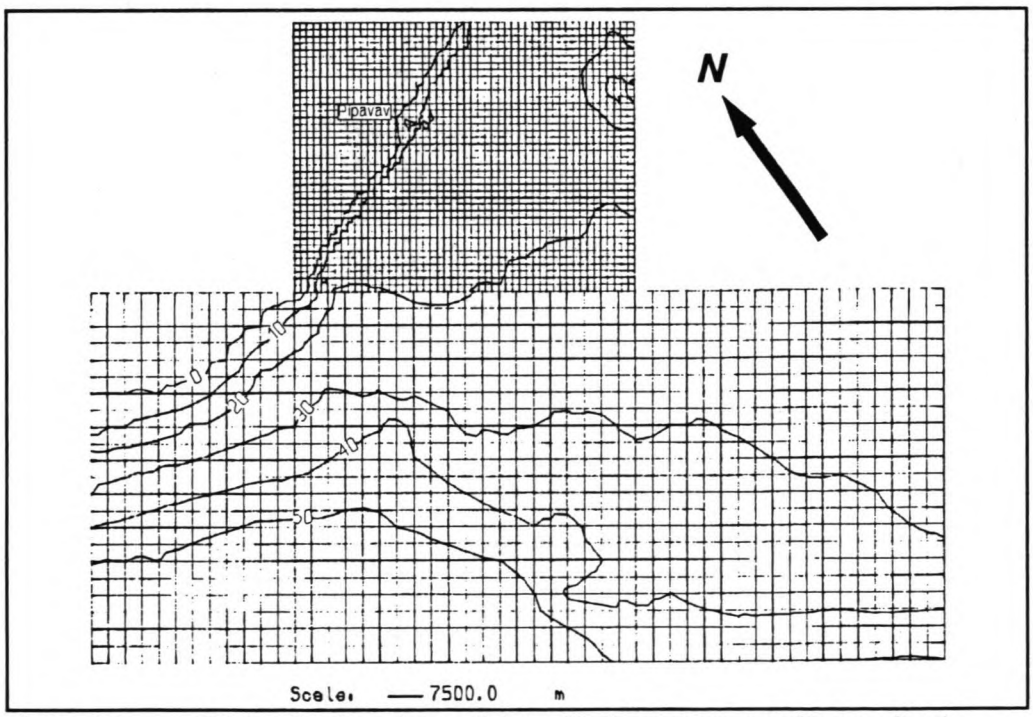

Figure 5.4 Schematization of the offshore depth contours near Pipavav for the determination of the near shore wave climate with PORTRAY.

In the Pipavav case this would mean a mesh size varying from 2.5 * 40m (5s) = 100m to 2.5 * 225m (12s) = 560m, depending on the period of the incident waves. Using the available depth charts [5] this would mean a mesh size of 0.13mm-0.75mm and 90,000-2,800,000 grid points. Such a small mesh size is not possible when the bottom grids are prepared manually. Besides that, the maximum number of grid points possible with PORTRAY is 40,000, or a meshsize (in this case) of 850m. When the map of the offshore seabed is digitized, using specially designed programs, any desired resolution is possible. This will result, however, in much longer calculation time, because more values have to be processed each run. The best manual approximation that could be

realized, consisted of two integrated grids. The first part (up to the 20m depth contour) had a mesh size of 3750m and the second part (from the 20m contour to the entrance of the port) had a mesh size of 1500m (see figure 5.4). The latter meant a square size of 0.5cm on the largest available chart. The computation time for one run varied between 0:45 min and 1:10 min, depending on the angle of incidence and the ray density. The estimated computation time for a grid consisting of 40,000 grid points is 3:00 minutes per run.

The last variable for PORTRAY is the ray density, i.e. the number of rays per square that is sent out from the model boundary. Again several suggestions are made by various authors. Suggestions varied from 5 to 10 rays per square as an optimum between accuracy and calculation time. The results did not improve with an increased ray density, in the sense that this would result in a more stable wave pattern, as can be seen from figure 5.5. To save computation time, a density of 10 rays/square was used. A listing of the control files used for the offshore calculations can be found in appendix VIII.

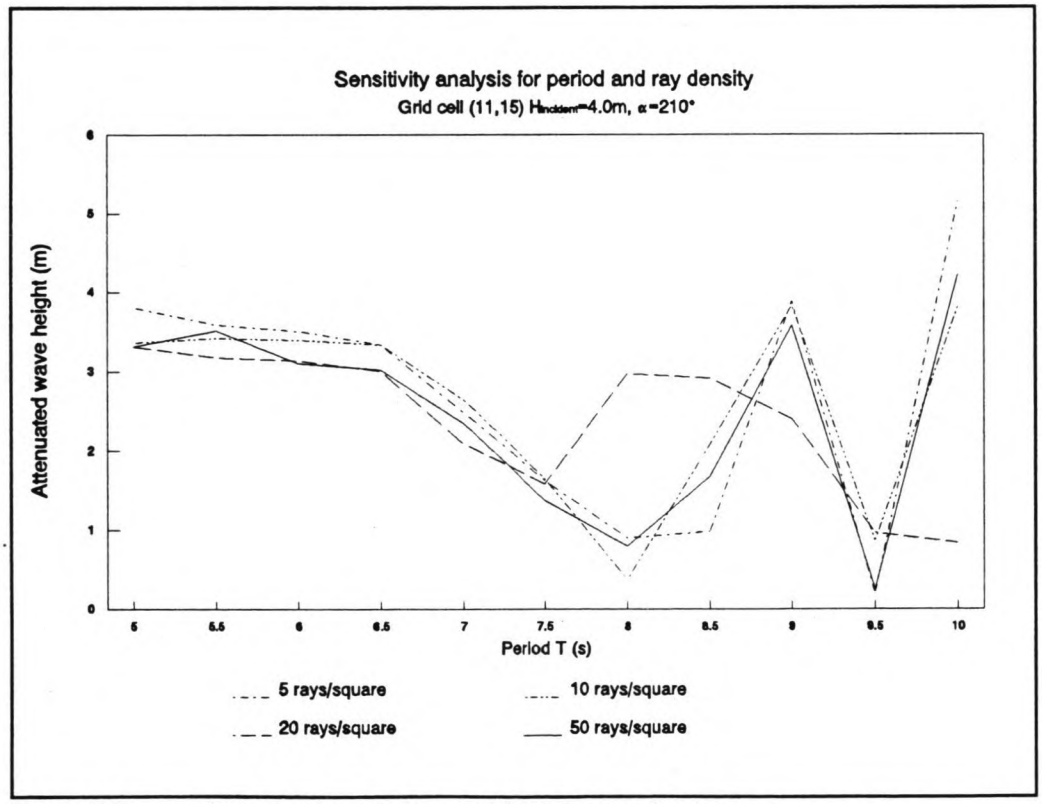

Figure 5.5 Investigation of the sensitivity for ray density.

The physical processes accounted for in the PORTRAY simulations are refraction, shoaling and wave breaking. Bottom friction was not incorporated, because frictional effects of a reasonably steeply seabed can be neglected.

The results of the offshore run were needed as input values for the port disturbance model. The results for a number of cells, at a depth of about 10m, near the entrance to the port, were stored. The results are presented in table 5.2.

Deep water		180°			210°			240°		
Hs	T	H,att	alpha	Kr*Ks	H,att	alpha	Kr*Ks	H,att	alpha	Kr*Ks
Sea for April to September										
0.5	3.0	0.41	180	0.81	0.43	209	0.87	0.29	237	0.58
1.0	4.0	0.80	178	0.80	0.67	208	0.67	0.70	229	0.70
1.5	5.0	1.13	178	0.76	1.32	205	0.88	0.99	229	0.66
2.0	6.0	1.51	176	0.75	1.68	202	0.84	1.37	222	0.69
2.5	6.5	1.93	178	0.77	2.07	202	0.83	1.63	224	0.65
3.0	7.0	2.33	174	0.78	2.50	200	0.83	1.96	217	0.65
3.5	7.5	2.70	178	0.77	2.64	198	0.75	2.36	212	0.68
4.0	8.0	3.08	179	0.77	3.36	204	0.84	2.70	213	0.67
4.5	8.5	3.45	181	0.77	3.77	200	0.84	2.98	142	0.66
5.0	9.0	3.68	183	0.74	4.08	207	0.82	3.30	210	0.66
5.5	9.5	3.97	178	0.72	4.38	205	0.80	3.62	203	0.66
6.0	10.0	4.19	175	0.70	4.63	200	0.77	4.03	202	0.67
6.5	12.0	4.41	184	0.68	4.83	198	0.74	4.23	207	0.65
Swell for April to May										
1.0	7.5	0.75	184	0.75	0.59	208	0.59	0.47	212	0.47
1.5	7.5	1.12	184	0.75	0.89	208	0.59	0.71	212	0.47
2.0	8.5	1.87	188	0.94	1.06	211	0.53	1.35	213	0.68
Swell for June to September										
0.5	8.0	0.22	181	0.43	0.49	198	0.98	0.31	213	0.62
1.0	8.5	0.65	179	0.65	0.91	200	0.91	0.65	213	0.65
1.5	9.0	1.08	178	0.72	1.36	207	0.90	0.93	210	0.62
2.0	9.5	1.46	180	0.73	1.80	205	0.90	1.29	203	0.65
2.5	9.5	1.90	180	0.76	2.24	205	0.90	1.73	203	0.69
3.0	9.5	2.27	180	0.76	2.66	205	0.89	2.15	203	0.72
3.5	10.0	2.65	183	0.76	3.09	0	0.88	2.63	202	0.75
4.0	11.0	2.96	184	0.74	3.47	202	0.87	3.07	202	0.77
4.5	10.5	3.28	176	0.73	3.83	201	0.85	3.40	203	0.76
5.0	12.0	3.51	183	0.70	4.23	197	0.85	3.54	202	0.71

Table 5.2 Calculation of the wave heights and directions at CD -10m for deep water waves from 180°, 210° and 240° with PORTRAY simulations.

As can be seen the same effects, i.e. the increase and decrease of the scaling factor, as for the manual method occur for the results of PORTRAY. The attenuation of the waves is just stronger than for the manual method.

The difference between the two methods can be explained by the fact that the breaking of waves is incorporated in the PORTRAY model. Furthermore the depth contours off the coast of Pipavav are slightly concave shaped. This means that the ray separation after refraction will be stronger than would be modelled with straight parallel depth contours. Or, the schematization, used in the manual method, was an underestimate. A further discussion on the results can be found in section 5.5.

5.4 HISWA simulations

The third determination of the offshore climate was done with the numerical model HISWA. This model calculates wave heights and directions across a grid instead of along a ray.

As input for the bottom grid the same files were used as those used for PORTRAY. The incident wave field was defined as a significant wave height with a mean wave period and a mean wave direction. For ease of comparison the same adapted wave field was used as the one used for PORTRAY and the manual calculations.

The only variable left was the fineness of the computational grid. After some experimenting it showed that no significant improvement could be reached for grid finer than 160 lines. To save calculation time[1], this was reduced to 80 lines. This is acceptable because the results obtained with the HISWA simulations for the adapted wave climate are just used for comparison of the various methods and not relevant in the determination of the port downtime. For this the approach will be somewhat different as will be described in chapter 6.

In the HISWA simulations of the near shore wave climate, the physical processes that are accounted for are, refraction and shoaling and surf dissipation. Current blocking and wind growth were not included in the simulations. The influence of wind on wave growth is very small in this case (approximately 5%) and the net result of ebb increased and flood decreased wave heights is zero.

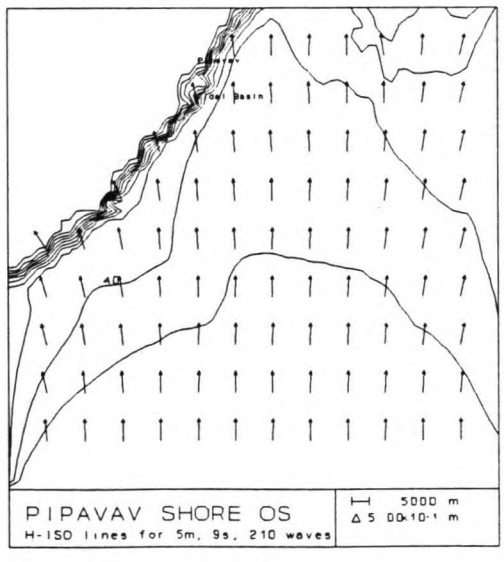

Figure 5.6 HISWA run with the offshore model.

The results of the HISWA simulations for the near shore wave climate are presented in table 5.3. A plot showing the iso-lines of H_s and the direction of energy transport is presented in figure 5.6. The direction of energy transport is same as the wave direction in the absence of currents, which is the case here. From the plot can also shows the disturbed regions at the edges of the computational grid. These regions originate due to an import of zero energy from the lateral boundaries. This is the reason that the computational grid has to be extended sufficiently to the left and the right to make sure that these regions do not influence the location of interest.

---

1 The reduction of computation time was approximately 3 minutes per run.

Deep water		180°			210°			240°		
Hs	T	H,att	alpha	Kr*Ks	H,att	alpha	Kr*Ks	H,att	alpha	Kr*Ks
Sea for April to September										
0.5	3.0	0.42	181	0.84	0.39	203	0.77	0.31	221	0.62
1.0	4.0	0.80	180	0.80	0.74	203	0.74	0.60	220	0.60
1.5	5.0	1.16	179	0.77	1.00	203	0.67	0.84	216	0.56
2.0	6.0	1.54	178	0.77	1.30	201	0.65	1.03	213	0.51
2.5	6.5	1.92	179	0.77	1.62	200	0.65	1.26	211	0.50
3.0	7.0	2.32	180	0.77	1.94	200	0.65	1.49	210	0.50
3.5	7.5	2.75	180	0.79	2.28	198	0.65	1.72	209	0.49
4.0	8.0	3.20	181	0.80	2.65	196	0.66	1.97	208	0.49
4.5	8.5	3.61	182	0.80	3.04	195	0.67	2.25	208	0.50
5.0	9.0	3.96	184	0.79	3.41	195	0.68	2.54	207	0.51
5.5	9.5	4.16	185	0.76	3.76	195	0.68	2.82	207	0.51
6.0	10.0	4.28	186	0.71	3.96	195	0.66	3.09	207	0.52
6.5	12.0	4.52	187	0.70	4.25	196	0.65	3.53	207	0.54
Swell for April to May										
1.0	7.5	0.81	178	0.81	0.67	199	0.67	0.50	209	0.50
1.5	7.5	1.21	178	0.81	0.98	199	0.65	0.75	209	0.50
2.0	8.5	1.71	179	0.85	1.35	199	0.68	0.98	208	0.49
Swell for June to September										
0.5	8.0	0.41	179	0.83	0.34	199	0.67	0.26	207	0.52
1.0	8.5	0.85	179	0.85	0.69	198	0.69	0.50	208	0.50
1.5	9.0	1.32	179	0.88	1.03	198	0.69	0.76	207	0.50
2.0	9.5	1.81	179	0.90	1.41	198	0.70	1.00	208	0.50
2.5	9.5	2.21	181	0.88	1.75	198	0.70	1.25	208	0.50
3.0	9.5	2.62	181	0.87	2.10	198	0.70	1.50	208	0.50
3.5	10.0	3.13	182	0.89	2.50	196	0.72	1.77	207	0.51
4.0	11.0	3.68	183	0.92	2.99	194	0.75	2.09	207	0.52
4.5	10.5	3.94	184	0.88	3.28	194	0.73	2.35	207	0.52
5.0	12.0	4.35	187	0.87	3.79	195	0.76	2.73	206	0.55

Table 5.3 Calculation of the wave heights and directions at CD -10m, near the entrance to the port, for deep water waves from 180°, 210° and 240° with HISWA simulations.

The results show, in almost all cases, smaller scaling factors for HISWA results than for PORTRAY and the manual method. The mean wave direction is generally closer to the original angle of incidence than for PORTRAY and the manual method, indicating a stronger refraction for the waves simulated with HISWA, although the difference is very small; in the range of 1 to 5°. The difference between the various methods is discussed in section 5.5.

5.5 Discussion and comparison of results

The graphs below show the results of the calculations of the near shore wave climate with the manual method versus PORTRAY and versus HISWA. Calculations have been made for three direction i.e. 180°, 210° and 240° bearing. For each direction distinction is made between sea waves (the same for both the Hot season and the SW monsoon) and swell waves for April-May (Hot Season) and June-September (SW Monsoon).

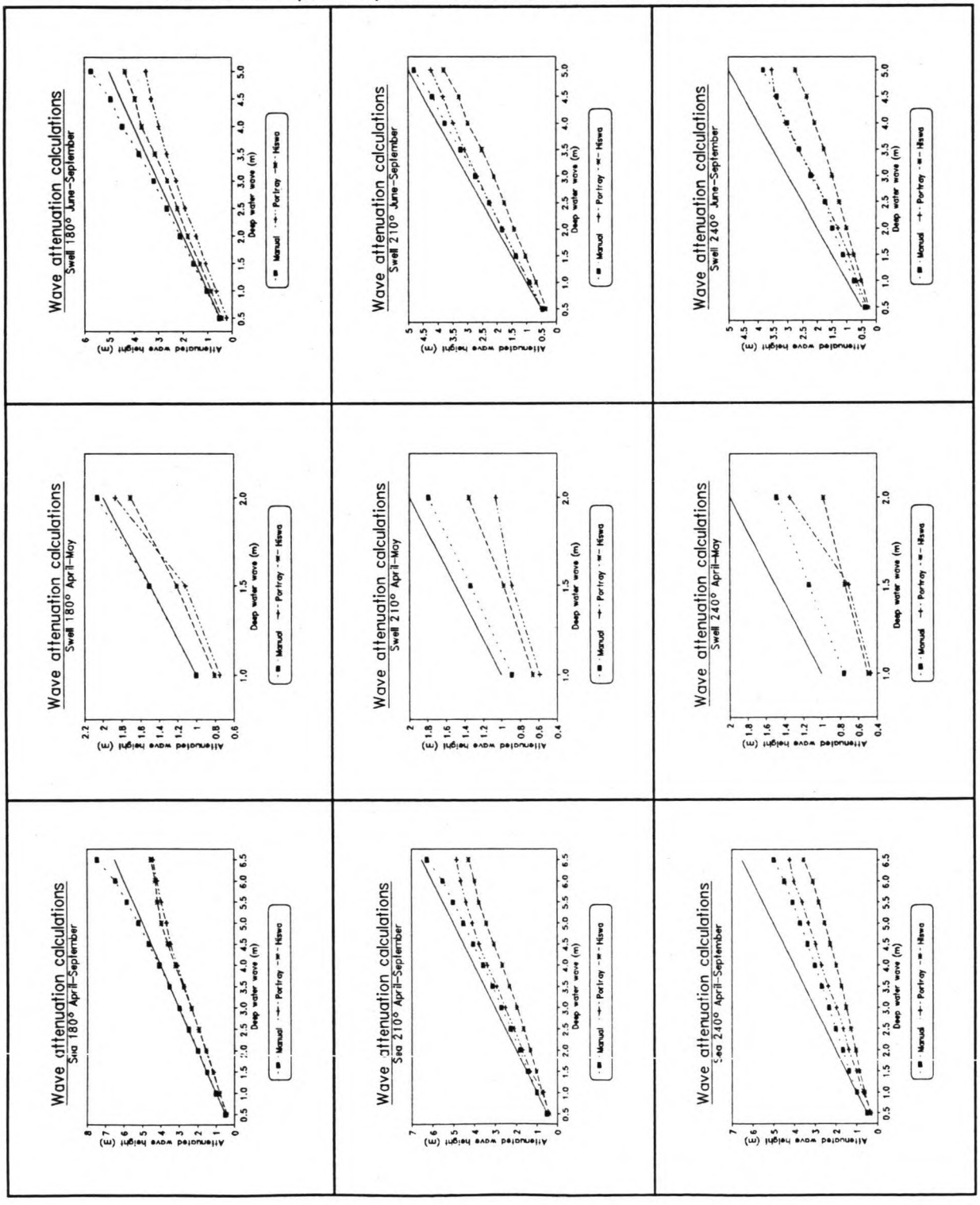

Several conclusions can be drawn from the results of the simulations.

1. If the bottom grid must be prepared manually, a translation of the deep water wave climate to a near shore wave climate, can become complicated, when the deep water boundary lies relatively far offshore.

2. In general, the HISWA simulations produce somewhat lower results, both in the wave height and in the refracted angle, than those of the manual method and the PORTRAY simulations.

3. HISWA simulations are very regular over the whole output boundary, contrary to the PORTRAY results, which show a large diversion between the various output cells as well as over the complete range of the adapted wave climate.

The problem indicated in the first conclusion can be solved by digitizing the bottom. This way, any desired meshsize is possible. This is limited however, to 40,000 grid points. It has to be noted that although PORTRAY was not written for translating a deep water wave climate over very large distances, it is possible. It was mainly intended for testing different port layouts, with one main breakwater.

The second conclusion indicates that during the HISWA runs more wave energy was dissipated than during the PORTRAY runs. The difference must be sought in the different ways that wave breaking is modelled, this being the only dissipation accounted for in both models.
PORTRAY works as follows. After the wave height has been altered by refraction and shoaling the dissipated energy is taken as the energy of the waves above H_B, the breaking wave height, multiplied by the breaking coefficient. HISWA, on the other hand, integrates the energy dissipation in the propagation of the waves across the grid.
The difference between these methods illustrates that PORTRAY calculations can underestimate the energy dissipation due to breaking, resulting in general higher wave heights.

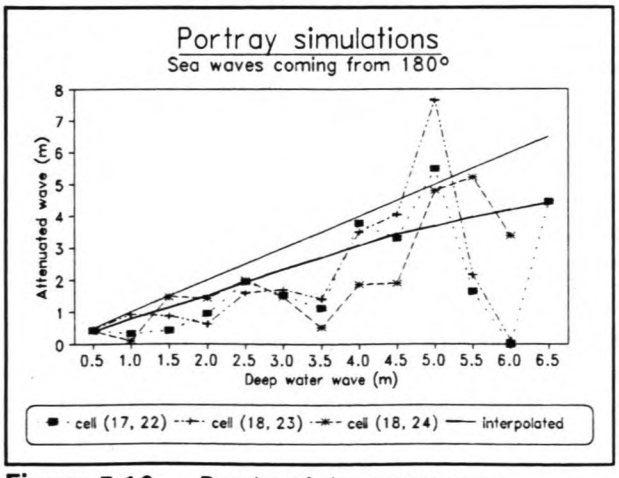

Figure 5.16 Results of the portray runs.

The third conclusion is illustrated below.
During a PORTRAY run, output is given in the centre of every cell of the bottom grid. Due to the coarseness of the grid this meant that the CD -10m depth contour, in front of the port, was represented by just three cells (i.e. cell 17,22 18,23 and 18,24). In figure 5.16 it can be seen that the results between the different cells can vary significantly. Also

Hiswa run H_s = 5.0m, T = 9.0s, Dir = 180°	
H_s (m)	Dir (°)
4.14	186.14
4.14	185.83
4.13	185.52
4.11	185.33
4.09	185.14
4.07	184.94
4.05	184.73
4.03	184.53
4.01	184.31
3.99	184.10
3.97	183.88
3.95	183.65
3.92	183.43
3.90	183.19
3.88	182.95
3.86	182.71
3.84	182.46
3.82	182.21
3.80	181.95
3.77	181.69
3.75	181.42
3.96	183.81

Table 5.4 Output for a HISWA run.

the results in total, are not regularly increasing as the deep water wave height (and period) increases. Especially for waves with periods longer than approximately 8.5s (H = 4.5m), the results become very irregular. The solid line in the figure is a graphical interpretation of the three separate lines of the three cells. This is the line that was used in the tables and the graphs of PORTRAY.

In HISWA the output is produced differently. During a HISWA run, output can be requested on specific locations. Independent from the mesh size of the bottom grid or the computational grid HISWA gives interpolated values of the wave height and the direction, see table 5.4. It can be seen that the values vary along this 6 km long output location, but certainly not as strong as for the PORTRAY run. Moreover the increase of the attenuated wave heights is just as gradual as the increase of the deep water wave height. The graphs at the beginning of this section show this. The interpolation procedure is very different from what was used for the PORTRAY results. The results of a HISWA run do not depend on the meshsize of the bottom grid, but on the meshsize of the computation grid. The latter can be increased independently from the bottom grid, attaining any desirable accuracy.

It has to be concluded that PORTRAY is less suitable as a program to calculate wave propagation over such a large foreshore area, particularly for the longer wave periods. This is a consequence of the limited number of grid points of the bottom and the computation grids. It has to be said that this program was not meant for foreshore calculations, but more specific for port basin calculations.

The results obtained with HISWA simulations, are more reliable and therefore more satisfactory. This is, because HISWA was specifically written to calculate wave attenuation on gently sloping seabeds. The validity of the results, however, can not be examined, because no observations or measurements of the near shore wave climate are available at this time.

6 Determination of the port wave climate

6.1 General

In this chapter the wave climate inside the port, known as the port wave climate, will be determined. The purpose of building a port wave climate simulation model is to be able to answer the question: 'How many times per year is a certain wave height of a certain period exceeded in front of the terminals, in the channel and at several offshore locations ?'.
This is part of the suitability investigation, stated in the main objective. To accomplish this, two models are constructed.

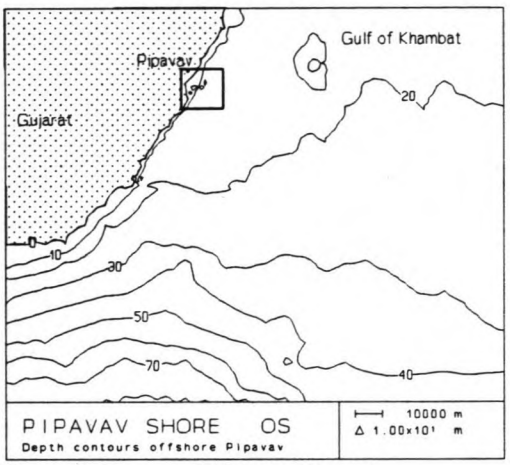

Figure 6.1 Offshore Pipavav.

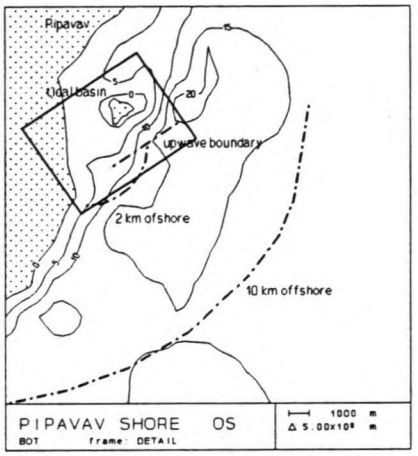

Figure 6.2 Entrance to port.

The first of these models is the offshore model, constructed to translate the deep water wave climate to a wave climate along the perimeter of the port area. The second model is the port model, that translates the near shore wave climate to wave conditions inside the port. The two models are linked together through an output location in front of the port in the offshore model that is the upwave boundary in the port model (see also figures 6.1, 6.2 and 6.3). Before the port wave model will be presented, a description will follow of a physical model of the Pipavav Port, that was built in India. This model can be used in validating the mathematical models.

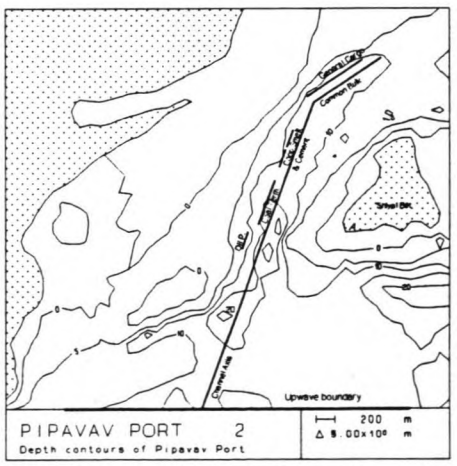

Figure 6.3 Pipavav Port, phase II.

Although the results with the near shore wave model built with PORTRAY were not very reliable, still the two mathematical models, PORTRAY and HISWA, will be used to construct a port wave model. The validation of the models will determine which will finally be used in the determination of the port downtime due to waves.

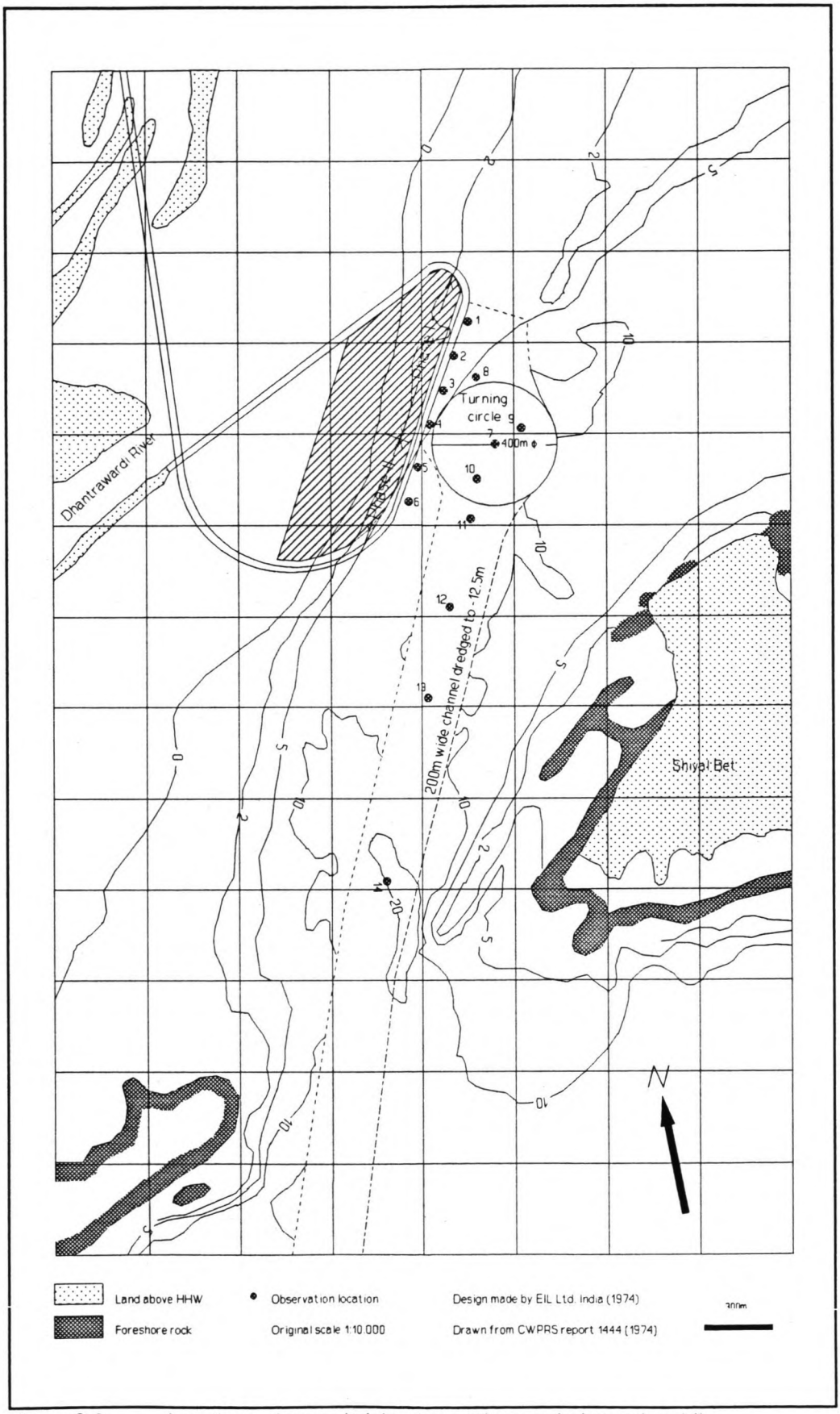

Figure 6.4 Locations of wave height observations and phases I and II.

6.2 Physical model

Validation is an important part in the process of constructing a simulation model. Validation can be done e.g. through comparison of the simulation results with (historic) measurements under similar circumstances.

No measurements of any kind are available for the validation of the port wave model, nor the offshore model for that matter. The only validation data available in this case are the results of a few test, obtained from a physical model built by CWPRS. Physical models are considered to give a reasonable representation of reality and can therefore be used in a validation process. Through lack of any other validation data, the CWPRS model will be used in this process.

In 1974 a physical model was built by the Central Water and Power Research Station (CWPRS), a hydraulic research institute in Pune, India. This was a model of the tidal basin near Pipavav with the port structures as they were designed by Engineers India Limited (EIL). This is presented in CWPRS report 1444 [27].

The port structures envisaged for the first and the second phase of the masterplan developed by EIL were modelled in a 1/150 scale model, covering the area shown in figure 6.4. Waves of 2m and 3m height and a period of 10s were tested in the model. Observations of wave heights at various locations (1-14) in the model (see figure 6.4) were made for existing conditions and for phases I and II of development. The observations were recorded at high water level.

Based on refraction calculations and model tests, made by CWPRS, the berths seemed to be *'more exposed to southerly waves than any other direction'* so therefore southerly waves, refracted to 192° were reproduced in the model. The results of the wave observations in the physical model are presented in columns two and three of table 6.1.

Location	Physical model		PORTRAY model		HISWA model	
	2m	3m	2m	3m	2m	3m
1	0.35	0.55	-	-	0.37	0.47
2	0.35	0.60	-	-	0.38	0.47
3	0.40	0.65	-	-	0.42	0.52
4	0.50	0.70	-	-	0.40	0.49
5	0.40	0.65	-	-	0.40	0.50
6	0.45	0.70	0.20	0.27	0.46	0.57
7	0.45	0.60	0.13	0.17	0.43	0.54
8	0.40	0.70	-	-	0.38	0.48
9	0.40	0.65	0.10	0.14	0.39	0.48
10	0.50	0.75	0.13	0.17	0.48	0.60
11	0.60	0.90	0.20	0.24	0.51	0.63
12	0.65	1.10	0.21	0.27	0.62	0.78
13	0.75	1.20	0.39	0.47	0.86	1.11
14	1.10	1.50	0.76	1.06	1.24	1.82

Table 6.1 Results of different models at incident conditions of 2m and 3m waves of 10s period coming from 192°.

From the table it can be seen that the wave heights in the port decrease towards rear of the harbour, as would be expected. It should also be noted that the wave heights were recorded with an accuracy of 5cm, which gives an indication on the attainable accuracy with the physical model.

6.3 PORTRAY simulations

For the construction of the port wave model with PORTRAY the bottom topography was translated into a grid file, to model the sea bottom and the existing reclaimed area. A mesh was laid over the drawing of the port and depth values were read off at the intersections, see figure 6.5. The mesh size of the grid was chosen at 100m, meeting the most stringent stability condition as formulated by Southgate [24], see also section 4.3.

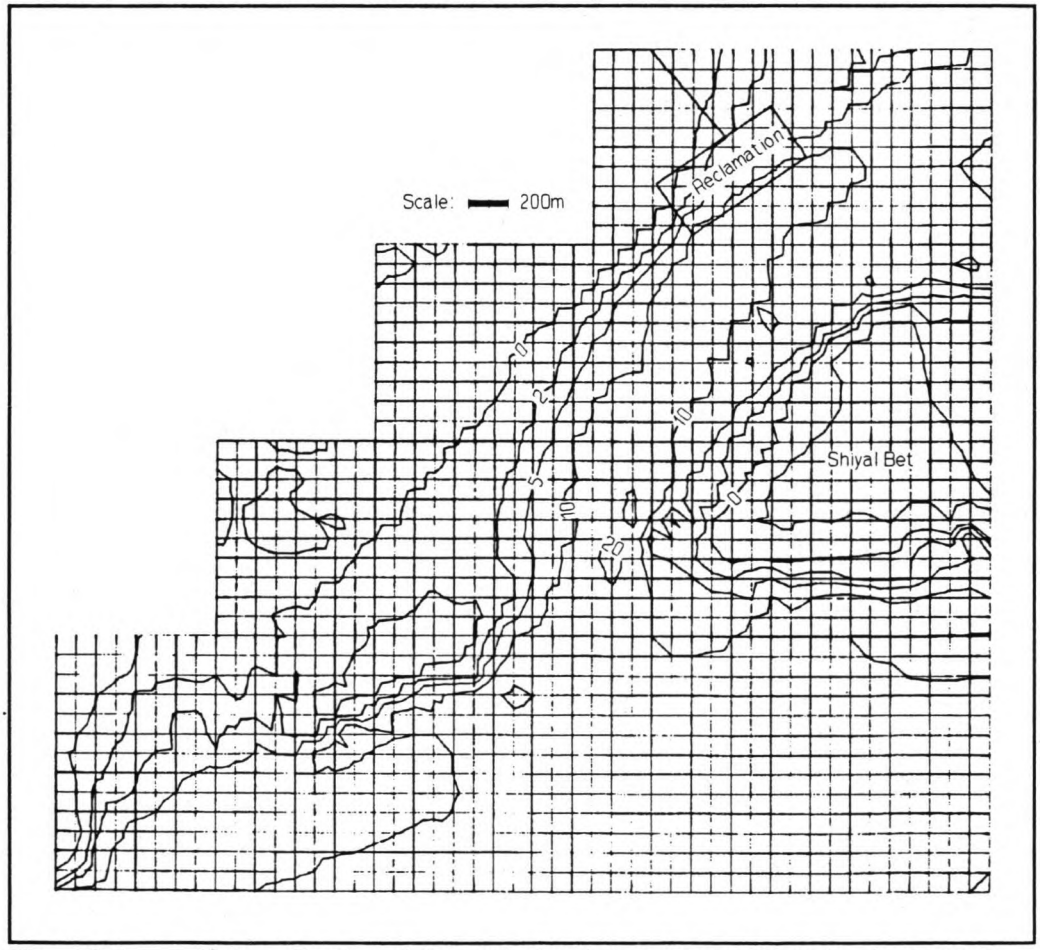

Figure 6.5 Schematization of the seabed and the port structures for the PORTRAY simulations.

Using the suggested ray density of 5 to 10 rays per square, large areas at the rear of the harbour showed a wave height of 0m, indicating that no energy had penetrated the furthest areas. Although this may sound very encouraging for the feasibility of this port design, it was thought to be rather unrealistic from a hydraulic point of view. The cause of these 'no energy' areas was the large divergence of the ray paths (this can be seen quite clearly in figure 6.6). This large divergence caused the rays separation to exceed the sides of several of the averaging squares at the rear

of the harbour[1]. Therefore the ray density had to be increased dramatically (up to 100 rays per square) to avoid these 'no energy' zones.

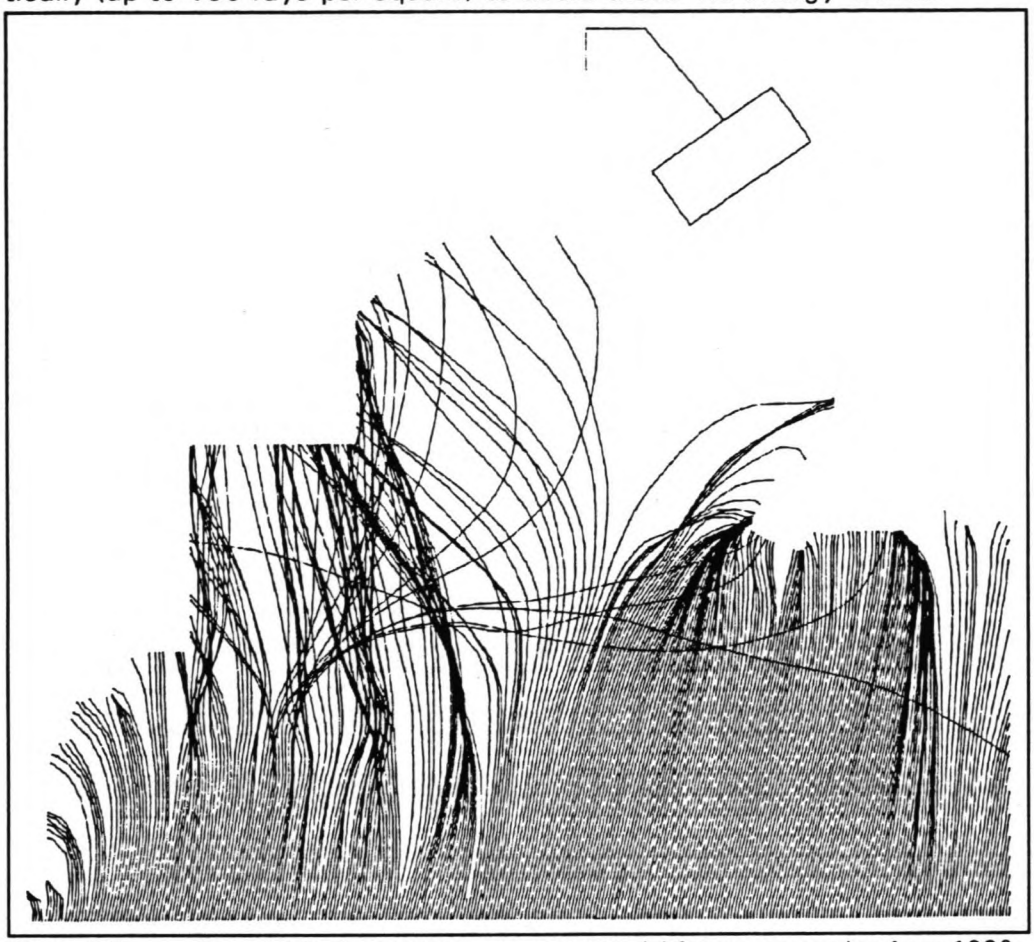

Figure 6.6 Ray plot in the PORTRAY port wave model for waves coming from 192°.

The wave heights, at the same locations as in the physical model, were noted for the same incident wave conditions. The results are presented in the fourth and fifth column of table 6.1. At locations 1 through 5 and 8 no results could be noted. This was a result of the way the basin was modelled. In the construction of the sea bottom grid files, the reclaimed area at the rear of the harbour was incorporated into these grid files covering the observation locations 1 through 5 and 8. A listing of the control file is given in appendix VIII.

It can be seen that the wave height decreases in the same manner as for the physical model tests, however, the results are significantly (29%-78%) lower for all locations due to the extreme ray separation. After consulting experts at Wallingford, DHV and DUT it was concluded that this was a result of the complex bathymetry of the tidal basin. Consequently PORTRAY is regarded to be unsuitable to build a port wave disturbance model for Pipavav.

---

[1] Changing the size of the averaging squares was not possible. It proved to be a fault in the program PORTRAY itself. This was corrected in the second version of PORTRAY.

6.4 HISWA simulations

The results of the PORTRAY validation called for implementation of a complete new model, HISWA. In this section the validation of this model and the construction of the HISWA port wave model will be discussed.

6.4.1 Validation

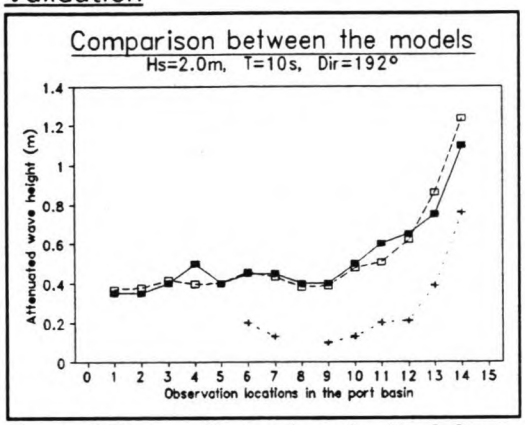

Figure 6.7 Comparison for H = 2.0m.

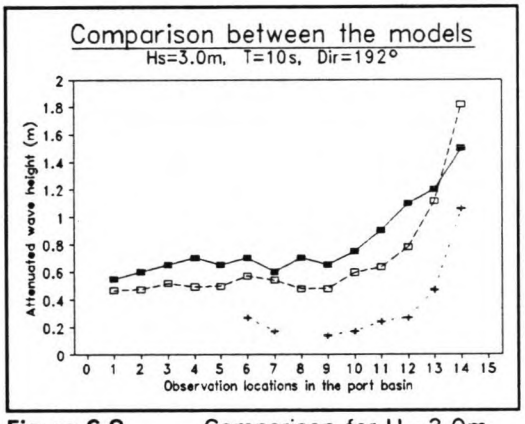

Figure 6.8 Comparison for H = 3.0m.

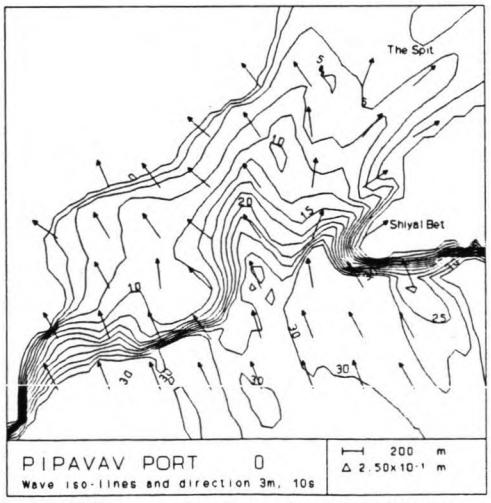

Figure 6.9 Iso-line plot of validation.

For this model the same depth file was used, as for PORTRAY. The incident wave field was defined using a significant wave height, its corresponding mean wave period and a mean wave direction. The same 2m and 3m waves with a period of 10s, coming from 192°, were used as incident wave field for comparison with the physical model.

In HISWA all waves are simulated with a directional spread, meaning that the waves are incident around the mean wave direction. The directional spread of swell waves is smaller than that of sea waves. By adjusting the directional spread, either sea waves or swell waves can be simulated.

In the physical model, the waves are induced as monochromatic waves. This implies that the waves come from one direction only, the incident wave direction.

The directional spread in the physical model is therefore 0°. The minimum directional spread possible in HISWA is 5.7°. Results of the simulations with waves with this directional spread are presented in table 6.1 and figures 6.7 and 6.8. Figure 6.9 shows an iso-line plot of the wave heights and the wave direction.

The results show the same trend as those of the PORTRAY simulations and the physical model, but with a much greater correlation to those of the physical model than in the case of PORTRAY. As can be

seen from the graphs, the results with the HISWA simulations show a great improvement. There still exists, however, a slight difference for 3m waves, between the results of the physical model and those of the HISWA simulations. When the results of the physical model are reviewed more critically the following stands out.

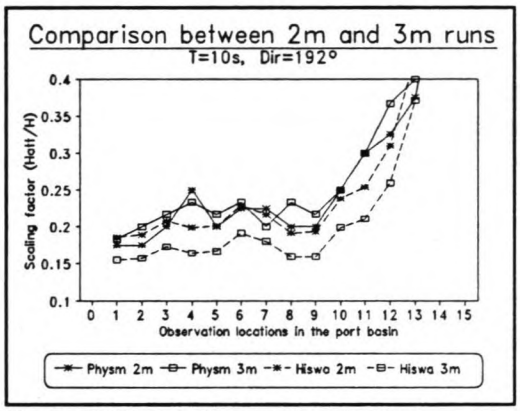

Figure 6.10 Attenuation factor.

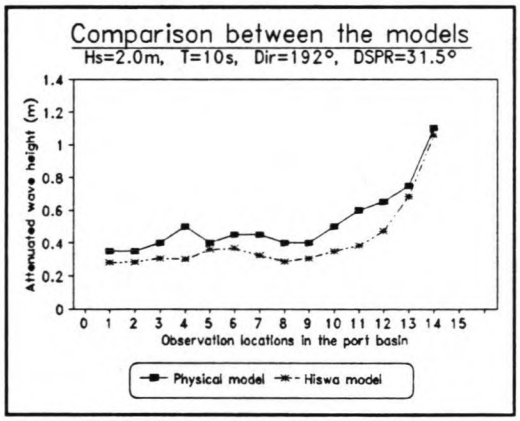

Figure 6.11 Comparison for H = 2.0m.

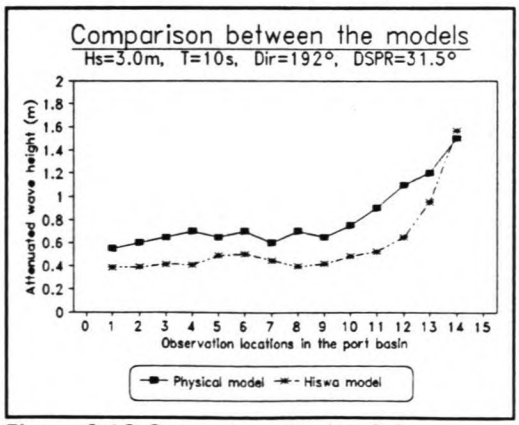

Figure 6.12 Comparison for H = 3.0m.

Looking at figure 6.10 it can be seen that, for the physical model, the attenuation factor of the 2m waves is the same as, or lower than, that of the 3m waves. For the HISWA results the attenuation of the 3m waves is lower at every location than for the 2m waves. The latter is to be expected, since the dissipation processes, such as diffraction, reflection and refraction, are linear with the wave height, resulting in lower attenuation factors for higher waves. This could lead to the conclusion that the results for the 3m waves should in fact have been lower, i.e. closer to the HISWA results.

Using monochromatic waves, as in the physical model, results in an incorrect assessment of the waves inside the port. There will always exist some directional spread, depending on the character of the incident wave field, more sea or more swell waves. Introducing a directional spread of 31.5° (the default option in HISWA) results in lower waves in the port basin, indicating that the results of the physical model were an overestimation.

Simulation results with the new directional spread are presented in figures 6.11 and 6.12. The fact that waves with a larger directional spread result in lower wave heights will be explained below.

The waves simulated in the physical model are of a rather long period (10s). These longer waves can penetrate the basin difficultly due to the fore shore rock on either side of the entrance channel. These rock formations cause a large absorption of energy. It can easily be imagined

that the effect of this energy absorption is higher as the original scatter of the wave rays is higher. This results in lower wave heights in the basin.

Another effect of the physical model is that the waves can be *diffracted* and *reflected* a little off the rock formations. These processes can not be simulated with HISWA. This can result in higher waves in the physical model. This would also mean that simulations with HISWA could be an underestimate of reality. However, it is believed that these contributions of diffraction and reflection off sloping banks and under water rock formations are too low to endanger the validity of the HISWA model.

Finally, models are always approximations of reality. Thus it cannot be expected of either model to represent reality completely. Besides this, the difference between the two models is not so great, that a new model should be implemented to get results that are even closer to those of the physical model. This would not give the amelioration, worth the energy and time that has to be investigated in such a new model.

Taking all these factors in consideration, the HISWA port wave model is regarded as being validated against the physical model, and its simulation results will be used in the investigation of wave climate inside the port.

In the determination of the port wave climate a directional spread of 31.5°[1] will be used to describe the incident wave field. This is done to get a more realistic incident wave field, for it was established before, that the approach of the physical model was an overestimation of the situation. The directional spread could be adjusted according to the character (sea or swell) of the incident wave field. This option is, however, not implemented in the port wave model simulations, to avoid a discussion on whether a certain wave height/wave period combination can be regarded as sea or as swell. This would be beyond of the character of this port study.

6.4.2 Determination of the port wave climate

Now that the HISWA port wave model is validated it can be used to determine the port wave climate. The sea bed files, used for the validation of the port model, were expanded with the dredged channel and turning basin for the first and second phase of development. Output locations were also added to the model, at locations where the terminals in both phases are situated (see also figure 6.3).

The incident wave field was defined using a significant wave height, the mean wave period and a directional spread of 31.5°. The influence of ebb or flood currents was not incorporated in the model. Although ebb currents can increase the local wave heights and flood currents can decrease them, these possibilities are ignored to limit the number of simulation runs. However, it should be borne in mind, that the wave

---

[1] This is the HISWA default value, see [28]

heights can be slightly higher during ebb. This increase can be of the order of 10%. In the simulation of the port wave climate only the effects of wind growth, surf dissipation, refraction and shoaling are accounted for. For a list of the control file see appendix VIII.

To determine the port wave climate the adapted wave climate, as it was used in the study of the near shore wave climate, was no longer used. This is because it is not interesting, from a port engineer's point of view, to know the distribution of the wave field in sea and swell waves. For calculations of downtime, information is needed on very particular wave height/wave period combinations, whether they are swell or sea waves. What these combinations are and how they are implemented in the determination of the terminal downtime is described in chapter 6. What *was* used will be explained below.

A literature study was made to establish the wave heights and periods for which operating limits at various locations inside and outside the port are exceeded. This study is discussed in chapter 3. The operational limits that evolved from this study were used to investigate what the deep water state of the waves had to be, so that these operating limits at the terminals and the other locations would be exceeded. In this investigation, the near shore and the port wave model, as constructed with HISWA, were used.

As a first step, it was investigated, to what general direction, waves are refracted to. Using the HISWA near shore wave model, waves coming from 180°(S), 210°(SSW) and 240°(WSW), were tracked to a depth of CD -10m offshore. This is the upwave boundary of the port model. It was established that waves coming from these directions are refracted to a mean of 179°, 197° and 206° respectively. This shows that the manual method, with the normal at 180°, was a good approximation.

Subsequently a backward calculating technique was followed, to track the waves from the terminals and other locations, to deep water. This means that the wave heights at the upwave boundary of the port wave model were increased until the operating limits at the terminals were exceeded. Subsequently the wave heights at deep water were increased until these upwave boundary conditions were exceeded, thus obtaining the deep water wave height for which the operating limits at the terminals are exceeded.

For some locations the waves at deep water had to be higher than any wave that ever occurred off the coast of Pipavav. This means that for these locations the operation criteria are never exceeded.

The port is envisaged to be developed in two phases. In the second phase (1997-2010) the vessels will have increased in size which results in deeper and wider basins and channels in the port. Also new commodities will arrive at Pipavav and existing cargo volumes will increase necessitating the construction of additional terminals and storage areas. In HISWA it is not possible to model port structures, yet the wider and deeper channels and basins can easily be added to the depth

files. The only difference for waves penetrating the harbour is that the wet cross sectional area is increased. The effect of this increase is a decrease of the wave heights in the second phase.

Although there is a difference in wave height between the two phases this did not mean that all the simulations had to be performed for both phases in order to determine the different downtime percentages of the two phases. The only terminals that exist in both phases, are the general cargo, the common bulk, the cement and the copper smelter terminal. Of these five terminals, the operation criteria are never exceeded, because the necessary wave height at deep water does not occur.

Terminal	H_p(m)	H_0(m)	T(s)	Dir	Refr	Exceed	Tot.
General Cargo	0.8	NA	-	-	3°	0.00	0
Common Bulk	1.0	NA	-	-	7°	0.00	0
Cement Term	1.0	NA	-	-	12°	0.00	0
Copper Smelter Ex	1.3	NA	-	-	11°	0.00	0
Copper Smelter Im	1.0	NA	-	-	11°	0.00	0
Coal Terminal	1.0	2.6	8-13	180°	1°	0.25	11
		2.2	13-20	180°		0.29	
		3.3	8-13	210°	3°	3.52	
		2.8	13-20	210°		0.11	
		4.4	8-13	240°	5°	5.88	
		4.0	13-20	240°		0.87	
Oil Products	1.5	2.1	8-13	180°	20°	0.34	20
		1.8	13-20	180°		0.31	
		2.6	8-13	210°	18°	6.01	
		2.2	13-20	210°		0.16	
		3.6	8-13	240°	16°	11.64	
		3.2	13-20	240°		1.12	
Fixed Crude oil	1.5	1.6	≥12	180°	53°	0.32	6
		1.9	≥12	210°	39°	1.75	
		2.7	≥12	240°	25°	3.96	
SBM Crude oil	2.5	2.6	≥12	180°	-	0.24	2
		3.2	≥12	210°	-	0.55	
		4.6	≥12	240°	-	1.15	
Port basin (mooring)	1.3	1.9	4-7	180°	-	0.00	11
		2.2	4-7	210°	-	2.73	
		2.8	4-7	240°	-	7.95	
Pilots 10km offshore	3.0	3.7	6-7	180°	-	0.00	1
		3.9	6-7	210°	-	0.47	
		4.5	6-7	240°	-	0.24	
Tugboats 2km offshore	1.5	1.9	4-7	180°	-	0.00	11
		2.2	4-7	210°	-	2.73	
		2.8	4-7	240°	-	7.95	

Table 6.2 Deep water wave heights, periods, directions and number of days for which the operating limits at these locations are exceeded.

The results of the simulations are listed in table 6.2. The first column lists the names of the locations. For a map of the project site, see appendix I. The second column lists the operational limits. The third column contains the deep water wave height, at which the operating limits are exceeded. The corresponding deep water wave period and direction can be found in the fourth and fifth column. The sixth shows the direction to which the waves are refracted, with respect to the terminal orientation. In the last two columns the corresponding number of days per year for which the limits are exceeded are presented. These days are obtained through linkage with the tables with observed wave heights as described in section 2.6.

From the table it can be seen that the wave heights at deep water coming from 240° need to be higher than waves coming from the other directions. This could be expected, for it was already concluded in the determination of the near shore wave climate, that waves coming from 240° were refracted stronger, resulting in lower wave heights in front of the port.

For some locations, the period range, for which the vessels are sensitive, was too long to give just one wave height that results in exceeding of the operating limits. For instance, it is assumed that the coal vessels are sensitive for waves of 1.0m with a period in the range 8-20s. It is not possible to give one deep water wave height for which this operating limit is exceeded. Subsequently, the period range was split up in a lower and a higher frequency part.
For other locations the waves were too short to reach the operating limits, due to exceeding of the wave steepness criterium (e.g. waves with a period of 4s can not reach a wave height of 3.0m to exceed the pilot criterium).

Several authors [17] and [7] specify that a downtime for approximately 1 week per year is acceptable. This means that these downtime periods due to waves are rather high.

6.5 Discussion and comparison of results

At the end of this chapter, the two mathematical models are compared and their (dis)advantages are discussed.

The main conclusion must be that the PORTRAY model was not suitable to build a mathematical simulation model of the tidal basin of Pipavav and the envisaged port structures. This can be explained as follows.

In ray models the paths of the individual rays, sent out from the upwave boundary, are tracked to the locations of interest. This approach to wave propagation is fairly easy to understand and to calculate. However, it is not taken into account, that the neighbouring rays travel at the same time towards the shore and can influence their neighbours through lateral transfer of energy. In conventional ray models this could also give rise to caustics and ray crossings, causing an unrealistic rapid variation of the wave height at these locations.

Elimination of the latter effects has been accounted for by the ray averaging method, incorporated in the PORTRAY model. This could not prevent, however, that almost all wave rays were strongly diverted away from the channel axis, towards the shore. This diversion was so extreme that although the ray density was increased, practically none of the rays could penetrate the tidal basin. The reason for this effect has to be sought in the large bottom gradients caused by the steep rock formations on either side of the entrance channel and the fact that the rays cannot laterally influence each other. It is a known feature of PORTRAY[1] that the model has more problems in modelling the propagation of long waves. Unfortunately, the only physical model tests available were the ones of waves with a period of 10s. Thus, it could not be investigated whether the model could be used for the simulation of just the shorter waves, or whether the bathymetry was too difficult all together.

Although the PORTRAY model was specifically written for the simulation of wave penetration in ports, the port layout apparently has to be much more straightforward than was the case in the tidal basin of Pipavav. It has to be stated that the bathymetry was indeed rather complex, with depth variations of 15m within a distance of only 500m. A possible remedy to intercept the ray separation effects is using a backtracking ray model, where the rays are tracked from the location of interest to deep water. Thus, it can be avoided that the rays never reach the location of interest. This is also interesting for a port engineer, because he would rather find out what the deep water state of the waves has to be to exceed certain values inside the port, than how the complete incidence wave field develops, propagating towards the coast.

A good feature of the PORTRAY models was that the port structures could be modeled easily and that these structures could also reflect and diffract the waves as they propagate through the port basin. The fact that it is not possible to model this in HISWA, has to be noted as a disadvantage of this model. On the other hand HISWA was not written to model port basins and it can model current patterns and wind generated waves within the model area, which can significantly influence the simulations results.

A point were HISWA excels in over PORTRAY is the way that output can be requested at any desired location, where PORTRAY just gives output on *all* the nodes of the computation grid which is the same as the bottom grid. This also implements that the bottom grid determines the calculation stability and accuracy. In HISWA distinction is made between a bottom and a computation grid which gives the user more freedom in determining the detail of the bottom grid.

In the ideal situation, HISWA could be used to translate the deep water wave climate to a location just outside the main breakwater of the port. PORTRAY, subsequently translates this to wave heights in front of the terminals and any other location of interest.

---

1 According to consulted experts at Wallingford.

7 Nautical investigation

7.1 Ship manoeuvrability

To obtain a better insight in the possibilities and restrictions of vessels and infrastructure, under several environmental conditions, of the Pipavav port design presented in volume I, the mathematical model SHIPMA was used. The theory behind this mathematical model is described in chapter 4.

As described in chapter 4 several input files are needed to perform a simulation run. The ship that is used in the simulations of the Pipavav port design is a 58,750 DWT bulk carrier[1] with the following characteristics:

BUL 242 A			
Designation	Symbol	Unit	Magnitude
Type of ship	-	-	bulk carrier
Length over all	L_{oa}	[m]	225.0
Length between perpendiculars	L_{pp}	[m]	217.0
Beam	B	[m]	32.2
Depth	h	[m]	18.4
Draught midships	T	[m]	12.0
Draught aft ship	T_a	[m]	12.0
Draught forward ship	T_f	[m]	12.0
Displacement	Δ	[m^3]	69450
Deadweight	D_{wt}	[tons]	58750
Shaft power	P_s	[kW]	10810
Max. number of propeller revolutions	n_{max}	[rpm]	91.0
Service speed	V_s	[knots]	13.5
Manoeuvring speed	V_m	[knots]	12.0
Frontal windage area	A_{wx}	[m^2]	668.0
Lateral windage area	A_{wy}	[m^2]	2286.0
Number of propellers	-	-	1
Propeller diameter	D	[m]	5.9
Propeller type	-	-	fixed pitch
Number of blades	Z	-	4
Direction of turning	-	-	right handed
Number of rudders	-	-	1
Type of rudder	-	-	mariner
Total rudder area	A_r	[m^2]	47.0
Rudder deflection rate	d_p	[deg/s]	3.0
Maximum rudder angle	δ_{max}	[deg]	35.0

Table 7.1 Main particulars of the vessel, the rudder and the propeller.

[1] This is the vessel that is standard supplied with the program SHIPMA. Additional mathematical models of the same or other ships are rather expensive. Fortunately, it is approximately the same as the largest expected vessel inside the port in the second phase (a 60,000 DWT coal bulk carrier).

The coefficients for windage areas, wind angles, wave-drift, and bank-suction are determined by model test performed by MSCN. They are applicable for h/T ratios (see figure 7.3) between 1.2 and 5. That means for depth values between $1.2*12 = 14.4$m and $5*12 = 60$m. That means for channel depths of CD -12.4m and CD -14.2m in the first and second phase of port development, the minimum value of the water level should be CD +2.0m and CD +0.2m respectively. Furthermore the wave-drift coefficients only apply for waves with a period of 10s. This means that the wave input file should only contain wave heights simulated for an incident wave with a period of 10s.

7.2 Test programme

The objectives of the SHIPMA study are listed below:

- Investigate the general character of the port under all circumstances. This means answering questions like:
  - 'Is it possible to enter the harbour and keep the drift angle tangent below 0.25?'
  - 'What is the amount of space used by the sailing vessel?'
  - 'What are the applied rudder angles and tug forces?'
  - 'What are the revolutions per minute of the propeller and is the use of power bust necessary for track control?'
- Investigate the possibility to stop the vessel in the turning circle.
- Investigate whether assistance by two tugs is sufficient to guarantee safe passage through the harbour.

To get an impression of the general character it will be investigated whether it is possible to manoeuvre the design vessel into the rear of the harbour, so that it is at complete stop in front of the general cargo terminal, see for instance figure 7.5. While performing this manoeuvre the vessel has to decrease speed and make a turn at the same time. The philosophy behind this is that when it is possible to manoeuvre the largest design vessel in front of the general cargo terminal, it is certainly possible for all smaller vessels.

The circumstances that are investigated are tug assistance, or no tug assistance, ebb or flood and regular (50% exceeded) or extreme (1% exceeded) wind, wave and current conditions. This results in six different test cases. Beforehand it was assumed that under extreme conditions tug assistance will always be needed.

Whether it is also possible to stop the vessel in the turning circle is investigated in run TM1 (see figure 7.19). This manoeuvre may seem easier at first, because the vessel does not have to make a turn, but the consequence is that the vessel also has less channel length to bring it's speed from 6-8 knots down to 0.

The berthing manoeuvre and port departure will not be investigated, for these kind of manoeuvres can not be simulated using SHIPMA. These manoeuvres are only briefly discussed in section 7.11.
The seven test cases that will be investigated, are presented in table 7.2.

Runid	Current (m/s)	Wind (m/s)	Waves (m)	Tugs
PP1	1.14 (50%)	W/5.5 (50%)	0.85m	no
PP2	1.14 (50%)	W/5.5 (50%)	0.85m	2*200 kN
PP3	1.69 (1%)	W/15 (1%)	1.50m	2*200 kN
PP4	-0.72 (50%)	W/5.5 (50%)	0.85m	no
PP5	-0.72 (50%)	W/5.5 (50%)	0.85m	2*200 kN
PP6	-1.47 (1%)	W/15 (1%)	1.50m	2*200 kN
TM1	1.40 (20%)	W/15 (1%)	1.50m	2*200 kN

Table 7.2 Seven cases of the test programme for the manoeuvrability study.

The current velocities presented in the second column of the table are the velocities measured at location 4, in the navigation channel see map in appendix I. This is the highest flow velocity and all other locations are related to this one. The wind direction is West in all cases. This is the most common direction (see section 2.3) and also the most troublesome, for ships sailing in a north-south direction. The wave height that is exceeded at the entrance of the channel for about 50% of the time is 0.85m. The maximum wave height is 1.50m, for this is the operating limit for tugboats and other service crafts. The distribution of the wave heights over the port area is obtained by performing two runs for 0.85m and 1.50m waves with a period of 10s, using the HISWA port wave climate model. When tugboat assistance is provided this will initially consist of two tugboats with a bollard pull of 200 kN each. If this proves to be insufficient it will be adjusted.

7.3 General setup

In this section the relevant aspects of the input files, needed for the simulation runs, are discussed. In appendix VIII some of these input files, needed for one simulation run, are presented. Reference is made to the SHIPMA manual [20] for a more detailed discussion of the input files.

Harbour layout

The harbour layout used for the SHIPMA runs is the layout of the second phase (see appendix I). This is because the ship used in the simulations is the design vessel of the second phase. This means that all the terminals are built and the channel and turning circle dimensions of the second phase are used. These dimensions are: - channel width: 170m,
- turning circle diameter: 400m.

The desired manoeuvre

The vessel will enter the harbour with a speed between 6 and 8 knots, depending on the flow velocity of the ebb or flood current and whether or not tugboat assistance is provided. If assistance is provided the maximum sailing velocity at which tugboats can tie up is 6 knots. The tie up

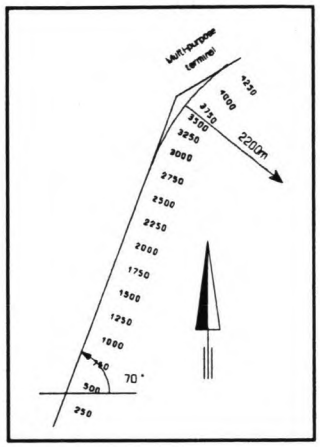

procedure takes approximately 15 to 20 minutes. The maximum sailed distance is then 3600m. This point is near the projected coal terminal, just before the dredged part of the channel begins. The vessel then has to reduce speed to end up berthing at the general cargo terminal, which is also called the multi-purpose terminal together with the common bulk terminal.

This manoeuvre is schematized by two track lines of 3000m and 500m each, connected by a circle section with a radius of 2200m. This makes up a total track length of 4200m. The track is then roughly divided in 8 or 9 track sections to indicate where a new number of propeller revolutions is desired. A typical propeller setting would look like:

```
**-----------------------------------
** Record 6b: Start position of track sections.        [m]
0  1000 2000 2800 3000 3700 3900 4100
**-----------------------------------
** Record 6c: Propeller revolutions per track section. [1/s]
.6  .5  .4  .3  .4  -.4  -.6  -.7
**-----------------------------------
```

Figure 7.2 Setting of rps for run pp1.

For this kind of manoeuvre the autopilot is set in a track keeping mode. Subsequently an anticipation distance (Δs) has to be chosen. This Δs is typically set between 1 and 2 times the ship's length. In this case it is set to 1.5. This means that the autopilot compares the present course of the vessel to a point at a distance of 1.5, further along the track. Judging the difference in the tangent of the track and the actual ground course and the offset from the desired track it adjust the rudder angle and it possibly gives power bursts, to get the ship back on track.

Reducing the length of the anticipation distance, to say 1.25, would result in a closer track keeping, but also in more 'nervous' rudder deviations and power burst control. So, if the available space for track deviation is sufficient, as it would be in port approach channels, the anticipation distance can be set to a higher value to get a more calm manoeuvre.

Tug assistance

When tug assistance is provided it consists of two tugboats, one for and one aft, with a bollard pull of 200 kN each. The tugs will be standby as from track position 2000m, which is about 3000m from the point where they start the tie up procedure. The time needed for tugs to reach their maximum tug force is 10s, since this cannot be realized instantly. The

tug controller is not set in lining-up mode, meaning that the tugs will always try to manoeuvre the vessel towards the desired track instead of sailing parallel to it. The use of power burst by the ship is suppressed, as this may be inconvenient during tug assistance.

Bank suction

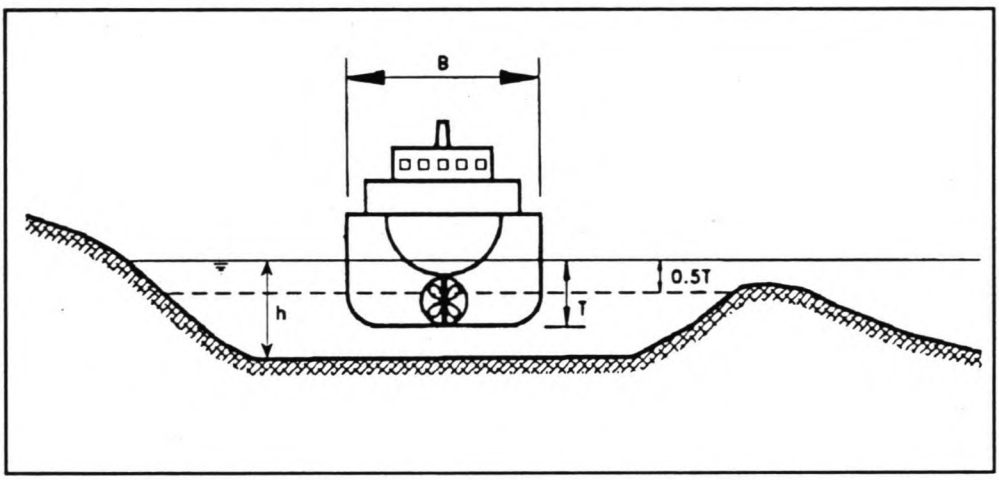

The influence of banks on a sailing vessel can be modelled by incorporating bank suction into the simulation runs. Bank suction becomes noticeable when the ship sails within, say 50m or 100m of the point where the water depth is approximately half of the ship's draught. In the Pipavav case this would be the 5m depth contour. This too far from the channel axis to be of influence on the ship's trajectory.

In the next sections the various runs of the test program will be discussed. The success of the runs are measured on the next four characteristics.

- Cross-track deviation, *dy* The is the distance, in (m) from the ship's origin perpendicular to the tangent of the track.
- Course deviation, *dpsi* This is the angle the ship makes with the channel axis. The tangent of this angle should not exceed 0.25 ($d\psi_{max} = 14.04°$).
- Ship's speed, *u* This is the longitudinal speed of the ship, measured in m/s.
- Rudder angle, *d* This is the rudder angle δ, which can vary from -35° to +35° maximum. When the desired rudder angle is twice the maximum possible angle, the propeller revolutions are set to power burst values. The rudder angle should preferably stay below ±35°.
- Tug force, *Ytug* This is the tug force in the ship's transverse direction (in kN) with a maximum of 400 kN for two tugboats.
- Swept path, *swept path* This shows the total used space by the ship, i.e. a summoning of *dy* and *dpsi*.

7.4 Run PP1; regular flood conditions, no tug assistance

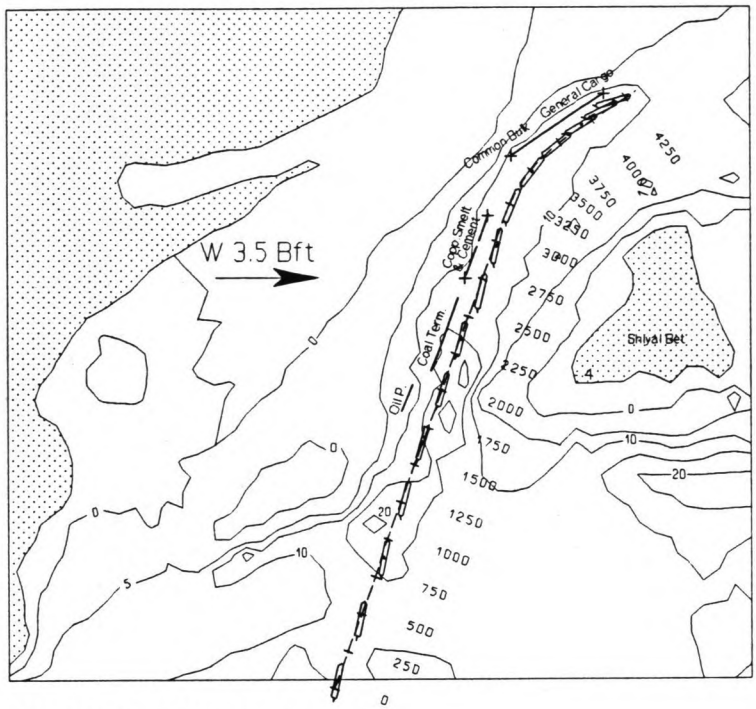

Figure 7.4 Track plot for pp1.

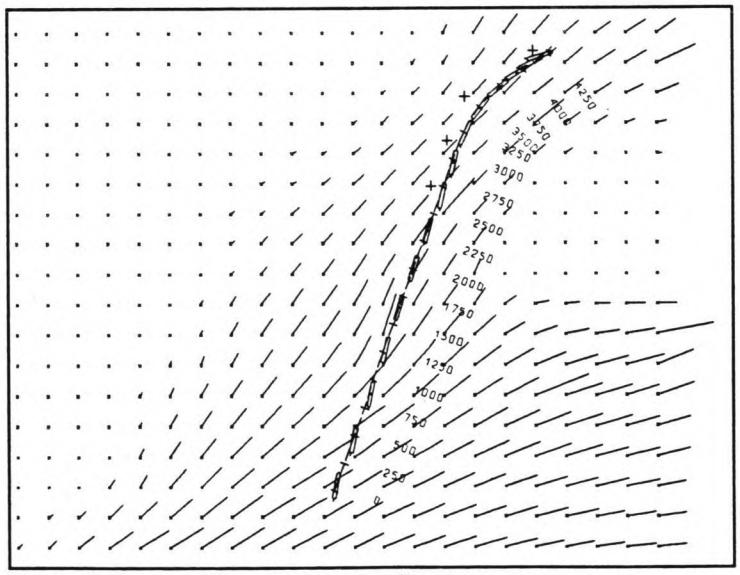

Figure 7.5 Flow pattern for flood.

Figure 7.4 shows the sailed track under regular flood conditions. Figure 7.5 shows the current pattern for flood[1]. It stands out that the angle that the current makes with the desired track, at the beginning of the channel, is considerable (approximately 38°). This, combined with a wind

[1] The current pattern is illustrated using a base and a current directions rather than using arrows. It is derived from [4]

blowing from the west, causes the vessel to sail with a small drift angle, resulting in a small cross track deviation (dy) of about 18m (see tables 7.3 and 7.4). The drift angle (dpsi) does not exceed 8° during the channel passage.

```
**-------------------------------------
** Record 6b: Start position of track sections.        [m]
0  1000 2000 2800 3000 3700 3900 4100
**-------------------------------------
** Record 6c: Propeller revolutions per track section. [1/s]
.6  .5  .4  .3  .4  -.4  -.6  -.7
**-------------------------------------
```

Figure 7.6 RPS setting for PP1.

From the track plot, the data tables and the rps setting it can be concluded that it is possible to manoeuvre the vessel into the rear of the harbour and to come to a complete stop at the end of the track. However, the cross track deviation, the drift angle, and the rudder angle at the end of the sailed track, are of such magnitude that this indicates that obliging vessels to always ask for tugboat assistance is not just necessary for turning the vessel in the turning circle.

7.5 Run PP2; regular flood conditions, *with* tug assistance

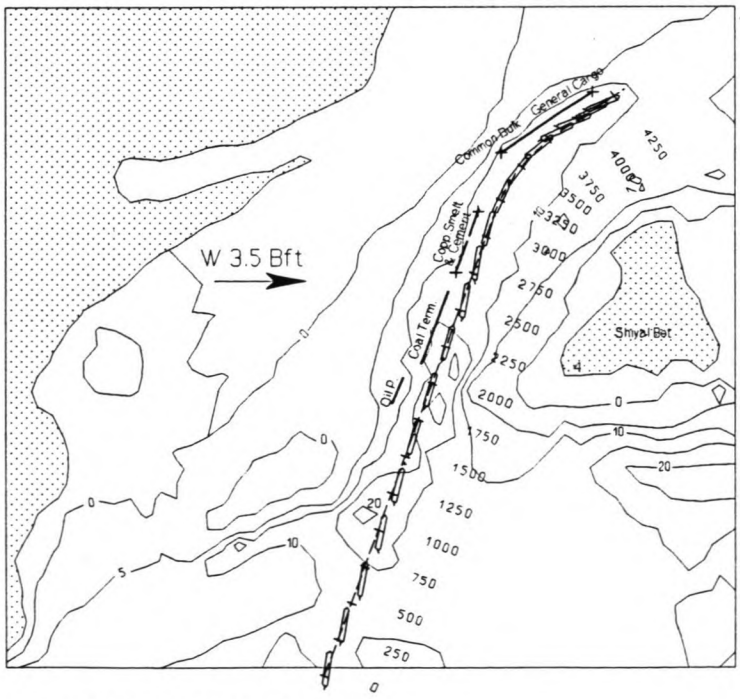

Figure 7.7 Track plot for pp2.

Although the entrance manoeuvre can be completed successfully without tug assistance, the manoeuvre is also investigated with tug assistance, see figure 7.7. The current pattern is the same as shown in figure 7.5.
The entrance speed of the vessel in PP1 is 3.7 m/s. When the vessel is

sailing in the beginning of the channel in PP2, the tie-up procedure is engaging. The sailing velocity is therefore restricted to a maximum of 3.0 m/s (6 knots) [18]. Because of the lower sailing speed the initial drift angle and the cross track deviation is larger. The automatic pilot is forced to use larger rudder angles to keep the vessel on track, see tables 7.3 and 7.4. Despite these higher values for *dy* and *dpsi* at the beginning of the channel, it is still possible to manoeuvre the vessel into the rear of the harbour. Stopping the vessel is now much more controlled.

```
**-------------------------------------
** Record 6b: Start position of track sections.          [m]
0  1000 1500 1900 2100 2200 2600 3600 3850 4000
**-------------------------------------
** Record 6c: Propeller revolutions per track section.   [1/s]
.6 .6  .5  -.5 -.4 .52 .53 -.65 -.3 -.7
**-------------------------------------
```

Figure 7.8 RPS setting for PP2.

The initial drift angle and course deviation could possibly be reduced by reorientation of the first part of the entrance channel, aligning it more to the prevailing flow direction (see also figure 7.5). This would result in additional dredging, since the water depth west of the channel rapidly decreases.

7.6 Run PP3; extreme flood conditions, *with* tug assistance

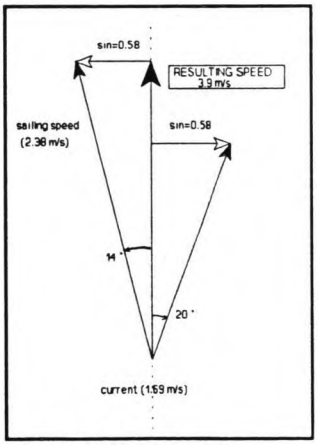

Figure 7.9 Velocities.

In this case the flood current velocity is 1.69 m/s. According to figure 7.10 this necessitates a sailing speed of the order of 4 knots to compensate the drift angle, caused by the current. This can be explained as follows (see also figure 7.9).

A current of 1.69 m/s at an incident angle of 20° to the desired track has a cross component of *1.69*sin20° = 0.58 m/s*. The ship has to sail under a drift angle to compensate this cross component. Assuming a maximum drift angle tangent of 0.25 the compensation speed of the vessel should be *0.58/sin14° = 2.38 m/s (4.6kn)*, with respect to the water. The resulting ground course speed is now 3.9 m/s, too high for tugboat tie-up. Aside from this tie-up criterium there is a minimum forward speed criterium and the speed of the vessel with respect to the water should also be large enough (approximately 3 knots [18]) to have sufficient pressure for the rudder deviations to be effective (to have enough rudder control). A diagram from which the final required sailing speed of the vessel can be read, is presented in figure 7.10. With a current velocity of 1.69 m/s (3.3 knots) this sailing speed would have to be of the order of 6.2 knots. This is too high for tug boats to tie up. Entering at a lower speed (6 knots) results in a drift angle higher than 14°. It is therefore not possible to

enter the harbour under these circumstances. Subsequently it was investigated what the maximum flood velocity may be at which entrance is still possible. According to the graph in figure 7.10, this is approximately 1.4 m/s (2.7 knots). This current speed is exceeded for 20% of the time, see figure (2.1). The resulting track plot is shown in figure 7.11. The corresponding data is presented in tables 7.3 and 7.4. The cross-track deviation is still significant 38m, but the drift angle is kept below 14°; the manoeuvre is controllable.

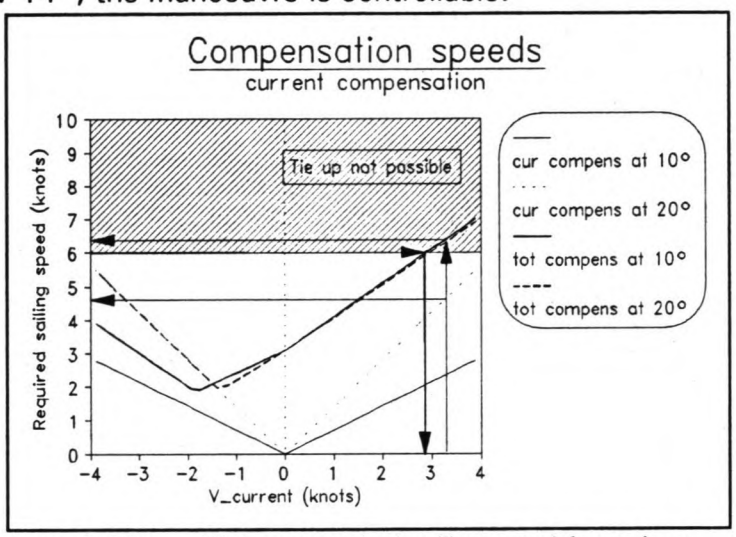

Figure 7.10 Minimum required sailing speed for various flow velocities.

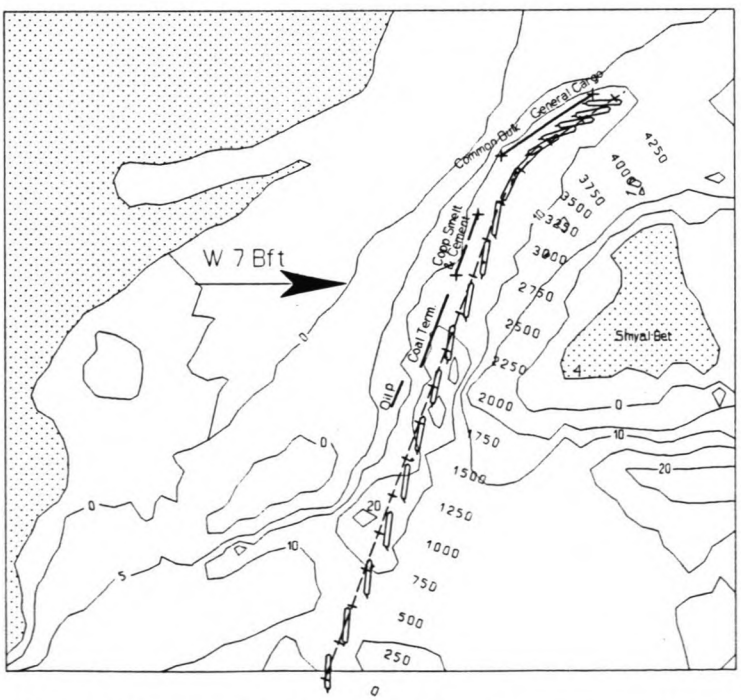

Figure 7.11 Track plot for pp3, with a current velocity of 1.4 m/s.

It can be concluded that under the extreme conditions, of a wind of 15 m/s coming from the west and a flood current with a flow velocity of 1.4 m/s, it is possible to complete the entering manoeuvre.

```
**-----------------------------------
** Record 6b: Start position of track sections.          [m]
0  400 1200 1900 2100 2200 2600 3650 3850 4000
**-----------------------------------
** Record 6c: Propeller revolutions per track section.   [1/s]
.65 .7 .65 -.5 -.4 .55 .52 -.65 .3 -.7
**-----------------------------------
```

Figure 7.12 RPS setting for PP3.

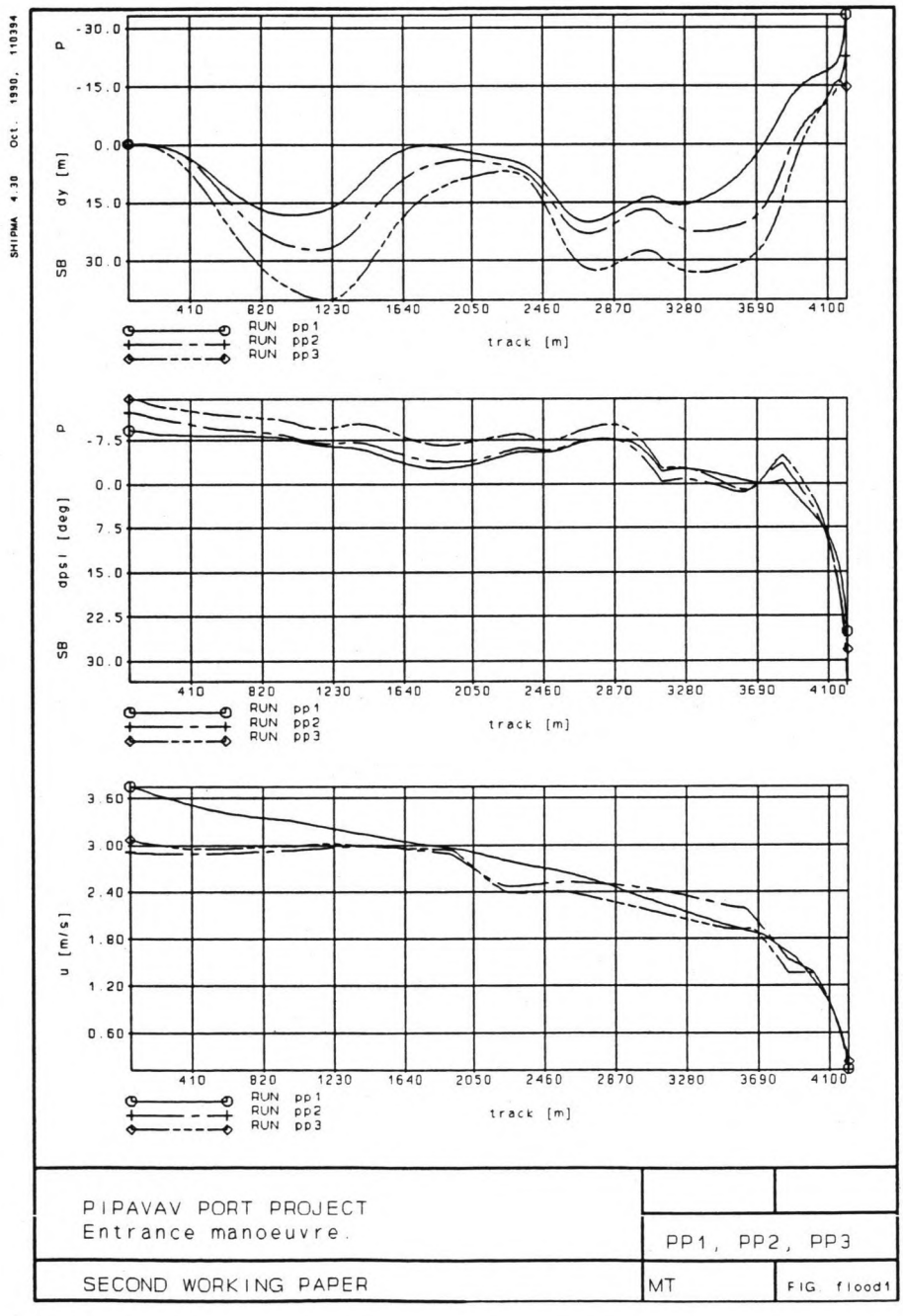

Table 7.3 Data tables, showing the cross track deviation, the drift angle and the longitudinal speed of the vessel for pp1, pp2 and pp3.

According to the swept path plot, the vessel needs at least 65m to starboard and 45m to port. It is also clear that two tugboats is enough to guide the ship into the harbour. Although it may seem possible to perform the entrance manoeuvre in the first part of the channel, judging from the rudder angle, the swept path and the applied tug forces, at the end (near the general cargo terminal) the conclusion should be that this is the most critical procedure, and conditions should be less to guarantee safe passage.

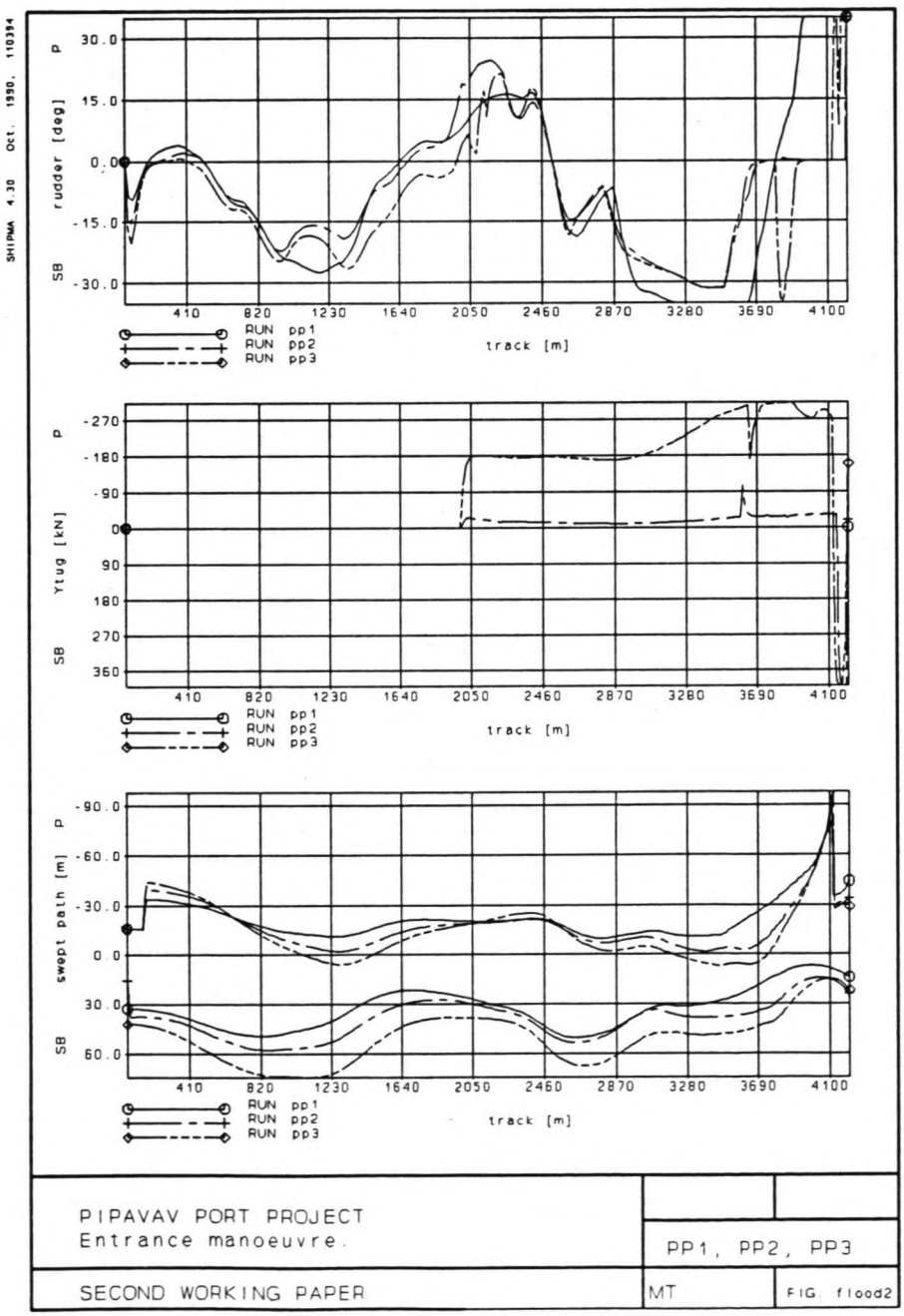

Table 7.4 Data tables, showing the rudder angle, the tug force in ship's transverse direction and the swept path for pp1, pp2 and pp3.

7.7 Run PP4; regular ebb conditions, no tug assistance

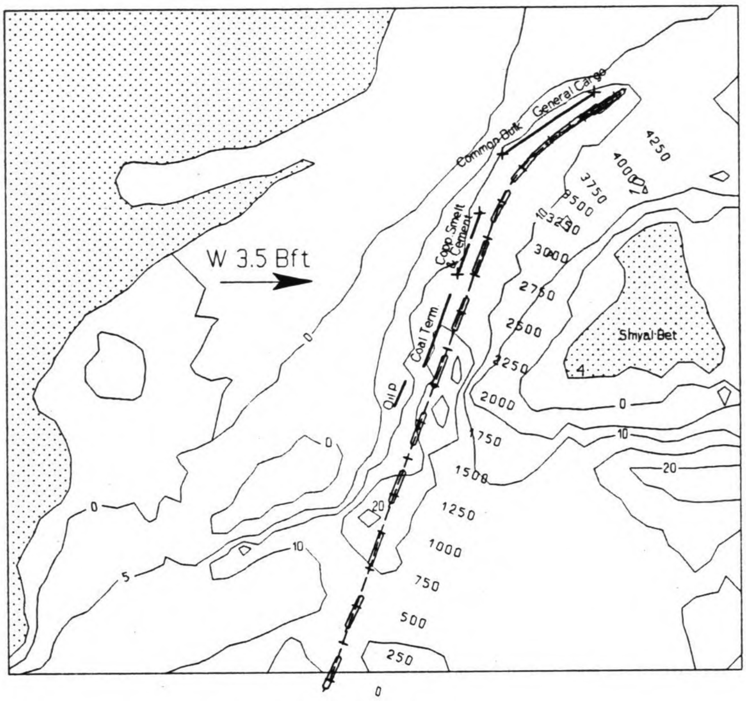

Figure 7.13 Track plot for pp4.

Figure 7.13 shows the track plot under regular ebb conditions. The current pattern is similar to the one shown in figure 7.5, except that the direction is reversed. The data results of this run are shown in tables 7.5 and 7.6. It can be seen that it is fairly easy to enter the harbour without the assistance of tugboats. The cross track deviation is minimal and the drift angle does not even exceed 5°. Even at the end of the track, the *dy* and *dpsi* are small, indicating that it is possible to stop the vessel under its own power. Also the rps setting indicates a smooth manoeuvre.

```
**-------------------------------------
** Record 6b: Start position of track sections.            [m]
0 1000 2000 2200 2800 3000 3600 3800 4000
**-------------------------------------
** Record 6c: Propeller revolutions per track section.     [1/s]
.9 .8 .7 .5 .6 .5 -.6 .1 -.4
**-------------------------------------
```

Figure 7.14 RPS setting for PP4.

7.8 Run PP5; regular ebb conditions, *with* tug assistance

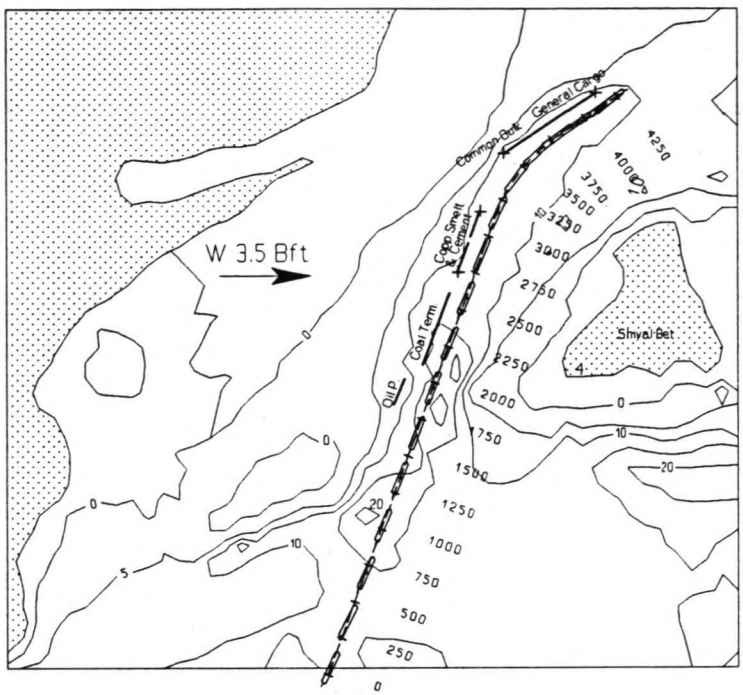

Figure 7.15 Track plot for pp5.

Although the entrance manoeuvre can be completed without tug assistance during ebb, it is recommended to always use tug assistance, to be able to assist in emergency situations and to turn and berth the vessel. That this is a fairly easy manoeuvre, is shown in figure 7.15, the rps setting and the corresponding data tables 7.5 and 7.6. The cross-track deviation and the drift angle are similar as for pp4 and moreover, the whole manoeuvre is more controlled.

```
**-------------------------------------
** Record 6b: Start position of track sections.          [m]
0  1000 1900 2300 2500 2850 3650 3800 4000
**-------------------------------------
** Record 6c: Propeller revolutions per track section.   [1/s]
.8 .7  .6  .55 .55 .6  -.4 -.5 -.5
**-------------------------------------
```

Figure 7.16 RPS setting for PP5.

7.9 Run PP6; extreme ebb conditions, *with* tug assistance

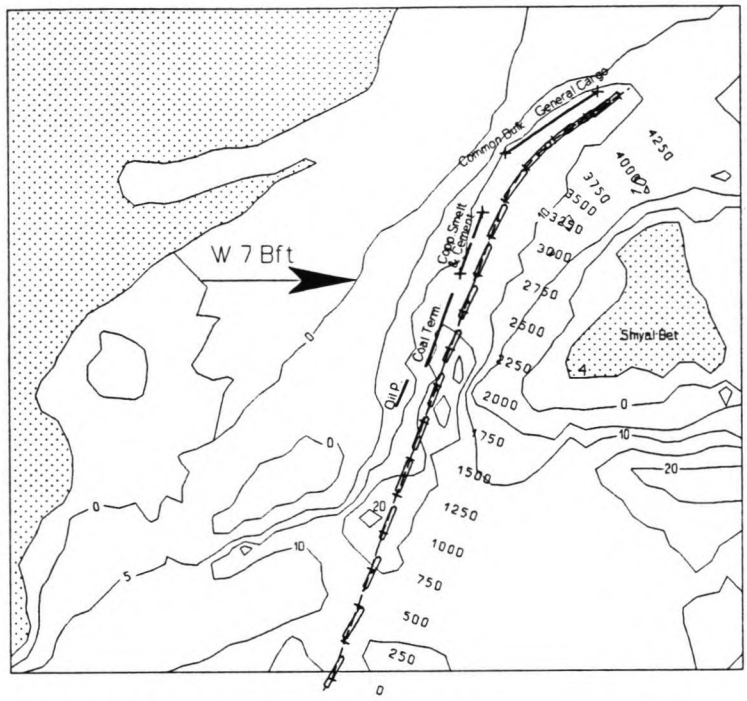

Figure 7.17 Track plot for pp6.

Even under extreme ebb conditions (1.47 m/s, exceeded for 1% of the time), combined with an extreme wind of 15.5 m/s coming from the west), it appears to be possible to enter the harbour, judging from the track plot (figure 7.17), the rps setting and the data tables 7.5 and 7.6. The autopilot has to use larger rudder angles to keep the vessel on track, but the drift angle never reaches the critical value of 14° and also the cross track deviation is very acceptable with only 12m to starboard. The average time needed to complete the entrance manoeuvre varies from 1740 seconds for PP1 to 2124 seconds for PP4. The tying up of tug boats starts at a distance of approximately 1000m before the SHIPMA runs start. This would take about *1000m / 3.0 m/s = 330 seconds*. The average time for entering the harbour and coming to a full stop is approximately 40 min.

```
**-------------------------------------
** Record 6b: Start position of track sections.        [m]
0  1000 1800 2300 2500 3000 3500 3700 4000
**-------------------------------------
** Record 6c: Propeller revolutions per track section. [1/s]
1  .9   .9   .9   .8   .7   -.3  .3   -.5
**-------------------------------------
```

Figure 7.18 RPS setting for PP6.

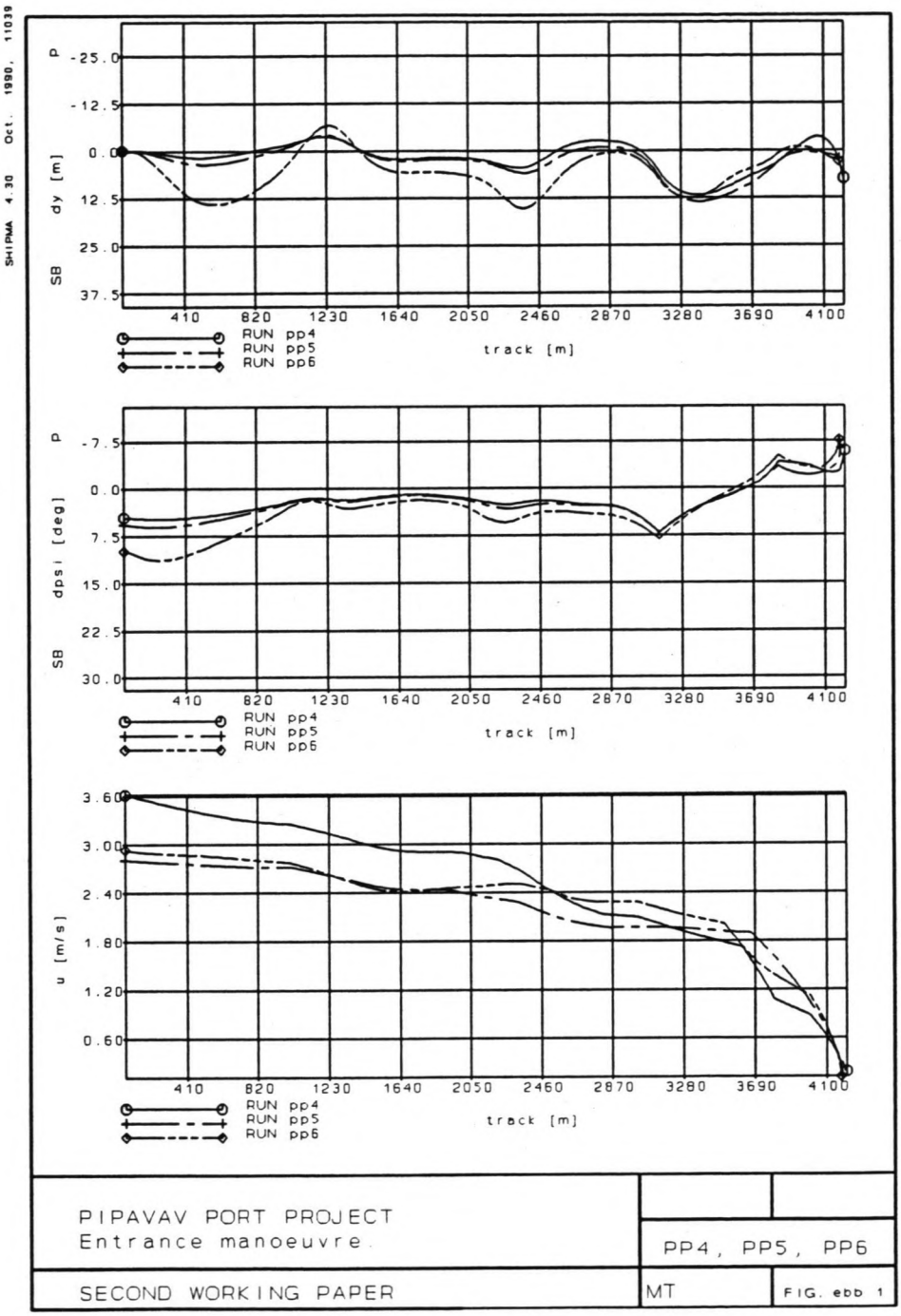

Table 7.5 Data tables, showing the cross track deviation, the drift angle and the longitudinal speed of the vessel for pp4, pp5 and pp6.

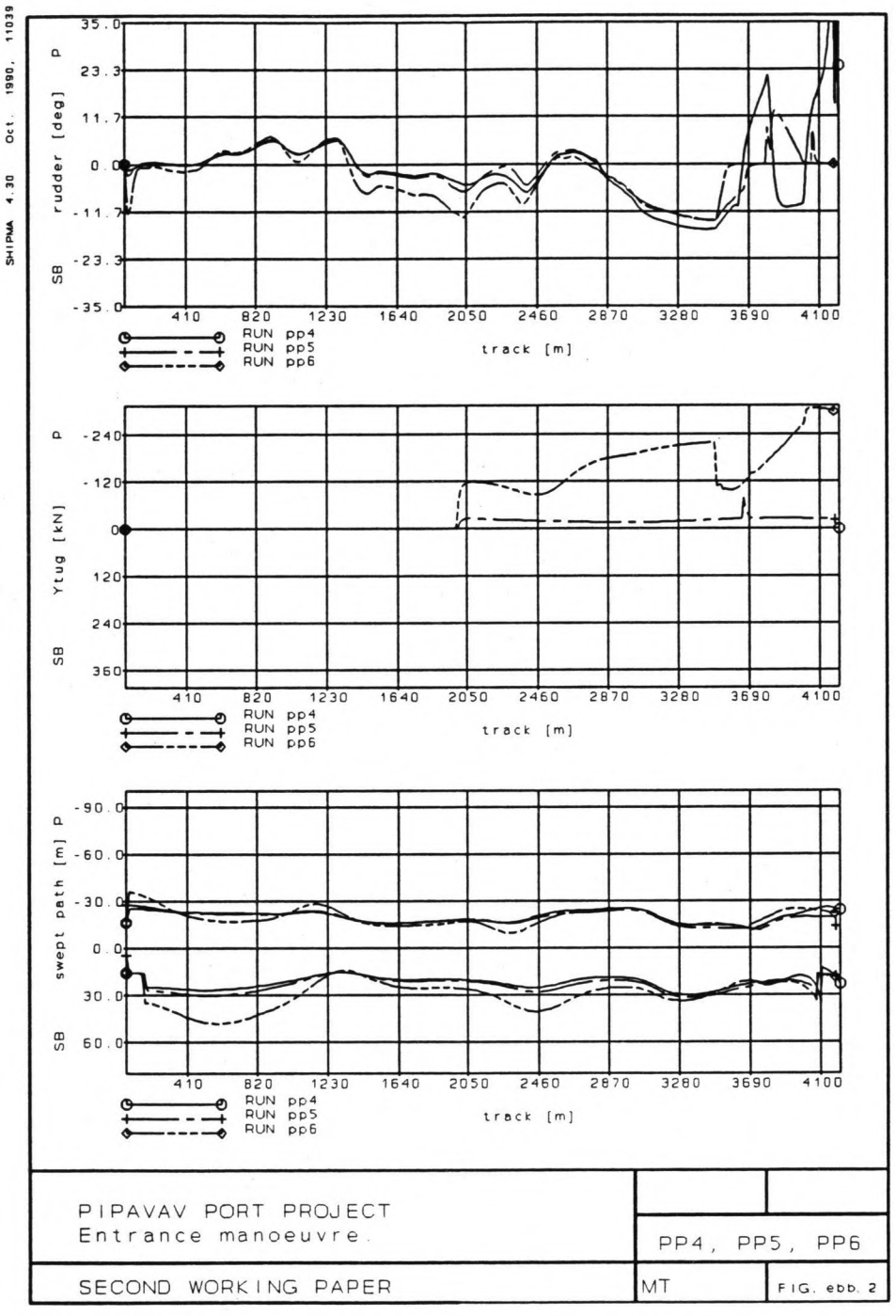

Table 7.6 Data tables, showing the rudder angle, the tug force in ship's transverse direction and the swept path for pp4, pp5 and pp6.

7.10 Run TM1; 15% exceeding conditions, with tug assistance

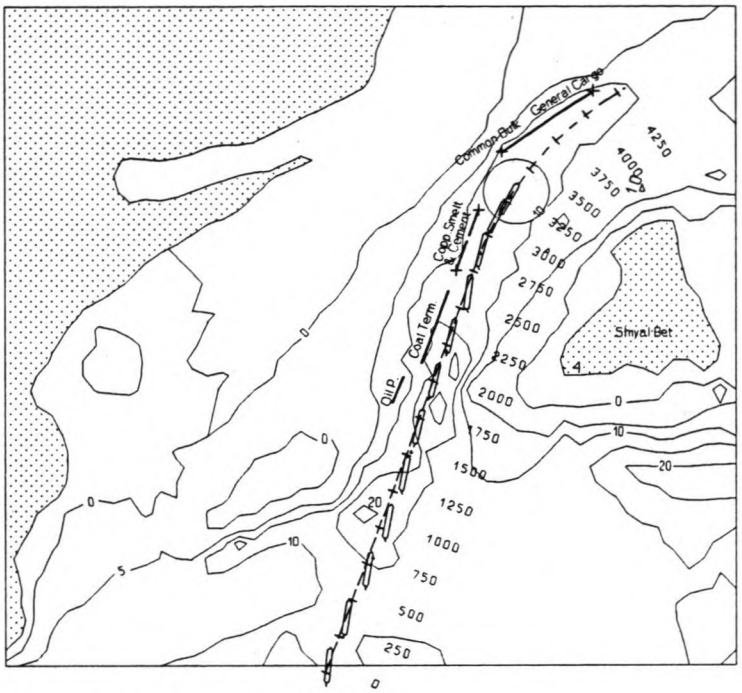

Figure 7.19 Track plot for tm1.

It was investigated in this run, if it is also possible to come to a full stop in the turning circle, between the cement and the multi-purpose terminal. It is inconvenient for vessels, that want to berth at the cement or the coal terminal, to come to a full stop only in front of the multi-purpose terminal. They then have to be towed backwards towards the turning circle, where they can be turned and berthed at other terminals. If it is possible to stop in the turning circle, the remainder of the channel can serve as a safety stopping-distance.

As can be concluded from the previous sections, entering the harbour under extreme flood conditions, is the most difficult manoeuvre. Therefore, if it is possible to stop in the turning circle under these conditions, it is also possible to stop under regular flood and regular and extreme ebb conditions.

```
**-------------------------------------
** Record 6b: Start position of track sections.        [m]
0  1000 1500 1900 2000 2500 2900 3000
**-------------------------------------
** Record 6c: Propeller revolutions per track section. [1/s]
.55 .5  .5  .45 .45 .5  -.7 -.9
**-------------------------------------
```

Figure 7.20 RPS setting for TM1.

The track plot of this manoeuvre is presented in figure 7.19. The corresponding data tables are presented in tables 7.7 and 7.8. Judging

from the track plot and the data tables, this manoeuvre is difficult. The cross-track deviation is practically the same as for pp3. The drift angle and the rudder angle, however, are slightly larger. This is caused by the larger speed reduction that has to be accomplished on a shorter sailing distance. The swept path does not claim any more space than the previous runs. Swept path and drift angle suggest that this manoeuvre is possible, but the applied rudder angle is at a maximum of 35° for some 300m. This is possible, but with this computer simulation the manoeuvre should be performed better to have some safety margins in practice. These margins then serve for the human element and rudder and engine failure, which happens only too often in a real life situation.

Altogether it can be concluded that this manoeuvre is the ultimate situation for safe passage. It will be practice, in stead of sailing to the end of the channel (PP1 through PP6), to keep the remaining part of the channel for safety purposes, in case the tie up manoeuvre is completed later than anticipated or even fails completely. The risk of a ship colliding with the multi-purpose terminal is higher than the other ones, because of its different orientation. The curve the ship has to make ro prevent collision is not very acute but a ship adrift is uncontrollable. In case the risk of collision is found to be too high, the terminal will either have to be relocated or at least reorientated, which could, however, involve rather high dredging costs.

The time needed to complete this manoeuvre is 1272 seconds. The average time needed for the entrance manoeuvre would therefore be approximately 25 minutes. The estimated time needed to turn the vessel and subsequently berth it at the designated terminal would be approximately 45 minutes. This is the same value as used in the entrance times of Volume I.

7.11 Turning manoeuvre and port departure

The turning manoeuvre itself will take about 10-20 minutes. In this period the ship is affected by wind and current. The tugboats will not be able to control the ship completely; it will start to drift during this manoeuvre. According to [17] the required tugboat bollard pull, for a 60,000 DWT vessel, in loaded and in ballast condition, for a 10 m/s wind and a 0.8 m/s current is approximately 570 kN. With a factor of 1.4 to compensate for uneven bollard pull when several tugboats are used and due to calculation inaccuracy this means that *800 / 200 = 4 tugboats* are needed to hold the ship against the forces due to wind and current. This means that 2 tugboats can compensate about 50% of the drift force. Assuming that the drift speed is about equal to the current speed results in a drift speed of approximately 0.4 m/s. Assuming that the vessel can not compensate the drift force on its own for about 15 minutes of the total manoeuvring time this results in a drift distance of approximately 350m. This extra drift length will have to be provided inside the turning basin.

When a vessel enters the port during flood, it will first sail to the turning basin where it will be turned to be able to berth the vessel with its bow

directed against the current. During ebb it will berth first. This is done to make sure that the vessel can assist the tugboats during berthing by letting the engine work and thus compensate for current forces. Deberthing the vessel for port departure will require the same vessel-assistance as in the case of port entrance. It may happen, however, that the ship is berthed with the current coming from astern.

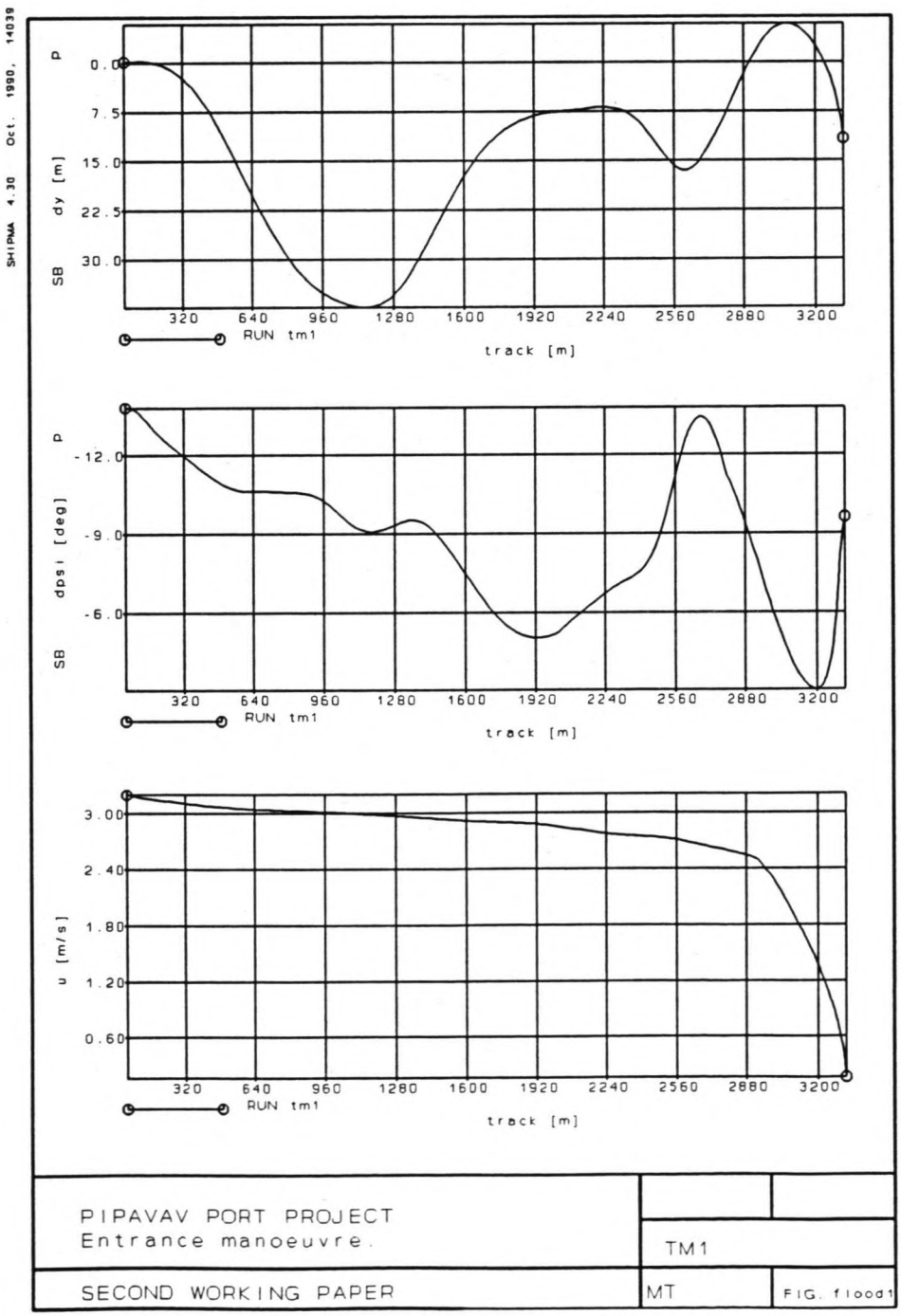

Table 7.7 Data tables, showing the cross track deviation, the drift angle and the longitudinal speed of the vessel for tm1.

In that case, the vessel will be unable to compensate for current forces (full astern will cause uncontrollable ship movements, due lack of rudder control) and the ship will start to drift on the current. As seen above, the tugboats can compensate for about 50% of these forces. It is believed that this is enough to guide the ship either to the navigation channel to leave port or else to the turning basin to be turned and then leave port.

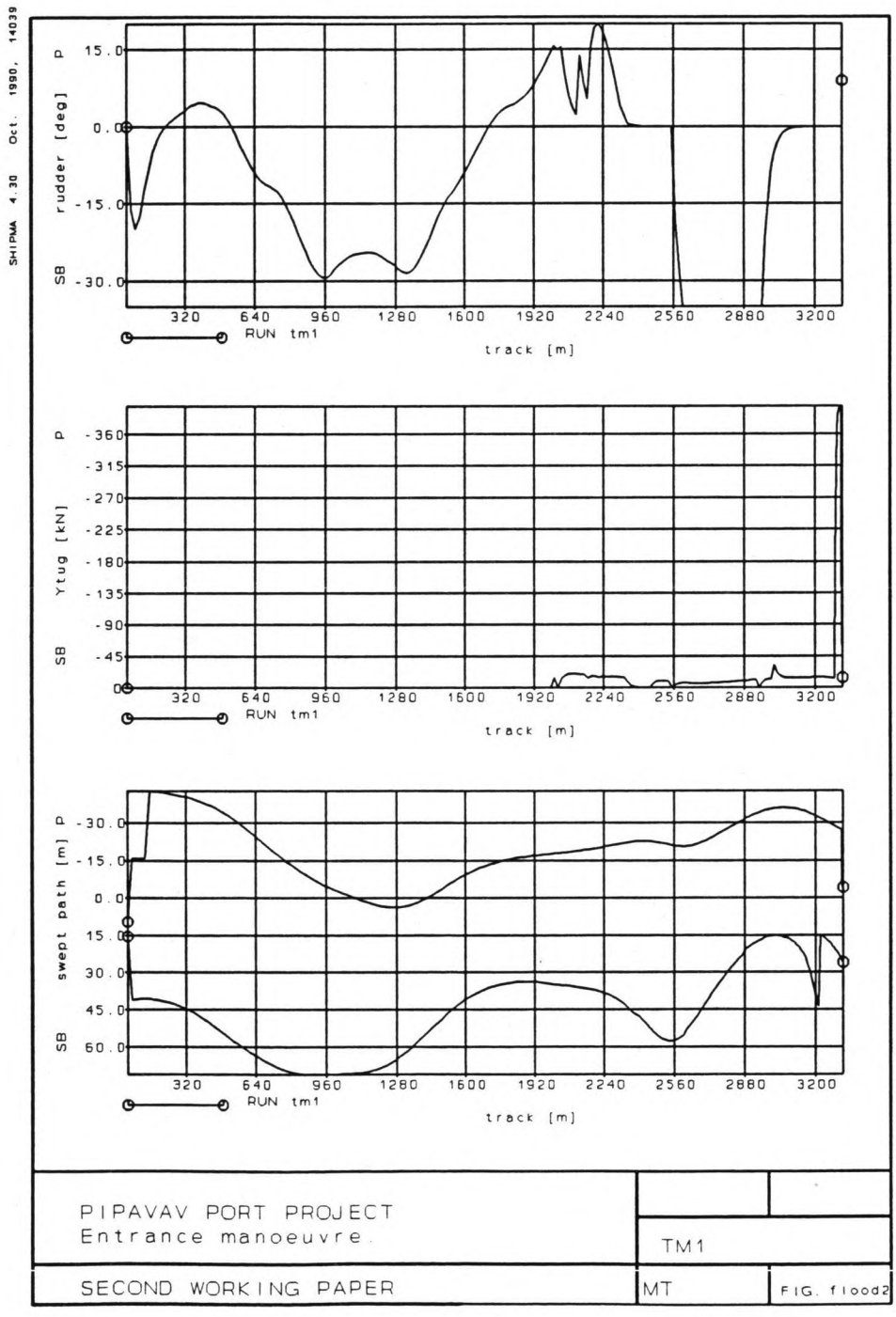

Table 7.8 Data tables, showing the rudder angle, the tug force in ship's transverse direction and the swept path for tm1.

8 Evaluation of design variables

In this chapter the results of all the previous chapters will be used to evaluate the design variables of the Pipavav Port based on the newly obtained insight in some of the parameters. This evaluation will lead to a more detailed design of the port and its facilities.

8.1 Downtime

As discussed before, downtime can be caused by various factors:
- Breakdown of cargo handling equipment and periodical maintenance of the terminals and installations.
- The combination of winds and currents for vessels sailing in the channel.
- Wave height/period combinations for pilot boarding, tugboat tie-up and vessels berthed at the terminals.

Maintenance and breakdown

Downtime due to breakdown and maintenance was evaluated in section 3.2.6. Breakdown is based on 90% average availability of the equipment. Depending on the terminal occupancy, maintenance can be scheduled in such a way, that it does not significantly influences the terminal availability. Only when the occupancy is high and cargo handling operations can not temporarily be carried out by other equipment, will it really cause downtime. Based on the estimated average terminal occupancy, this amounted to:

Event causing downtime	Days/year in phase I	Days/year in phase II
Periodical maintenance	0	0
Breakdown of cargo handling equipment	9	15

Table 8.1 Maintenance and breakdown downtime.

Currents and wind

Downtime due to current/wind combinations was investigated with the nautical simulation model SHIPMA. The limit for ships entering the harbour appeared to be a flood current of 1.4 m/s, combined with a wind of 15 m/s, coming from the west. The current flow velocity occurs with a tidal range of approximately 3.0m which is exceeded for about 20% of the time, see figures 2.4 through 2.5. Naturally this does not mean that the port is also closed for 20% of the time. This velocity of 1.4 m/s or higher can only occur twice a day and then only for a limited period of time. This is illustrated in figure 8.1. The summarized time that the flood current is equal to or higher than 1.4 m/s is, 45.29 for a standardized month of 28 days, or:

*365/28 * 45.29h / (24h * 28 days) = 0.9 days/year.*

The results of the nautical investigation are summarized in table 8.2.

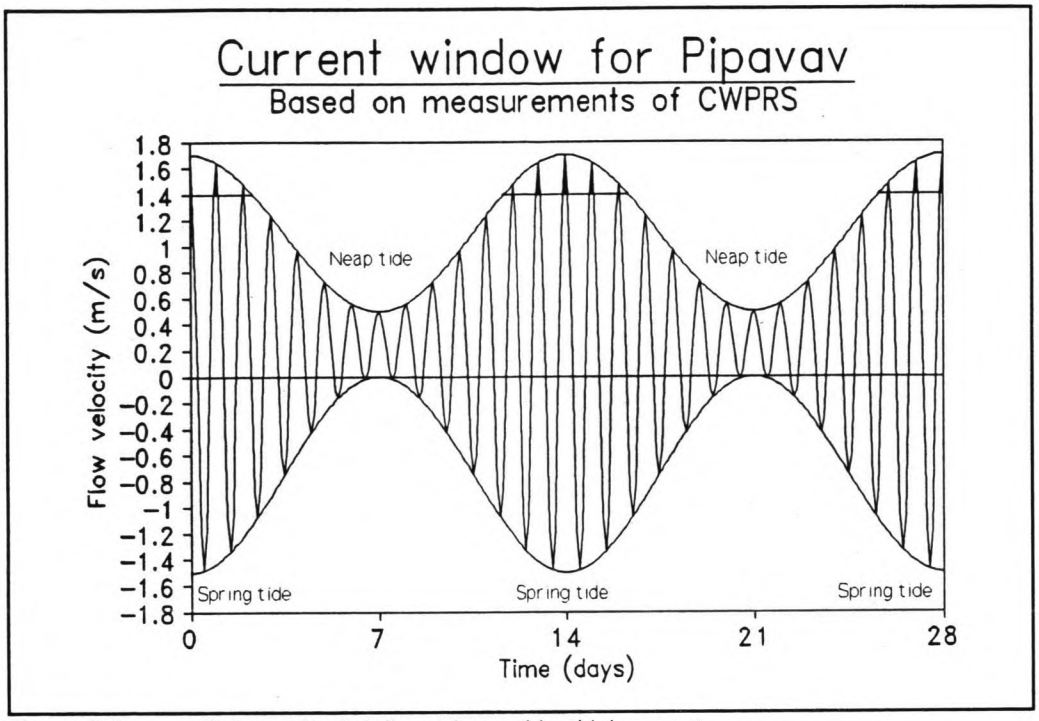

Figure 8.1 Schematized daily and monthly tidal current.

Event causing downtime	Occurring (% of time)	Occurring (days/year)
Flood current with a flow velocity of ≥ 1.4 m/s	15%	0.9
Ebb current with a flow velocity of > 1.47 m/s	<1%	0
Wind coming from west with a speed of > 15 m/s	<1%	0

Table 8.2 Current and wind downtime.

The current window would have to be applied approximately 10 times a month (that's when the flood flow can surpass 1.4 m/s) and the maximum durations of such a window would be 2h 25min during a spring tide. It has to be noted that all downtime figures are given as the total number of days that a certain operation is impeded, rather than the chance a ship has to the port or the terminal closed.

Waves

Suspending of cargo handling operations due to certain wave height/-period combinations at the various berths was evaluated in section 6.4.2. Simulations with the numerical model HISWA resulted in the following presented in table 8.3.

The correlation between downtime, caused by maintenance/breakdown, wind/current and waves is so small that the events are considered to be totally not correlated. This means that the number of days of downtime, caused by the various events, can be summed up to get the total number

of days of downtime per terminal.

Terminal/offshore location	$H_{location}$(m)	Days/year
General Cargo Terminal	0.8	0.00
Common Bulk Terminal	1.0	0.00
Cement Terminal	1.0	0.00
Copper Smelter Export Terminal	1.3	0.00
Copper Smelter Import Terminal	1.0	0.00
Coal Terminal	1.0	10.93
Oil Products Terminal	1.5	19.57
Fixed Crude Oil Jetty	1.5	6.03
SBM Crude Oil	2.5	1.94
Launches and mooring boats in port basin	1.3	10.67
Pilots 10km offshore	3.0	0.71
Tugboats 2km offshore	1.5	10.67

Table 8.3 Terminal downtime for cargo handling and port downtime for entering.

The port may not be entered without the assistance of pilots, tugboats and other auxiliary craft, such as mooring boats. From table 8.3 it can be seen that these events are exceeded for 0.71, 10.67 and 10.67 days/year respectively. These specific events however are highly correlated. It is no use to let pilots board the vessel with a deep water wave height of 4m, when at the same time the tugboats are unable to tie up. The assistance of auxiliary harbour craft in the port basin is influenced in the same manner as the tie-up procedure for tugboats. Either event can therefore be normative for causing port downtime. The tie-up procedure is supposed to start at a distance of approximately 2km outside the port, after which the ships are accompanied to the turning circle between the cement and the multi-purpose terminal, to be turned and berthed. For oil product tankers this manoeuvre seems unnecessarily long an risk-full. These vessels will have to pass three terminals, then turn, and then sail back to the oil products terminal, with all possible dangers of this manoeuvre. It seems more appropriate to turn these tankers outside the port and then berth them directly at the oil products terminal near the entrance of the harbour. This would mean that the tie-up procedure has to start further offshore and consequently that the port downtime for this specific terminal would increase significantly. Since it's terminal downtime is already the highest of all relocation or special protection of this terminal should be considered. For now, the more risk-full procedure is considered, to get an equal basis of comparison for all terminals.

The obtained port downtime is highly correlated with the terminal downtime. When a storm is building in the open sea, first the port will close, due to the inability of tugboat tie-up. Later, when the wave heights keep

increasing the terminals will close, because cargo handling is no longer possible. When the storm dies down, first the terminals will open and then the port will open again. It can also happen, however, that a vessel can slip through during a more quiet period of the storm. So when determining the available working hours per year one cannot include the complete port downtime. An example calculation for the coal terminal is described below. It will be determined how many days out of the port downtime, due to tugboat tie up impediment, actually cause terminal impediment.

# of storm days: *10.7 days/year*
storm chance: *10.7/365=0.03*
estimated storm duration: *18 hours/storm*
average waiting time: *9 hours/storm*
average waiting time: *9*0.03=0.26 hours/ship*
# of ship arrivals: *178 ships/year (2010)*
total waiting hours: *178*0.26/24=1.93 days/year*

terminal waiting time: *5.47 days/year*
available working hours: *(365-(1.93+5.47))*24=8582 h/a*

As can be seen the influence of port downtime on the total available working hours per year is minor, even though a relative high average storm duration was used. This average storm duration should be investigated and may possibly be lower. With this higher average duration, however, a pessimistic approach is followed to be on the safe side. For the other terminals the available number of working days per year is summarized below.

		Port downtime (d/a)	Terminal downtime (d/a)	Occupancy	Breakdown (d/a)	Current/wind (d/a)	Total downtime (d/a)	Workable hours (h/a)
A	Common bulk export	0.89	0.00	0.23	8.51	0.90	10.31	8513
	Common bulk import	0.71	0.00	0.27	9.87	0.90	11.48	8484
B	Cement terminal	0.41	0.00	0.10	3.81	0.90	5.11	8637
	Copper smelter exp Copper smelter imp	0.46	0.00	0.12	4.55	0.90	5.91	8618
D E F	General cargo Containers Ro-ro	1.15	0.00	0.44	15.96	0.90	18.01	6940

Table 8.4 New values for above mentioned variables for phase I of development.

8.2 Number of berths

The number of berths for one terminal depends upon many variables. Among these are the effective loading capacity, the number of ship calls, the time needed for entering the harbour and berthing the vessel, the cost ratio between additional berths and ship waiting time, etc. All these factors have not changed, however. The only variable that was significantly influenced by the results of the mathematical models is the number of workable days/year of the various terminals. In Volume I this was roughly assessed based on a diffraction study made by DHV. Now this is more accurately determined based on the results of HISWA and SHIPMA. The resulting new berth occupancies and workable hours/year are presented in table 8.4.

		Port downtime (d/a)	Terminal downtime (d/a)	Occupancy	Breakdown (d/a)	Current/wind (d/a)	Total downtime (d/a)	Workable hours (h/a)
A	Common bulk exp	1.69	0.00	0.36	13.08	0.90	15.67	8384
	Common bulk imp	1.16	0.00	0.35	12.66	0.90	14.72	8407
B	Cement terminal	1.06	0.00	0.22	8.04	0.90	10.00	8520
	Coal terminal	1.95	10.93	0.63	23.07	0.90	36.85	7876
	Copper smelter exp Copper smelter imp	1.58	0.00	0.39	14.08	0.90	16.57	8362
C	Oil products	2.44	19.57	0.48	17.49	0.90	40.40	7790
	Crude oil jetty	0.73	6.03	0.12	4.31	0.90	11.97	8473
D E F	General cargo Containers Ro-ro	3.12	0.00	0.63	23.08	0.90	27.10	6758

Table 8.5 New values for above mentioned variables for phase II of development.

The values for the berth occupancies and the workable hours/year slightly ameliorated for all terminals (approximately 350 h/a), except the oil products terminal (compare with table 3.7 in Volume I). The oil products terminal has approximately 28 days less available for terminal operations. This is caused by a higher port and terminal downtime due to waves, compared to the former study. The location of this terminal appears to be less favourable than expected. This is caused by the fact that the wave height attenuation does not start to set in significantly until near the oil products terminal (see also the wave height iso-line plot in figure 6.9 and figure 8.2).

The berth occupancy of the oil products terminal has consequently slightly increased with 0.04. The berth occupancies of the other terminals have decreased (varying from 0.01 to 0.07). These values mean a gain or loss in the turn-around time per vessel of a couple of hours. All this has not resulted in a change of the required number of berths.

8.3 Quay length, height and type of berths

The length of the quay depends upon the required number of berths per terminal and the average and maximum length of the expected ships at that terminal. Neither one of these has changed, as a result of the studies undertaken in this paper.

The height of the berths depend upon the expected wave height at the terminal, the water level variation in the basin and the ship's freeboard.
The freeboard of a ship is the difference between its moulded depth and its maximum or ballast-loaded draft. For the type of ships, expected at Pipavav this would typically range between 3m and 10m.
The berth should be constructed in such a way that it is protected from waves hitting the bottom of the deck (in case of open structures) and for flooding. The design criteria used in this paper is 1/20 year. The water level that is exceeded for about 0.01% of the time is CD +4.25m. The wave height that is exceeded for approximately 0.01% at deep water is 9m. The wave height at the terminal depends on the wave period and the location of the terminal in the basin. It varies between 0.6m at the general cargo terminal to 7.5m at the oil products terminal and 9m at the crude oil jetty. Flooding of the oil terminals is less arduous, because there is no direct storage at these terminals. When the flood criterium is softened to, say 1% for the oil terminals, the new berth heights may be:

Crude oil terminal (fixed jetty)	CD +8.75m
Oil products terminal	CD +7.75m
Coal terminal	CD +7.75m
Copper Smelter terminal	CD +6.35m
Multi-purpose terminal	CD +5.15m

This makes the berth height of the multi-purpose terminal a little lower than in Volume I and by CES. These reports recommended CD +5.50m.

The type of berth structure, closed or open, mainly depends upon the soil characteristics and the need for storage directly behind the apron. The expected wave heights and periods and the ship's wave response characteristics, also play an important role, because of reflection of wave energy by closed type structures.
The soil structure is discussed in section 2.7. It seems that both berth constructions, a solid gravity type berth and an open, pile supported deck, are possible, based upon the soil profile in appendix IV. Reflection of wave energy off a solid berth will not directly influence the moored ship, the ship behaves as a vertical mass structure itself. Only the wave response will increase with increasing wave height. During berthing, the enclosed water mass between ship and berth, can be more troublesome in case of a closed type berth. It can also serve as a buffer, avoiding high collision speeds.

Also, high wave activity in the port basin, can cause restless water for sailing ships. Open berth structures would, therefore be recommended from a navigational point of view. Since wave activity is rather low, however, and berthing primarily depends on good communication between the tug boat operators and the ship's captain, the type of berth structure will probably be decided through cost comparison, rather than nautical preference.

8.4 Location & orientation

Evaluating the results of the studies undertaken in this paper, with regard to the direction of waves and currents, the following can be concluded:

- The waves penetrate the harbour at an angle of 0°-20° to the berth orientation, the most favourable direction for moored ships (head sea). Only the fixed oil jetty has waves at 25°-53°, see table 6.2.
- The wave height decreases towards the rear of the harbour, to approximately 90% near the oil products terminal up to 10% near the multi-purpose terminal, see figure 8.2.
- The various terminals are reasonably aligned to the flood and ebb currents, with angles varying from 0° to 10°, see figure 7.5.

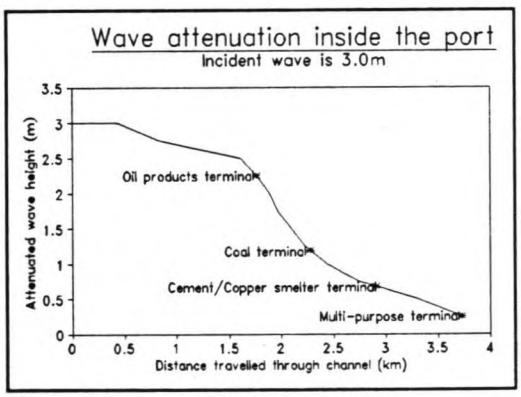

Figure 8.2 Wave attenuation.

These conclusions indicate that the alignment of most terminals is good, keeping in mind the comment made in section 7.10, with regard to collision risk of the multi-purpose terminal. The orientation of the fixed oil jetty, however, is less favourable, with respect to incident waves. It is therefore suggested to turn the jetty some 20° as a compromise between wave direction and current alignment.

As for the location of the terminals, the first two terminals, for oil products and coal, should preferably be moved more towards the rear of the harbour, to increase the advantage of the wave height decrease.

8.5 Width & depth of channel and basins

The width of the channel should be such that a vessel assisted by tugs can enter the channel, even under extreme flood conditions. The swept path-results, from the various SHIPMA runs, can give a good indication of this required width. The swept path of run PP3 shows a maximum deviation to starboard of approximately 75m and 45m to port. At the point where the dredged channel starts this is 65m to starboard and 25m to port. This means a minimum channel width of 120m decreasing to 90m near the entrance of the channel. When the speed of a vessel is almost zero it can easily start rotating and because of this it requires some extra space. Assuming that vessels will usually be stopped in the turning circle, this extra width is present and does not result in an extra

channel width. This minimum width requirement does not compensate for information inaccuracy on the ship's position, nor does it foresee in a safety margin, to compensate sudden wind gusts, the stochastic nature of human behaviour or other extreme factors. It is therefore recommended to increase the minimum required width with twice the beam of the design ship. This means an extra $2*33.5=67m$, which results in a channel of 190m at the entrance of the navigation channel, decreasing to 170m near the beginning of the dredged part of the channel.

The diameter of the turning basin was firstly estimated at 380m and 440m in the first and the second phase. In this estimation the influence of drift during turning, due to current and wind forces has not been incorporated. The tugboats will be able to control the vessel, but can not prevent that the vessel will have some displacement. It is assumed that the tugboats can reduce the drift speed for about 50% (see section 7.11), so that an extra drift length inside the turning basin would have to be provided of some 350m.

The depth of the channel and basins is made up of several factors, summed up below.

Sailing vessel	Moored vessel
* Ship's draught	* Ship's draught
* Tidal window	* Minimum water level
* Vertical ship motion (heave, pitch, roll)	* Vertical ship motions
* Squat, trim	
* Sedimentation buffer	* Sedimentation buffer
* Dredging inaccuracies	* Dredging inaccuracies
* Depth sounding inaccuracies	* Depth sounding inaccuracies

Vertical ship motion

In section 3.1 it was already discussed what factors influence the vertical ship motions of sailing and moored ships.

For a sailing ship the risk exists that the apparent wave period can become equal to the natural period of oscillation of the ship. When this happens, resonance can cause rather large vertical movements. Depending on the size of the ship and the height of the waves this can vary between 0.5m and 2.0m. When it is assumed that the maximum vertical deviation is at the most 2/3 of the significant wave height [17] this amounts to 2/3 * 1.5m, for 1.5m is the limiting wave height for which ships are still allowed in the channel.

A moored ship starts to resonate when the period of the external forces equals the period of the mass spring system, made up by the ship and the mooring lines and fenders. Resonance due to this occurrence will hardly happen, for the natural period of such systems usually lies significantly higher than the wave periods expected at Pipavav. Nevertheless the expected vertical motions will be of the order of 0.5m to 1.0m.

Squat

Squat is the phenomena that a sailing vessel has a downward displacement, under specific conditions, due to a return current along the sides and under the keel of the ship. Dr. C.B. Barrass [2] has developed a formula to calculate the squat of sailing ships:

$$\xi = \frac{V^2}{2g} \cdot 3.75 \cdot C_B \cdot S_2^{3/4} \cdot \left(\frac{V}{V_s}\right)^{1/12}$$

$$S_2 = \frac{S}{(1-S)}$$

$$S = \frac{bd}{BD} = \frac{d}{D} \cdot \frac{1}{7.7 + 45 \cdot (1 - C_w)}$$

$$C_w = \frac{A_s}{bL_s}$$

ξ = squat
V = vessel's speed
C_B = block coefficient
S = blockage factor
V_s = vessel's service speed
C_w = water plane area coefficient

Using the values of the ship used for the SHIPMA simulations, this gives a squat of 0.12m at a sailing speed of 4 knots and a channel depth of 14.2m.

Sedimentation buffer

The average depth in the channel is CD -11m. This means that there has to be done some dredging to provide enough water depth for ships to sail and be moored. This dredging will be of the order of 2m-3m. In section 2.9 it was estimated that the annual siltation would be about 20%-30% of the capital dredged volume. The sedimentation buffer would have to be 0.4m-0.9m.

Tidal window

As explained in Volume I is probably uneconomical to provide unrestricted access for all vessels expected at Pipavav. A tidal window of 4 hours minimum per tidal cycle, for all ships with a draft larger than 9.10m in the first phase and 10.6 in the second, is guaranteed CD +2.40m.

The estimated channel and basin depth requirements are:

Sailing vessel		Moored vessel	
* Ship's draught	11.5m/13.0m	* Ship's draught	11.5m/13.0m
* Tidal window	CD +2.40m	* Minimum water level	CD +0.00m
* Vertical ship motion	1.00m	* Vertical ship motions	0.80m
* Squat, trim	0.12m		
* Sedimentation buffer	0.65m	* Sedimentation buffer	0.65m
* Dredging inaccuracies		* Dredging inaccuracies	
* Depth sounding inaccuracies	1.00m	* Depth sounding inaccuracies	1.00m
Channel bed in phase I	CD -11.87m	Basin bed in phase I	CD -13.95m
Channel bed in phase II	CD -13.37m	Basin bed in phase II	CD -15.45m

Comparing to the results of Volume I, the channel depth is slightly less and the basin depth is slightly more.

9 Conclusions

Conclusions with respect the site conditions

- The principal wind direction is between SW and NW, blowing with an average wind speed of 3.5 Beaufort and a maximum of 7 Beaufort.
- The average flow velocities during ebb and flood are 0.72 m/s and 1.14 m/s, with a maximum of 1.47 m/s and 1.69 m/s.
- The most interesting seasons, with regard to waves, are the Hot Season (April-May) and the SW-Monsoon (June-September).
- The principal wave directions affecting the site of Pipavav are between 165°-255°.
- The wave height exceeding at deep water is larger than originally assumed in the study performed by CES, Consulting Engineers India.
- The top layer of the channel bed consists of soft mud, with more solid layers, directly below.

Conclusions with respect to the models

- Although the mathematical model PORTRAY could be used for the translation of the deep water wave climate to the near shore wave climate, the model HISWA is more suitable and easier to operate for these kind of translations.
- Although HISWA can very well be used inside port basins, such as the Pipavav Port basin, PORTRAY is more suitable to be used for translation of the near shore wave climate to the port wave climate, especially when reflection and diffraction by port structures is expected to be of influence.
- Ideally the two models should be combined to make a translation of the deep water wave climate to the near shore wave climate with HISWA and then use the thus obtained near shore wave climate with PORTRAY to predict the wave activity inside the port.
- Although PORTRAY was specifically written to be used for the prediction of wave activity inside harbours, it was not suitable for Pipavav Port, mainly due to the complexity of the basin.
- Although HISWA was specifically written to model wave propagation over a slowly rising foreshore seabed, it could be used to model the port wave climate of Pipavav Port.

Conclusions with respect to the wave climates

- The near shore wave climate can be described as follows:
  - Waves coming from 180° are refracted to approximately 82% of their original wave height and to a new direction 181°,
  - waves coming from 210° are refracted to 69% and 198° and
  - waves coming from 240° are refracted to 52% and 209°.

  (For a more elaborate discussion of the near shore wave climate and the difference between the models is referred to section 5.5.)

- Impediment of the port activities is mainly caused by waves, breakdown of cargo handling equipment and combined wind current forces on a sailing ship.

- The port wave climate can be described as follows:
  - Waves at the multi-purpose terminal are refracted to approximately 8% of the wave height at the port boundary and to an angle of 5° with the terminal orientation,
  - at the cement/copper-smelter terminal this is 23% and 11°,
  - at the coal terminal this is 40% and 3°,
  - at the oil products terminal this is 75% and 18° and
  - at the crude oil terminal this is 100% and 39°.

  (For a more elaborate discussion on the port wave climate and the difference between the models is referred to section 6.5.)

Conclusions with respect the navigability

- The navigability of the port is good. Under more extreme conditions it becomes difficult to manoeuvre safely through the harbour, which however, only results in an downtime of the channel of circa 1 day per year, divided over the monsoon period.

- The limiting condition for vessels entering the harbour is a wind coming from the west, with a speed of 7 Beaufort, a flood current, with a flow velocity of 1.4 m/s and a wave height of 1.50m at the channel entrance. Under these conditions the vessel can enter the harbour and come to a full stop in the turning circle between the cement and the common bulk terminal, with the assistance of two tugboats, where it can be turned by the tugboats to be berthed at the terminal of destination.

- The tie-up by tugboats is the determining downtime factor for all terminals. The combined downtime due to wave exceeding at the terminal and port closure is:
  - circa 1 day or less for all terminals in the first phase,
  - circa 1½ days for the common bulk, cement and copper smelter terminal in the second phase,
  - circa 3 days for the general cargo terminal in phase II,
  - circa 7 days for the crude oil jetty,
  - circa 13 days for the coal terminal and
  - circa 22 days for the oil products terminal.

General conclusions

- The orientation of the multi-purpose terminal should be reconsidered, for with the current orientation there is a high risk of collision between vessels manoeuvring in the channel and vessels berthed at this terminal or the terminal itself. This would have to be cost evaluation between relocation costs (dredging) and collision risk.

- The orientation of the first part of the channel is at an angle of 38° to the current and this can be changed to ameliorate the navigability of this part of the channel.

- The orientation of the crude oil terminal should be changed with approximately 20° counter clock wise, to get a better compromise between alignment of this terminal with the mean wave direction and the mean current direction.

- In locating the terminals it should be tried to relocate the coal terminal and the oil products terminal in a way that they are placed more towards the rear of the harbour, to get a better protection for wave penetration for these specific terminals and thus decreasing the terminal downtime.

- The port is fairly to well protected from wave penetration from the Arabian Sea by the islands and the foreshore rock formations. This, combined with the good navigability of the port, would have lead to the conclusion that the feasibility of this port is acceptable, from a nautical/hydraulic point of view.

- This study has shown that the port wave climate is very favourable in the rear of the harbour, but that the wave height increases fast towards the entrance, resulting in the high terminal downtime of the oil products terminal. This includes that port expansion will be difficult an expensive. Either extensive dredging has to take place to enlarge the protected area or the exposed area will have to be protected with the use of breakwaters.

10 Recommendations

The recommendations made in this chapter are a supplement on the recommendations done in chapter 6 of Volume I.

It is recommended to do additional measurements on

- the prevailing flow velocities of the flood and ebb current, for they have a significant influence on the wave height outside and inside port and the navigability of the channel.
- wave heights and periods of waves outside and inside the port basin to get actual wave data for design purposes and for calibration of the mathematical offshore and port wave climate models.
- the soil material and structure, for reasons of nautical depth, dredging quantities and terminal foundation.
- the suspended load and bed load transport, to get reliable estimates of sedimentation rates in the basin.

Furthermore it is recommended to perform additional studies on

- the range of wave height and wave period combinations that the vessels expected at Pipavav are sensitive to.
- the transfer functions of the expected vessels at Pipavav, to establish the vessel movements resulting from a certain wave attack, at various loading stages.

Furthermore to

- perform additional navigation simulation studies, with some of the other vessels expected at Pipavav, to get a more complete view on the navigability of the port for all ships. In particular studies with container vessels and product tankers are recommended, for their behaviour is significantly different from that of a bulk carrier.

The following recommendations are done with respect to the mathematical models used in this study.

PORTRAY

- Disconnect the computation grid from the bottom grid, to be able to use less depth values to represent the sea bed, without jeopardizing the accuracy of the results.
- Add the possibility to let the user ask for specific output locations where he wants results, to improve the readability of the output.
- Add the possibility of post processing of the model results, to get a better presentation of the simulation results. This ask for a disproportional amount of the study time.
- Include some examples of imaginary or real situations into the user manual to get a better comprehension of the theory and the importance of the variables and model settings.
- Add comment lines to the input files to make it easier to adjust the setting of variables.

HISWA

- Add the possibility of post processing of the model results, to get a better presentation of the simulation results. This ask for a disproportional amount of the study time.
- Include some examples of imaginary or real situations into the user manual to get a better comprehension of the theory and the importance of the variables and model settings.

SHIPMA

- Add the possibility to plot the bottom contours, the wind field and the orientation and position of the grids with respect to one another.
- Make it possible for the user to determine the scale of the graphs of the variables, to make it possible to get an exact comparison between two or more sets of results.

References

[1] A comparison of the performance of three mathematical models of wave disturbance in harbour approaches, J.V. Smallman and N.P. Tozer, 1990.

[2] A unified approach to "squat' calculations for ships, Dr. C.B. Barrass, MSc., C.Eng, F.R.I.N.A.

[3] Admiralty Tide Tables, Volume 2, 1992.

[4] Admiralty Chart no. 2034, Naval Hydrographic Office, India, Compiled from various hydrographic surveys to 1964, with additions and corrections to 1968.

[5] Admiralty Chart no. 1474, Hydrographic Office, 1991.

[6] Classification of soils & rocks to be dredged, bulletin 47, PIANC, 1985.

[7] Criteria for ship movements in harbours, Jensen, Vigossen, Thomsen, Bjordal, Lundgren, Chapter 223 199207005, reference to PIANC.

[8] Field investigations for the development of Pipavav Port (Gujarat State), nr. 2310, CWPRS, India, 27-3-86.

[9] Field data collection for the determination of the alignment of the steamer berth at Pipavav Port (Gujarat), nr. 2584, CWPRS, India, 1-12-88.

[10] Lectures on ship hydrodynamics, steering and manoeuvrability, rep. no. HY-5, M.A. Abkowitz, Hydro and Aerodynamics Laboratory, Copenhagen, Denmark, 1962.

[11] Masterplan for the development of Pipavav Port, Consulting Engineering Services (CES), June 1989.

[12] Methods for analyzing wind, wave and swell data to estimate on an annual basis the maximum duration of periods during which port and ship operations will be impeded by these elements, bulletin 32, PIANC Working Group I, 1979.

[13] Model studies for the alignment of guide walls for the steamer berth at Pipavav Port, Gujarat, nr. 2677, CWPRS, India, 22-11-89.

[14] Pipavav Port - Hydraulic model studies with the modified layout suggested by M/S. Engineers (India) Limited, nr. 1555, CWPRS, India, 4-3-76.

[15] Planning and design of ports and marine terminals, H. Agerschou, e.o., Norwich, Great Britain, November 1985.

[16] Port Engineering, Volume 1, Harbour planning, Breakwaters and Marine terminals, P. Bruun.

[17] Port design, guidelines and recommendations, C.A. Thoresen, 1988.

[18] Ports and Terminals, Prof.ir. H. Velsink, January 1993.

[19] Rules for the design of hoisting appliances, Federation Europeene de la Manutention, Paris

[20] Shipma 4.30 user manual, Delft Hydraulics, The Netherlands, 1990.

[21] Shore Protection Manual, Volume I, US Army Corps of Engineers, Washington DC, USA, 1984.

[22] Studies on the behaviour of moored ship at Pipavav Port, Gujarat, nr. 2756, CWPRS, India, 9-8-90.

[23] Studies on a tidal model for the development of port facilities at Pipavav Port, nr. 1490, CWPRS, India, 11-6-75.

[24] Techniques of ray averaging, International journal for numerical methods in fluids, H.N. Southgate, 1984.

[25] The PORTRAY harbour wave disturbance model, training and user manual, Dr. J.V. Smallman and Mr. G.J. Eadie, Ports and harbours group, Hydraulic Research, Wallingford, November 1991.

[26] Tidal observations taken at the new port site of Port Pipavav, period from 3-2-88 to 8-4-88, India, 1988.

[27] Tranquillity studies for the Pipavav Port, nr. 1444, CWPRS, India, 3-12-74.

[28] User Manual for the program HISWA, N. Booij, L.H. Holthuijsen, Delft, March 4, 1992.

[29] Wave flume studies for the design of reclamation bund at Pipavav Port, Gujarat, nr. 2401, CWPRS, India, 13-1-87.

[30] West Coast of India Pilot, 11th edition, 1975.